HADES
(Hatton Deep Seismic)

Geological interpretation and synthesis of the Irish Rockall and Hatton margins

L. Gernigon[1], P.M. Shannon[1], P.W. Readman[2], B.M. O'Reilly[2]

[1]UCD School of Geological Sciences, University College Dublin, Belfield, Dublin 4, Ireland. http://www.ucd.ie/geology

[2]Dublin Institute for Advanced Studies (DIAS), 5, Merrion Square, Dublin 2, Ireland. http://www.dias.ie/

Draft Final Report

Prepared for PIPCo RSG Limited

Contract No. 12.29.2003

February 2006

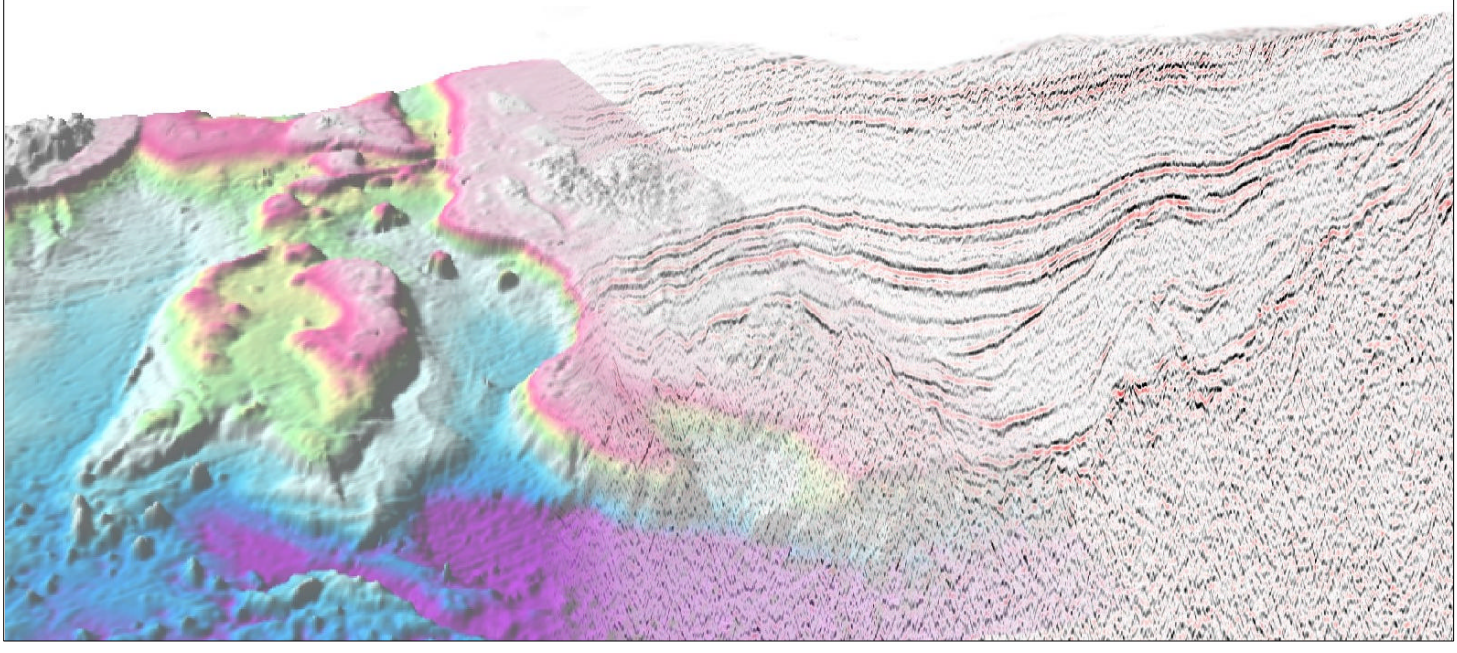

Table of Contents

List of figures

Executive summary

Defining the exact location and nature of the transition between continental and oceanic crust is of key importance to understanding the structure and evolution of continental passive margins. The Irish margins provide an excellent natural laboratory for studying such processes, as they display a large variety of styles, including narrow, wide, volcanic and non-volcanic margins. Integration of the Hatton Deep Seismic (HADES) results, with new seismic, potential field and well calibration data clarifies the structure and stratigraphy of both the West Hatton Margin (WHM) and the south Rockall/Hatton margin (SHRM). A set of regional to semi-regional maps place the Irish margins in their geodynamic context. The WHM represents a Late Palaeocene-Early Eocene volcanic margin, as suggested by the typical volcano-stratigraphic sequence (Inner SDRs, Outer High, Outer SDRs, oceanic crust) observed near the beakup axis. Thin and intruded sediments and continental crust typically underlie the Inner SDRs wedges. Oceanwards, the deep structures of the Outer High and outer SDRs features are underlain by a massive, uniformly thick, high-velocity lower crustal body interpreted as breakup underplating that probably controlled the emplacement of structures than produced the Seaward Dipping Reflectors (SDRs) by a mid-crustal updoming. To the south, the SHRM is a complex rifted zone linking the WHM with the Celtic and Iberian non-volcanic margins. The SHM was also influenced by an earlier Cretaceous phase of break-up and, compared to the WHM, the nature of the continent-ocean transition is different. Close to the C34 magnetic anomaly, the continent-ocean transition is defined by a sharp contrast between a smooth oceanic basement and block-faulted structures that exhibit both syn- and post-breakup features. Close to the oceanic crust, the C34 may not necessarily represent ‘true’ oceanic crust but the complex may reflect a combination of serpentinized peridotites and/or intruded continental basement. No SDRs are imaged, but evidence of magmatism is identified. Thin lava flows and transgressive sill complexes, magmatic plugs and seamounts intruding the Cretaceous oceanic crust are observed near the SRHM. Close to the Charlie-Gibbs Fracture Zone the East Thulean Rise, defining the southern end of the volcanic province, is also imaged. It probably represents a thick Palaeocene oceanic volcanic plateau, uplifted and block faulted during Cenozoic time and interacting with the oceanic spreading initiated earlier in the Porcupine Abyssal Plain. The age of the magmatism along the SRHM and adjacent basins is controversial. Evidence of Palaeogene magmatism is seen but Early Cretaceous igneous activity is also indicated. The best example is the Barra Volcanic Ridge, which is reinterpreted here as a structural horst (serpentine or continental block) cut by Early Cretaceous extrusives and intrusives and subsequently by Cenozoic dykes. Detailed stratigraphic analysis documents the contrasting subsidence/uplift patterns that differentiate the sedimentary architecture of the WHM and the SRHM.

1 INTRODUCTION

The NE Atlantic domain (Figure 1) contains a set of large Late Palaeozoic to Cenozoic sedimentary basins that have undergone a multiphase evolution from rifting through to rift-drift and continental rupture to form a complex passive margin. These episodes of rifting thinned and heated the continental crust and lithosphere, which then subsided to form a complex set of marginal basins. Recent academic research and industry exploration have yielded a wealth of basic information that has greatly improved our understanding of the fundamental processes of lithospheric extension, continental rifting and breakup that have formed these margins (Shannon et al., 1994, 1995, 1999; O'Reilly et al., 1996; Robert et al., 1999; Doré et al., 1999; Naylor et al., 1999).

Results from existing data confirm that the Hatton, Rockall and Porcupine region, offshore Ireland, contains thick sedimentary successions, which show indications of possible large-scale structural features (Shannon et al., 1995). However, the West Hatton Margin (WHM) and the South Rockall/Hatton Margin (SRHM) are poorly understood regions, straddling the continental/oceanic margin and strongly affected by Early Cenozoic magmatism.

The overall aims of the HADES (Hatton Deep Seismic) projects were to define the structure and refine the tectonic development model of the Rockall/Hatton area. The P2 project is one of three linked HADES projects. It involves the synthesis of existing geological and geophysical data and integration of the results with information from the HADES wide-angle seismic profiles. This report also includes the preliminary interpretation of new 2-D seismic reflection data provided by Petroleum Affairs Divisions (PAD) of the Department of Communications, Marine and Natural Resources. The specific objectives of the geological interpretation and synthesis project (P2) are to:

- Identify the structural architecture of the sedimentary strata in the WHM and SRHM region.
- Identify, classify and interpret the different volcanic seismic facies observed in the region.
- Integrate the results from the wide-angle modelling and interpretation into the other available geophysical (seismic reflection, gravity and magnetic) and geological (borehole and well) information from the region.
- Develop a regional geological model to explain the velocity structure of the HADES wide-angle transects.
- Define the total thickness of sedimentary strata in the Hatton Basin and document the large-scale sedimentary geometries within the basin.
- Evaluate the structural style and nature of the Hatton continental/oceanic boundary and investigate the role of underplating and asthenospheric anomalies during the breakup and post-breakup development of the margin.

This report focusses on the geological investigations being carried out in parallel with the wide-angle processing and modelling.

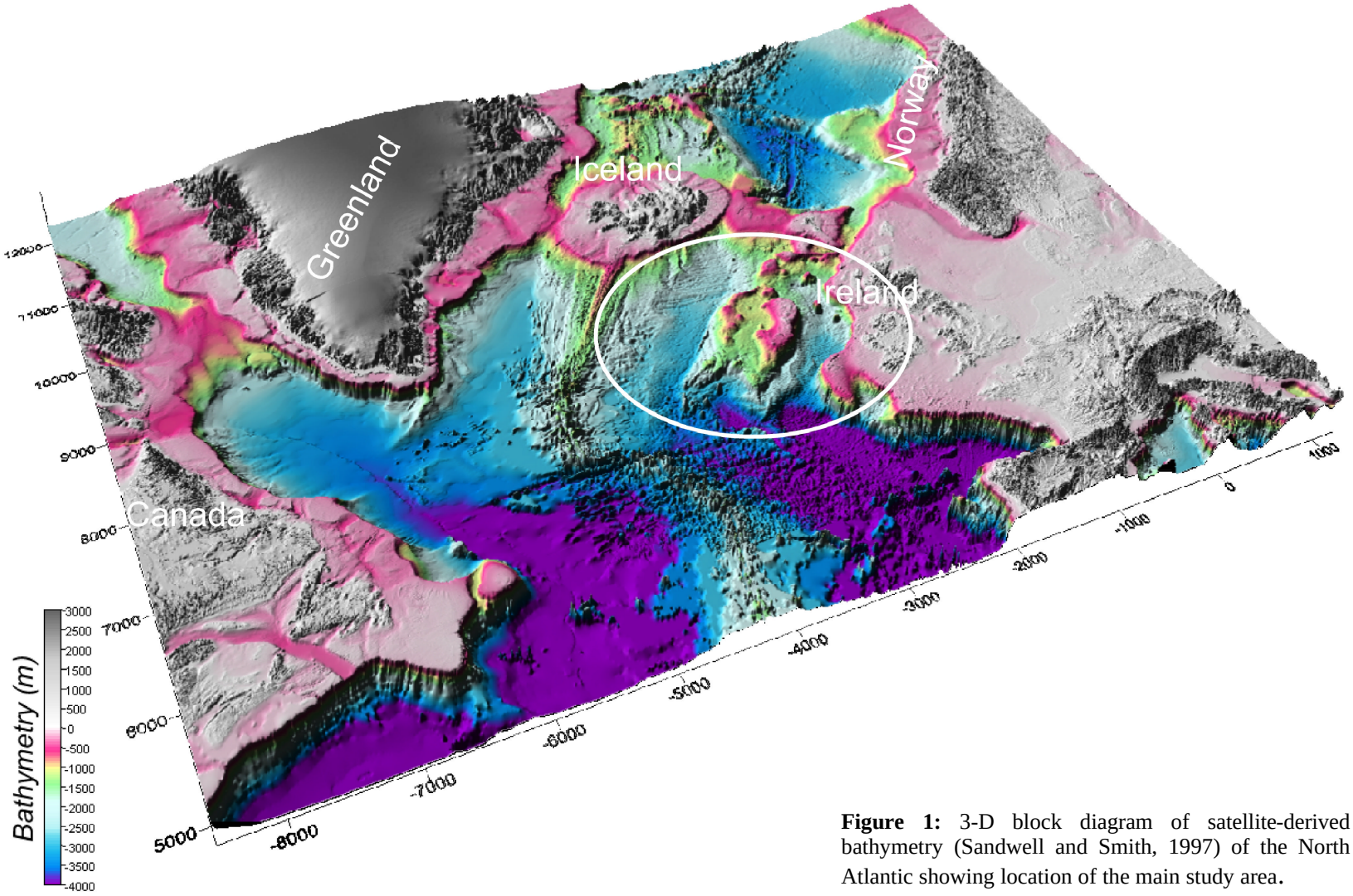

Figure 1: 3-D block diagram of satellite-derived bathymetry (Sandwell and Smith, 1997) of the North Atlantic showing location of the main study area.

1.1 Methodology

Potential field and seismic methods have an important place among the wide variety of methods in applied geophysics. In this study, potential field techniques were used intensively as complementary tools in the interpretation of the 2D seismic and wide-angle data and also to test the validity of other geophysical models. A set of potential field maps has been produced with relevant filtering to enhance the main structural change and magmatic features observed along the Irish margins.

1.2 New refraction/reflection data

For the integrated regional study, the geological investigation is based on the wide-angle seismic, potential field and seismic reflection data acquired in the Rockall/Hatton area in 1995 (PAD95 survey). The 2D reflection lines have facilitated the refinement of the structure and basin architecture from the Goban Spur to the West Hatton Margin. The HADES wide-angle and the older RAPIDS 1 and 2 crustal models were used to constrain the deep structures of the margin.

1.3 Potential field data

Available potential field datasets for the region have been compiled. The compilation includes public domain data, together with high-resolution ship-track data provided by the Geological Survey of Ireland (GSI). Satellite-derived free-air gravity data were used to constrain the structure of the basin. The data used are the 2x2 minute grid (v7.2) of satellite altimetry derived marine gravity data of Sandwell and Smith (1997). High-resolution ship-track bathymetry and gravity from the Irish National Seabed Survey were used to better refine the structure of the Hatton and Rockall basins and to constrain the gravity modelling of the HADES transects. Unfortunately, the survey does not overlap the PAD95 seismic reflection lines to the south and along the West Hatton Margin (WHM) segment.

The magnetic data were taken from a compilation of aeromagnetic and shipborne data described in detail in Verhoef et al. (1996) and Murphy (1993). The onshore data come from a compilation by Morris (1989). The compilation was initially done in a Sanston-Flamsteed projection with a cell size of 2 km. A fourth order difference filter was applied to clean the data, using a cutoff value of 1000, and no points were replaced. After this cleaning, the data were regridded to a standard 5 km Transverse Mercator grid. UTM 28 projection was used for the maps offshore Ireland and the UTM 35 projection for the maps of the North Atlantic.

1.4 Other data

Onshore topography has been included on some maps and comes from the SRTM30 dataset. SRTM30 is a near-global digital elevation model (DEM) comprising a combination of data from the Shuttle Radar Topography Mission, flown in February

2000 and the U.S. Geological Survey's GTOPO30 dataset. It can be considered to be either an SRTM data set enhanced with GTOPO30, or as an upgrade to GTOPO30. SRTM30 is a digital elevation data set that spans the globe from 60° north latitude to 56° south latitude. It has a horizontal grid spacing of 30 arc-seconds. Elevations in GTOPO30 are regularly spaced at 30-arc seconds (approximately 1 km). The GTOPO30/SRTM30 dataset is available for download from the website http://edcdaac.usgs.gov/gtopo30/gtopo30.html.

Sediment thickness data for the North Atlantic have been regridded in the standard projection in order to illustrate the main depocenters of the Irish margins and the conjugate system. K. Louden from Dalhousie University initially compiled the data (Louden et al., 2004).

A seismic tomography velocity model (100 km depth) has also been included in our compilation. It reflects the heterogeneities in the upper mantle/continental crust and the distribution of the Iceland mantle anomaly. The model values files give the percentage shear velocity deviation on a 2 by 2 degree grid at different depth levels through the Earth. We have shown the model for 100 km depth (see Appendix 1; Map 15). The grid is described in Grant et al. (1997)

Seismicity from 1973 to present is also included in the compilation even though the level of seismic activity on the Irish margin is extremely low. The data used have been downloaded from the U.S. Geological Survey website (http://neic.usgs.gov/neis/epic/epic_rect.html).

1.5 Enhancement of potential field anomalies (filtering)

Gravity and magnetic anomalies whose wavelengths are long relative to the dimensions of the geological bodies or structures in a particular investigation are called regional anomalies. Regional anomalies are usually thought to reflect the effects of relatively deep features. Anomalies whose wavelengths are similar to the dimensions of the geological bodies are called local anomalies. In processing gravity data, it is usually preferable to attempt to separate the regional and local anomalies prior to interpretation. The regional anomaly can be estimated using a variety of analytical techniques. Once this is done, the simple difference between the observed gravity anomalies and the interpreted regional anomaly is called the residual anomaly. The techniques used to separate regional and local gravity anomalies take many forms and can all be considered as filtering in a general sense (e.g. Blakely, 1996). Many of these techniques are the same as those employed in enhancing traditional remote sensing imagery.

The initial gravity and magnetic datasets were filtered in the frequency domain in order to facilitate interpretation. The initial and filtered data have been used to constrain the seismic interpretation of the PAD95 lines and to support the validity of the velocity models deduced from the wide-angle seismic modelling. The most common types of filtering carried out are as follows:

Directional filters are used to select anomalies based on their trend. In addition, a number of other specialized techniques have been employed to visually enhance anomalies.

First derivatives calculate the slope or gradient of the surface along a given direction. First derivative grid files produce contour maps that show isolines of constant slope along lines of fixed direction. This filter can be used both for gravity, magnetic fields and bathymetry. *Second derivative filters* produce contour maps that show isolines of constant rate of change of slope across the surface.

In 2-D, *a directional filter* can be use to enhance a particular direction. Directional derivatives provide information about the slope, or rate of change of slope, of the gridded surface in a specified direction. This filter was particularly useful to enhance the magnetic trends of the oceanic crust, offshore Ireland (NW-SE-oriented in the Porcupine Abyssal Plain and NE-SW-oriented in the Iceland Basin).

The *first derivative filter* also computes the vertical or horizontal rate of change in the magnetic or gravity fields. The vertical derivative of the magnetic anomaly highlights the variation of magnetic properties in the rocks of the Earth's crust, and therefore provides an indication of the composition, and the deformational and metamorphic history of the underlying rocks. Compared to the total magnetic intensity, the vertical derivative reflects sources closer to the surface. Higher vertical derivatives are generally associated with highly magnetic rocks (for example, iron-rich volcanic rocks). Lower derivatives are generally associated with non-magnetic rock). In this technique, faults and other abrupt geological discontinuities (edges) can also be detected based on the high horizontal gradients that they produce. A pronounced maximum in the gradient is interpreted as a discontinuity such as a fault. These features are easy to extract graphically to be used as an overlay on the original gravity or magnetic map. The algorithms used for the 2-D profiles are described in Gunn (1975). For the 2-D grid, we used techniques discussed by Swartz et al. (1974).

In addition to the usual *wavelength filters*, a variety of specialized filters have been used for gravity-magnetic data that include:

Upward continuation is a process that simulates the result if the survey had been conducted at a higher elevation. This process is useful to estimate the depth of anomalies.

Reduction to the pole of the magnetic total field - The shape of any magnetic anomaly depends on the inclination and declination of the main magnetic field of the Earth. Thus the same magnetic body will produce an anomaly of different shape depending on its location and orientation. The reduction to the pole filter reconstructs the magnetic field of a dataset as if it were located at the pole. This means that the data can be viewed in map form with a vertical magnetic field inclination and a declination of zero. In this way the interpretation of the data is made easier as vertical bodies will produce magnetic anomalies that are centred on the body symmetrically.

Analytic signal - The concept of the analytic signal of magnetic anomalies was developed by Nabighian (1972). The analytic signal is calculated by taking the square

root of the sum of the squares of each of the directional first derivatives of the magnetic field. The resulting shape of the analytic signal is independent of the orientation of the magnetization of the source expected to be centred above the magnetic body. This has the effect of transforming the shape of the magnetic anomaly from any magnetic inclination to one positive body centred anomaly.

1.6 Depth estimation methods

Spectral analysis can be used to analyse or to represent geophysical quantities of oscillatory nature. The Fourier transformation makes it possible to represent a set of equally spaced potential field data in the frequency domain. The mean depth, *d*, of the shallower and deeper magnetic sources can be determined, using the technique of Spector and Grant (1970), from the slope of the straight (regression) line in the logarithmic plot of the power spectrum versus the frequency (wavenumber). Estimation of source depth from this kind of analysis remains problematical with ambiguous solutions. The deepest boundary may suggest a real lithologic interface or may represent the median Curie temperature isotherm where rocks lose their ferromagnetic properties. This technique has been applied to the HADES transect P1.

2D Euler deconvolution has also been performed and combined with the preliminary results of the seismic inversion and gravity modelling. The Euler deconvolution method, published by Reid et al. (1990) serves to determine source positions and the depths of the geomagnetic inhomogeneities. The solving of Euler's equation requires horizontal and vertical gradients of the potential field data, calculated in the frequency domain. Different geological structures have characteristic "structural indices", e.g. indices from 0-1 provide the best fits for steeply dipping contacts and basin edges, whereas higher indices (2-3) provide best fits for geological features such as volcanic plugs or dykes or basement contact (see Thomson, 1982; Reid et al., 1990; Cooper, 2002). Solutions for a range of structural indices are shown where comparisons with the seismic velocity/density model can be made (see later in the report). For the Euler deconvolution, we used a code provided by Cooper et al. (2002).

The work presented in this report is focussed on a methodical study of selected profile interpretation methods (so-called semi-automated interpretation methods) in situations, which are typical in gravimetry and magnetometry. *Euler deconvolution* is useful to indicate areas of interest, which can then be modelled in greater detail. However, the method had a tendency to generate large numbers of solutions, which can be confusing. Numerous sill intrusions in the sedimentary basins offshore Ireland, and the numerous sources of magnetism locally, provide inconsistent results.

1.7 Gravity modelling

Gravity modelling was undertaken to test the preliminary results of the first break tomography inversion of the seismic data from HADES profile P1 and other regional transects of interest. In the initial modelling, we used the British Geological Survey GRAVMAG software. These gravity models were mostly undertaken to check the

validity and regional consistency of the preliminary velocity models, and also to provide and confirm a preliminary overview of the deepest structures not covered by the ray coverage. An updated version of the initial model has now been developed using GM-SYS software recently purchased by DIAS.

Gravity anomalies are calculated using a modified Talwani method of summing irregular polygons (Talwani, 1973). Polygons for Profile 1 were generated from the seismic tomography model using key iso-velocity values (3000, 4000, 5200, 6500 and 7000 ms^{-1}) as the polygon boundaries. Densities were assigned using a velocity-density function (Ludwig et al., 1970) defined by a fourth-order polynomial equation:

$$\rho = -0.6997+2.2302v - 0.598v^2+0.0703v^3 - 0.0028311v^4$$

This velocity-density function is widely accepted as a standard for sedimentary basins (Chian et al., 2001). The average density for each polygon can then be calculated from the velocity isolines. The uncertainty is estimated to be about 0.2-0.5 Mg m^{-3}.

In order to remove edge effects, the polygon model was extended for further 100 km at each end of the transect. Deeper polygons are poorly constrained by the seismic tomography model so below the 6500 ms^{-1} level. The size, shape and density of the polygons were manipulated within realistic limits to obtain good agreement between the calculated and observed free air anomalies.

2 IRISH MARGINS: REGIONAL MAPS

Magnetic and gravity data facilitate two primary types of interpretation: (1) identifying sea-floor magnetic anomalies, and (2) modelling basement structures onshore or concealed beneath the sedimentary cover. Since the seismic database is extremely sparse along the Rockall/Hatton area, the filtered magnetic data maps were particularly useful to aid location of possible fault zones, intrusion and other dyke swarms when seismic information is not available. They have also been used to refine the location and geomorphological meaning of the continental-oceanic transition along the WHM. Slope attribute maps have been used to assist with the definition of superficial structures that represent surface expressions of deeper structures.

The following section is a presentation of the compiled dataset. Together with seismic data, gravity and magnetic data can be used for a better-integrated study of the Irish margins and HADES project. Maps 1-14 extend from 1°W to 30°W and 46° N to 58°N.

These preliminary maps were extended to a regional scale (Maps 15-18) in order to better constrain the kinematic relationships of the Rockall/Hatton area with the conjugate margins in Canada and Greenland that formed a triple junction before the North Atlantic breakup. Recent published data helped to constrain the geological model of the WHM and SRHM. To the west, the results from ODP leg 152 are useful in constraining the seismic interpretation of the WHM. To the southwest, the geological evolution of the Orphan Basin has included significant tectonic subsidence during the Tethys and Atlantic rifting phases. The geological evolution of the basin is similar to that of the adjacent Jeanne d'Arc and Flemish Pass basins, and is also similar to the history of the Porcupine Basin (Sinclair et al., 1994). Prior to the final rifting episode leading to the opening of the North Atlantic, the Porcupine Basin was located immediately to the east of the Orphan Basin. The structure and tectonic history of the Orphan Basin is extremely useful in constraining the geological framework of the SRHM.

2.1 Geophysical atlas

During the project the following maps were produced (Appendix 1):

Ireland 1: Bathymetry of the Irish margins and adjacent area based on the satellite-derived bathymetry of Sandwell and Smith (1997).

Ireland 2: Bathymetric/altimetry map of the south Rockall-Hatton area and location of the PAD reflection lines wide-angle seismic transects (RAPIDS1, 2, 3, COOLE and HADES), the location of ODP/DSDP wells and other seismic sections. Also included, for information, is the location of the recent GEOMAR survey in the Porcupine Basin. The digital elevation model, onshore Ireland, is based on the SRTM30 data.

Ireland 3: Bathymetry based on the GSI high-resolution dataset from the Irish National Seabed Survey.

Ireland 4: Sediment thickness map of the Rockall/Hatton area and conjugate margin system. The map also includes an interpretation of the magnetic trends in the oceanic domain.

Ireland 5: Slope attribute map applied to bathymetry. This filter highlights the different morphological features of the margin and is extremely useful in mapping the main trends of the margin that probably represent the superficial expression of deeper structures.

Ireland 6: Free Air gravity anomaly based on the satellite derived grid (v7.2) of Sandwell and Smith (1997). The Free Air data covers virtually all the marine areas with a reasonably dense and consistent grid. This kind of map is preferred to the Bouguer anomaly map as it is free of the interpretation factors required to correct for bathymetry and crustal geometry. This map has been draped on a digital elevation model of the bathymetry in order to include the combined effect of both the bathymetry and the gravity signature.

Ireland 7: Free-Air gravity map provided by the Geological Society of Ireland (GSI). This map is very similar to that produced from the satellite-derived data of Sandwell and Smith (1997). There is, however, a significant improvement in the Porcupine area where new trends are clearly highlighted. This shipborne data has also refined some structures in the Rockall-Hatton area.

Ireland 8: First derivative of the Free-Air gravity anomaly based on the satellite derived grid (v7.2) of Sandwell and Smith (1997).

Ireland 9: Bouguer anomaly based on the GSI high-resolution Bouguer Anomaly grid. Offshore, the Bouguer correction can effectively remove gravity anomalies due to sea bottom topography.

Ireland 10: Total magnetic field based on the regional data compilation of Verhoef et al. (1996). This map has been and draped on a digital elevation model of the bathymetry in order to include the combined effects of both the bathymetry and magnetic signatures.

Ireland 11: First derivative of the total magnetic field, based on the regional data compilation of Verhoef et al. (1996).

Ireland 12: 45°E derivative of the total magnetic field, based on the regional data compilation of Verhoef et al. (1996). This map enhances NW-SW magnetic anomalies.

Ireland 13: 135°E derivative of the total magnetic field, based on the regional data compilation of Verhoef et al. (1996). This map enhances NW-SE magnetic anomalies.

Ireland 14: Total magnetic field based on the regional data compilation of Verhoef et al. (1996) overlapped by the main Free-Air gravity anomaly contours.

North Atlantic 15: Tomography of the lithosphere (100 km) (Grant et al., 1997). Low percentages of the shear velocity deviation highlight the two main mantle anomalies of the North Atlantic: 1) the Iceland mantle anomaly and 2) the Azores anomaly to the south. Areas in purple represent the North Atlantic Large Igneous Province. Shaped contours with purple dashed lines represent the high magnetic provinces offshore Canada and in the southern part of the Hatton area.

North Atlantic 16. Thickness of the North Atlantic sedimentary basins. The main volcanic and oceanic magnetic anomalies have been draped on the sedimentary thickness grid.

North Atlantic 17: Free Air gravity anomaly of the North Atlantic based on the satellite derived grid (v7.2) of Sandwell and Smith (1997).

North Atlantic 18: Total magnetic field of the North Atlantic based on the regional data compilation of Verhoef et al. (1996).

2.2 Geodynamic setting

The Irish continental rifted margin system can be divided into internal and external basin systems. The internal basin system includes the Rockall Basin, flanked by the Rockall Bank to the west, and a chain of 'perched' early Mesozoic basins to the east. The perched basins include the Erris and Slyne basins, which are separated from the Rockall Basin by the Erris Ridge. Recent seismic interpretation indicates that a similar chain of perched basins may exist along the western margin of the Rockall Basin adjacent to the Rockall Bank (Corfield et al., 1999; Naylor et al., 1999). To the southeast, the Porcupine Bank separates the Rockall Basin from the Porcupine Basin.

The external basin system of the Rockall Plateau, underlain by continental crust, marks the transition between the internal basins (e.g. the Hatton Basin) and the oceanic domain of the Iceland Basin. The Rockall Plateau includes the Rockall Bank, the Hatton Basin, the Hatton High and the West Hatton Margin (WHM). To the south, the boundary between the internal and external basin systems and the oceanic crust form a different kind of continental margin, which we define here as the South Hatton/Rockall Margin (SHRM).

Wells in the Slyne, Erris, Porcupine and Rockall basins have penetrated the Upper Palaeozoic to Recent sediments and the basement (Croker and Shannon, 1987; Naylor and Shannon, 1999; Naylor et al., 1999, 2001; Shannon et al., 2005). To the west, data tie locally with pre-existing wells of the Deep Sea Drilling Program (DSDP) legs 12, 48, 81 and 95. Legs 48 and 81 include wells 405 and 406 located in the SHRM and wells 403, 404, 502, 503, 504 and 505 drilled along the SRHM (Laughton et al., 1972, Montadert and Roberts, 1979; Roberts et al., 1979, Roberts and Schnitker, 1984; Robert et al., 1986; Jansen et al., 1986). Unfortunately, the wells do not go deeper than the Eocene and do not allow any calibration of the pre-Cenozoic successions. Hitchen

et al. (2004) published some pertinent results of shallow cores along the UK part of the Hatton Basin indicating the presence of Cretaceous and younger strata.

In the absence of extensive borehole information from the Rockall Basin, one of the most important guides to depositional environments is the rifting history and geodynamic setting of the Irish basins and margins in the North Atlantic context.

2.2.1 Permo-Triassic

There is evidence for widespread Permo-Triassic rifting in most areas on the continental margins of eastern Greenland and northwestern Europe (Coward, 1995). Permo-Triassic rifting has been proposed throughout the Irish offshore basins (e.g. Croker and Shannon, 1987; Shannon, 1994; Shannon et al., 1995; Naylor et al., 1999, 2001). The regional stress and the strong Palaeozoic and older structural inheritance of the area controlled the rift architecture (Shannon 1991). Plate tectonic reconstructions support the idea of a Triassic rifting event with extensional strain of ~1.5 (Cole and Peachey, 1999). Permo-Triassic grabens and half-grabens extend from the Scotian Shelf through into the Scotian Shelf and other Grand Banks areas of offshore eastern Canada (Shannon et al., 1995). In the Porcupine Basin, the Permo-Triassic formations have limited preservation, mostly proved in the north Porcupine Basin and penetrated beneath Carboniferous (Zechstein) formations by wells in the Slyne and Erris basins (Croker and Shannon, 1987; Tate and Dobson, 1989; Naylor et al., 2005).

2.2.2 Jurassic

Several rifting episodes occurred in the Jurassic, with a climax during Late Jurassic earliest Cretaceous time. Early Jurassic rifting, leading progressively to the breakup of the Central Atlantic has been proposed along the Iberian margin, and its Canadian conjugate (Welsink et al., 1989; Robert et al., 1999; Funck et al., 2004). Further north, an early Jurassic event was reported in the Celtic Sea (Shannon, 1991) and along the Hebrides Basin (Morton, 1989). In the Orphan Basin the first episode of rifting in this basin could be as old as late Triassic to early Jurassic, based on seismic correlation and well data in the Jeanne d'Arc Basin, creating a deep trough immediately landward of the Flemish Cap - Orphan Knoll Ridge (Enaschescu et al., 2004). Prior to the final rift episode leading to the opening of the North Atlantic, the Porcupine Basin was located immediately to the east of the Orphan Basin. Rifting along the Porcupine, Slyne and Erris basins first occurred in the Permo-Triassic and then again in the late Jurassic (Tate, 1993; Chapman et al., 1999; Dancer et al., 1999). A significant Middle Jurassic extensional event occurred in the Slyne Basin (Dancer et al., 1999) where the Middle Jurassic stratigraphy is quite well documented (Trueblood and Morton, 1991). This extensional episode is contemporaneous with similar events recorded in the North Sea and in the Halten Terrace (Norway) (Koch and Heum, 1995; Erratt et al., 1999; Blystad et al., 1995).

The Middle Jurassic marks a period of local uplift and magmatism. Uplift has been described in the central North Sea sourcing the sand-prone Brent Formation (Underhill and Partington, 1993). It has been suggested in the central part of the Vøring Basin, which was also in a structurally high position during this period (Martinius et al., 2001; Gernigon et al., 2003), while a similar uplift event is interpreted northwest of the

Porcupine Basin (Roberts et al., 1999; Johnson et al., 2001). The meaning of these isolated uplifts is still unclear and could be explained by the presence of small-scale sub-lithospheric convection cells. Such vertical movements could explain the restriction of the seaway between the Boreal and Tethyan Sea in the Middle Jurassic (Doré et al., 1999) and the anomalous sand influx observed locally along the NE Atlantic sedimentary basins.

The Late Jurassic period was characterised by a major rifting episode which affected the North Atlantic (Ziegler, 1982, 1992). It is recognised in the Central Graben, Viking Graben and Moray Firth Basin (Erratt et al., 1999). The North Sea System extends to the north into the Møre Basin and in the Haltenbanken, offshore Norway (Koch and Heum, 1995). This event also influenced the East Greenland basins (Surlyk, 1990), the outer Norwegian margin (Gernigon et al., 2003) and the Faroes-Shetland Basin. The northernmost expression of this rift system is documented in the Hammerfest Basin in the Barents Sea.

Close to the study area, the late Jurassic rifting event is interpreted from the Bay of Biscay to the Celtic Basin (Shannon, 1991; Ziegler, 1982). North-south expressions of the rift system are recorded on the Newfoundland-Iberia margins, in the Jeanne d'Arc Basin and on the conjugate Galician Bank. Further north, the Porcupine Basin developed its north-south orientation during Late-Middle to Early-Late Jurassic time, with a moderate effect on the Slyne and Erris basins (Shannon et al., 1995; Cunningham and Shannon, 1997). Thomson and McWilliam (2001) also presented evidence for late Jurassic rifting in the Bróna Basin in the eastern flank of the Rockall Basin.

A second rifting phase occurred in the late Jurassic to early Cretaceous in the Orphan Basin. Deformation is recorded essentially in the eastern part of the West Orphan Basin (Enaschesu et al., 2004) but the oldest sediment appears to be early Cretaceous in age.

2.2.3 Cretaceous

Early Cretaceous extension is commonly interpreted as a different extensional event and represents a significant geodynamic change in the evolution of the North Atlantic rifted basins (Doré et al., 1999). This event marks the end of the rift activity in the North Sea and the development of a new NE-SW oriented rift axis lying from the South Rockall to Lofoten basins in Norway, and to the Tromsø and Bjørnøya basins in the Barents Sea. At the same time, a NW-SE oriented axis develops from the Iberia-Newfoundland margins to the future Labrador Sea. In the Faroes-Shetland Basin, Dean et al. (1999) constrained major syn-rift expansion along NE-SW trending faults to the Valanginian-Barremian interval.

The Rockall-Hatton area, to the south, was affected during this period by a regionally growing extensional phase leading to the opening of the Bay of Biscay and the Porcupine Abyssal Plain, usually identified by the Early Campanian C34 magnetic chron (~80 Ma). Due to the magnetic quiet period, magnetic trends older that C34 are not clearly evidenced from the Goban Spur to the SRHM. Plate kinematic investigations suggest that the breakup could have been initiated in Barremo-Aptian

time (M0, 118 Ma) (Figure 3) in the Bay of Biscay area (Sibuet et al., 2004). Upper mantle exhumation and the first evidence of oceanic accretion during Barremo-Aptian time was also proposed on the margin of the South American plate, where a probable peridotite ridge is imaged (Thinon et al., 2003). Further north, rifting started during Neocomian to late Aptian time and the breakup was initiated during the late Aptian to early Albian (Montadert and Roberts, 1979; de Graciancy et al., 1985). The main evidence of the breakup along the Goban Spur is the recovery of depleted tholeiitic pillow lavas drilled by DSDP well 500. Due to rock alteration, K/Ar failed to give a reliable age of emplacement but a late Albian age for the oldest sediments above the basalt has been proposed on the basis of palaeontological data.

There are two schools of thought concerning the history of rifting in the Rockall Basin. The first considers that the basin formed entirely by rifting during the Cretaceous (e.g. Musgrove and Mitchener, 1996), while the second considers that Cretaceous rifting was preceded by rifting during the Triassic and/or Jurassic (e.g. Shannon et al. 1995, 1999; Naylor et al., 1999). Both events may have affected the internal and the external basin systems. Given a history of Triassic/Jurassic rifting, it is likely that the Rockall Basin (or part of the Rockall Basin) was already a depocentre by earliest Cretaceous times.

Recent shallow drilling by BGS penetrated rotated Albian siliciclastics sequences suggestive of an early to mid-Cretaceous rifting event along the Hatton Basin. There is no information about the sand provenance, but a source in Greenland could be possible. Some of the sediment supplied from east Greenland during the Cretaceous would have accumulated in the Hatton Basin and along the proto-WHVM and possibly may have sourced part of the SRHM evolving south of the external system. An analogue for this scenario is the Norwegian margin, where well-constrained investigations of the outer Vøring Basin show that a huge amount of Cretaceous sands could be sourced from the Greenland mainland and reach the deep Vøring Basin (Kitilsen et al., 1999). Reworked Carboniferous, Jurassic and Cretaceous polymorphs have been recorded in Eocene sediments drilled on the eastern flank of Rockall Bank. It suggests the availability of local Palaeozoic and Mesozoic rocks in the area.

Offshore Labrador, syn-rift extension occurred between Barremian to Lower Campanian times (Balkwill et al., 1990). In the Hopedale Basin, Cretaceous extension started with the onset of a regional volcanic event characterised by the Alexis Formation (Barremo-Aptian in age). This extension episode was still active during Aptian-Aptian (Bjarni Formation) and the Mid(?) Albian-Campanian period (Markland Formation) (Balkwill et al., 1990).

A Late Cretaceous phase of extension leading to the breakup in Late Palaeocene-Early Eocene time is now well recognised in the North Atlantic (Doré et al., 1999). In Norway, this episode started in Early Campanian time but was not necessarily synchronous along the margin segments (Gernigon et al., 2003). The Late Cretaceous period coincides with the (a) the opening of the Labrador Sea (Roest and Srivastava, 1989; Chalmer and Pulvetaft, 2001); (b) the onset of the Alpine Orogeny (Ziegler, 1990); (c) the onset of the Eurekan Orogeny and (d) the impact of the Iceland mantle anomaly (White and McKenzie, 1989; Lawver and Müller, 1994; Nadin et al., 1997). During this period the onset of formation of the oceanic crust in the Labrador Sea,

lying in the trend of the SRHM, is however still controversial. Older models proposed that sea-floor spreading occurred in the Labrador Sea at chron 34 in Late Cretaceous time (Roest and Srivastava, 1989), but recent models suggest opening in the Palaeocene (Geoffroy et al., 2001; Chalmers and Pulverstaft, 2001).

2.2.4 Palaeocene

During the early Palaeocene, breakup was initiated in the Porcupine Abyssal Plain. In the Labrador Sea, a recent review (Chalmers and Pulverstaft, 2001) has suggested that the breakup did not start until C27 (Mid-Palaeocene) and stopped in Oligocene times at chron 13. In the Baffin Bay, the nature and age of the oceanic crust is controversial due to a disturbed magnetic pattern (Geoffroy et al., 2001). Sea floor spreading in Baffin Bay is assumed to have started at chron C27 (Chalmers and Pulverstaft, 2001) or chron 24 (Jackson et al., 1979). Activation of left-lateral strike slip displacement in the area of Nare Strait and Judge Daly is linked to coeval sea-floor spreading in Baffin Bay and the Nansen Gakkel Ridge. Assuming a connection between the two spreading systems, breakup in Baffin Bay should start between chron 25 and 21 (Saalmann et al., 2005). Sea floor spreading rates in Labrador slowed down substantially after chron C24, whereas spreading continued and increased along the WHM-Norwegian axis (Figure 2).

By analogy with other basins of the northeast Atlantic rifted system, a Late Cretaceous rifting event is also proposed here along the WHM. This rifting phase would have led to the breakup from the WHM to the Lofoten Margin in Late Palaeocene-Early Eocene time (C24, ~54 Ma). This last event was influenced by a significant volcanic event leading to the formation of the North Atlantic Igneous Province (NAIP). Following White et al. (1987) and White (1988) most workers interpret the early Palaeogene volcanism of the NAIP in terms of lithospheric impingement of the proto-Iceland ‘mantle plume’, referred to here as the Iceland ‘mantle anomaly’. There are a wide variety of ideas on the size, morphology and existence of the plume exist, from a single point (Lawver and Müller, 1994) to continental-scale mantle anomaly acting simultaneously on areas separated by some 2000 km (Smallwood and White, 2002). NAIP magmatism is usually divided into two phases (Saunders et al., 1997):

- A Middle Palaeocene phase (62-58 Ma) continent-based magmatism in Britain and West Greenland, and
- A second event in Late Palaeocene-Early Eocene (c. 56-53 Ma) leading to significant magmatism along the North Atlantic volcanic margins.

The Rockall Basin, like the Faroe-Shetland, Møre and Vøring basins, lies beneath several kilometres of water because the total volume of sediment supplied to the basin, especially during the Late Palaeogene and Neogene, was much less than the accommodation space created by differential subsidence. The geology of the Palaeogene to Neogene formations is summarised by Stoker et al. (2005).

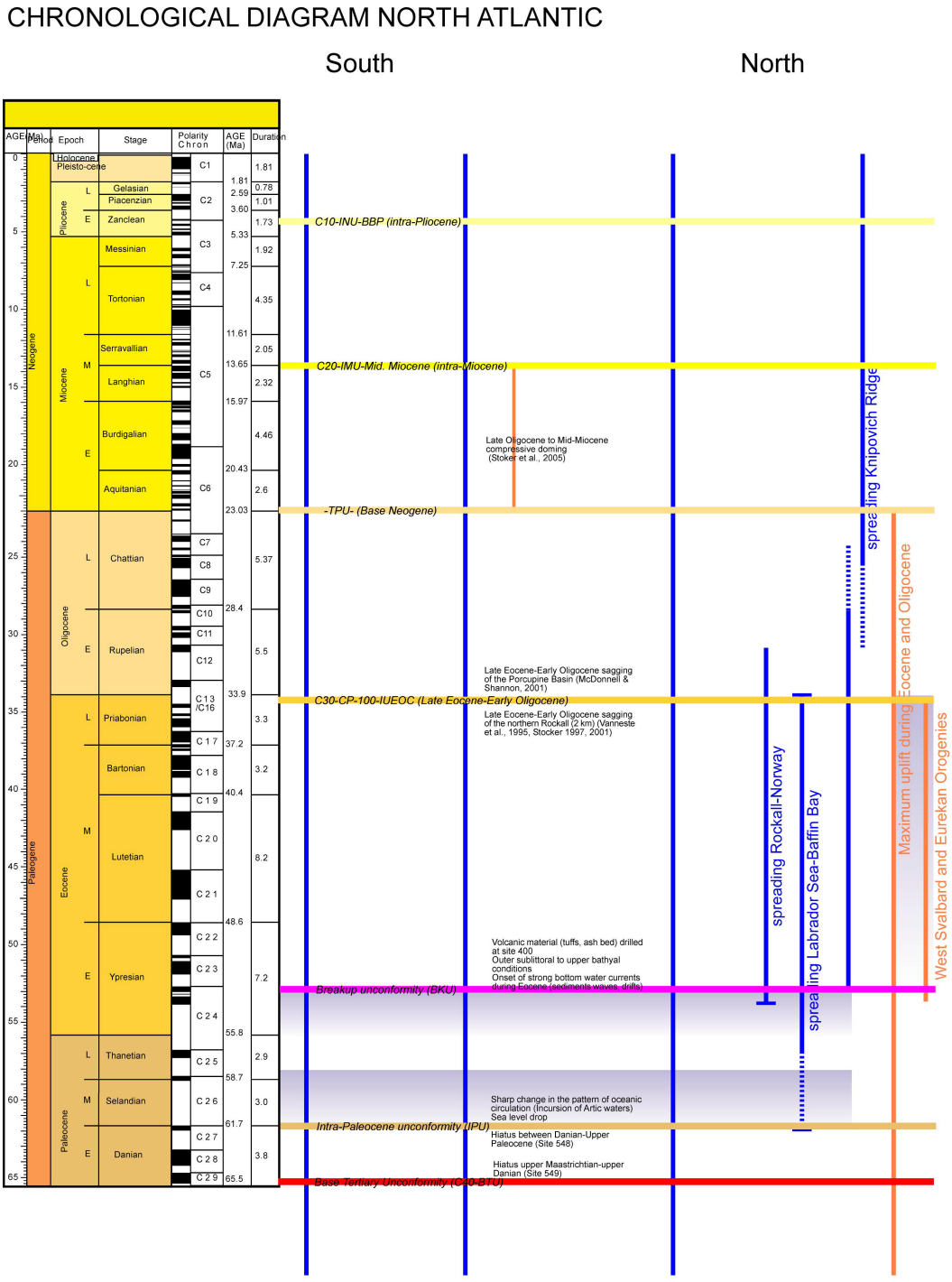

Figure 2: Tectonic calendar of the Irish Margin/North Atlantic area (continued on next page).

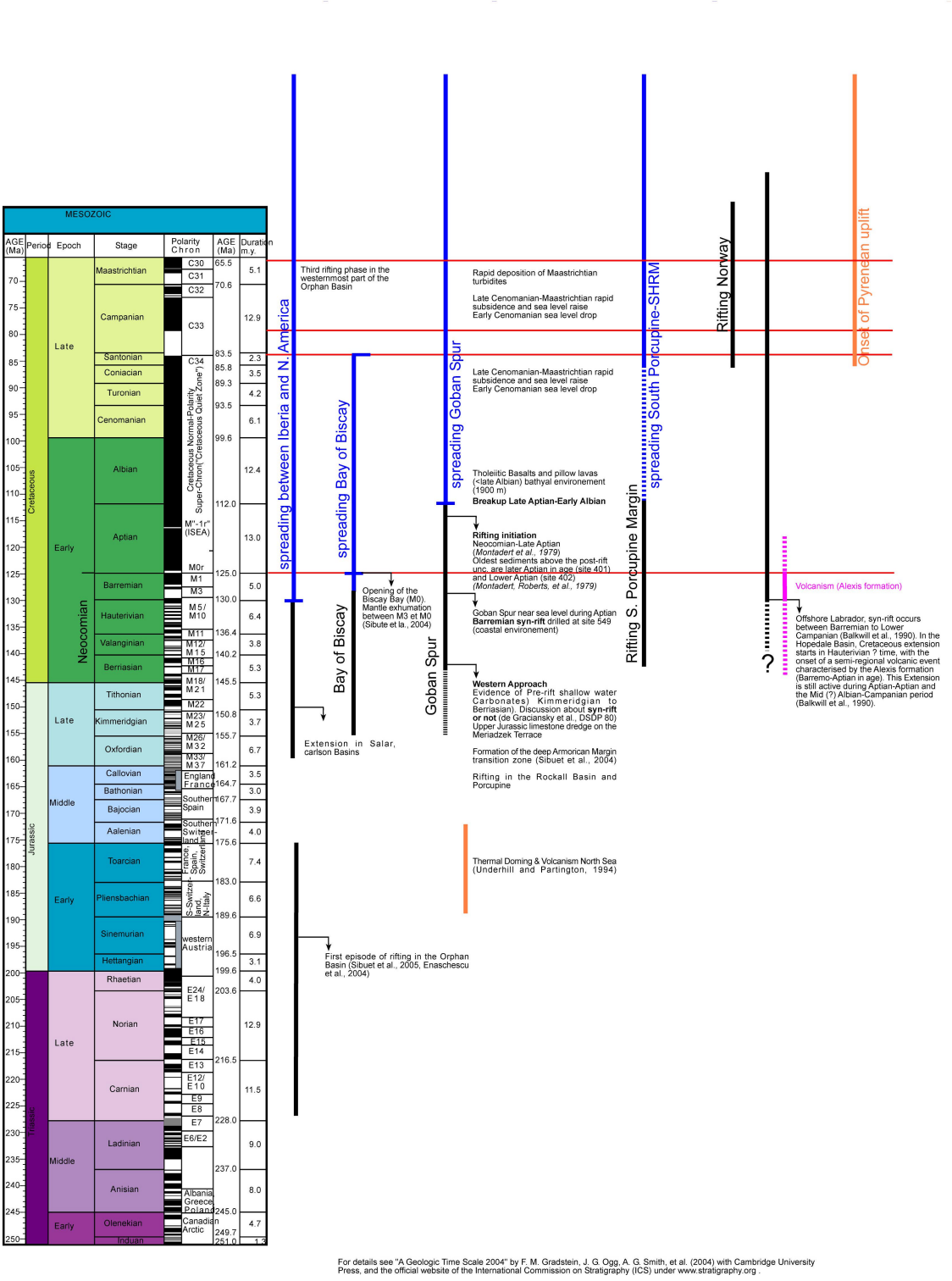

Figure 2: Tectonic calendar of the Irish Margin/North Atlantic area (continued from previous page).

3 STRUCTURE OF THE IRISH MARGINS

Integration of new seismic, potential field and well calibration data has facilitated the clarification of the structure and stratigraphy of the both West Hatton Margin (WHM) and the South Rockall/Hatton Margin (SRHM). Seismic sequences, on all the new PAD lines, were identified and line-drawing interpretations were completed for all the sections. Some of the sections have been calibrated with results from DSDP wells but some uncertainties exist due to the small number of wells and the complexity of the area. The interpretation underlines the contrasting style of the margins' segments that probably interacted with each other during the late Cretaceous.

3.1 Southern Rockall - West Porcupine Bank

The South Rockall - West Porcupine Bank segment is slightly different from the structure of a conventional non-volcanic passive continental margin like the Goban Spur or the Galician Margin. This margin segment characterises a 45°E oblique continental-oceanic transition between a crust extremely thinned (e.g. the Rockall Basin), and the oceanic crust (the Porcupine Abyssal Plain). During Jurassic to Early Cretaceous times, this area was probably a rift triple junction (R-R-R) formed by the Rockall Basin (N10ºE - N20ºE), the rift system stretching from the Goban Spur to the West Porcupine Bank (N100ºE - N120ºE) and a rift axis lay in the SRHM. It is likely that the Rockall Basin formed an aulacogen soon after the break-up of the Porcupine Abyssal Plain before Campanian time (C34), due to all the stress probably being focussed along the oceanic spreading axis. However, some reactivation along the main border faults of the Rockall Basin is expected in late Cretaceous and Palaeocene times.

3.1.1 Rockall Basin

The Rockall Basin has been a focus of geological and geophysical investigations for more than three decades since pioneering work of Scrutton and Roberts (1971) and Roberts (1975). Recent work suggests a sedimentary succession of Palaeozoic to Cenozoic sediments in the region of up to 7 km thick, overlying an extremely thin continental crust and serpentinized upper mantle (Shannon et al., 1994, 1995, 1999; Hauser et al., 1995; O'Reilly et al., 1996; Mackenzie et al., 2002; Morewood et al., 2004). The GSR96-0116 seismic profile (Figure 4) is a key regional line to illustrate the structure of the Rockall Basin. It also stretches along the RAPIDS3 wide-angle seismic Profile 33 of Mackenzie et al. (2002) and our gravity model based on the previous velocity model.

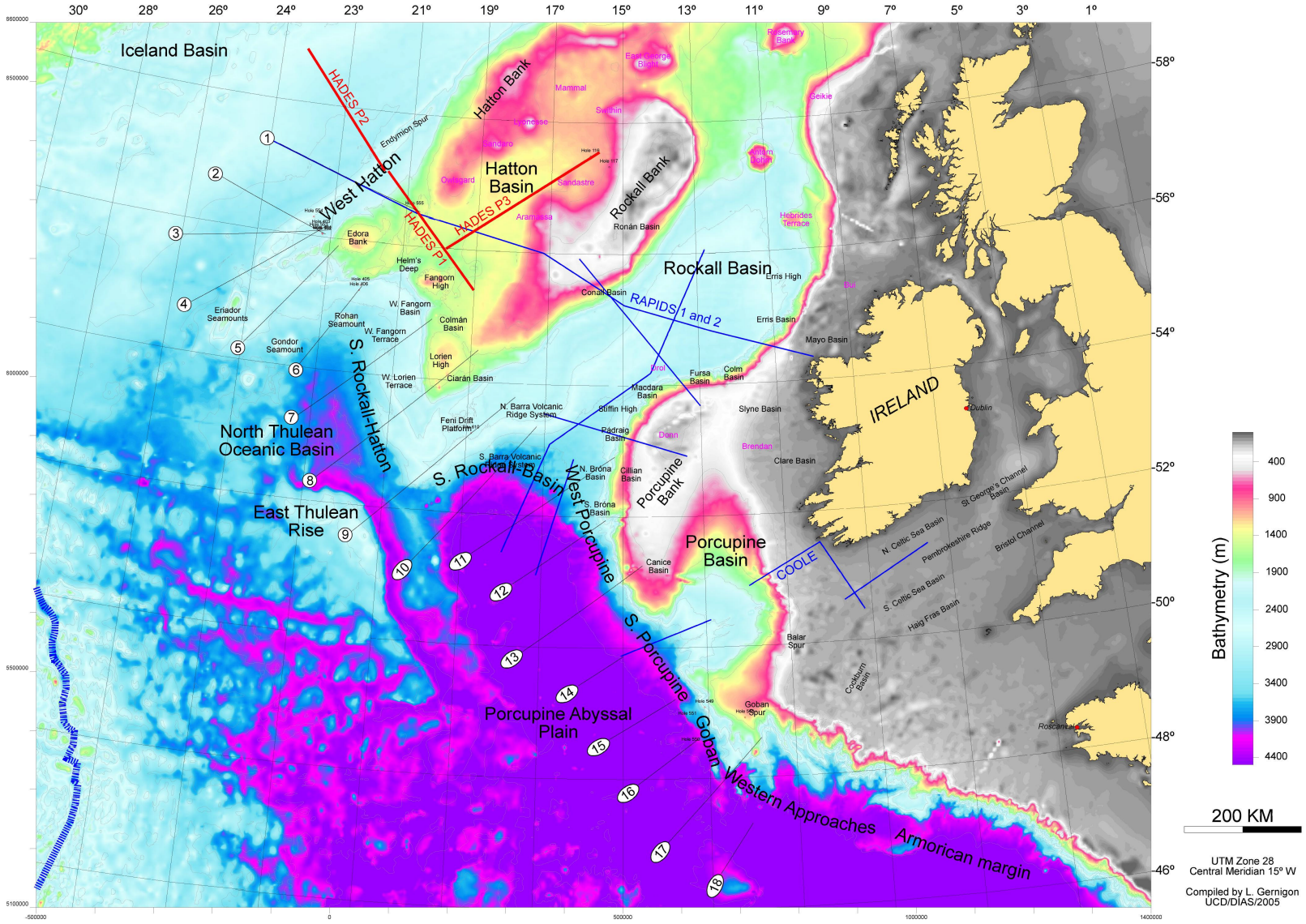

Figure 3: Bathymetry map of the Hatton-Rockall-Porcupine area showing the location of the Southern Rockall - West Porcupine Bank (section 3.1), the South Rockall Hatton Margin (section 3.2) and the Hatton Basin and West Hatton Margin (section 3.3). Bathymetry is the satellite-derived bathymetry of Sandwell and Smith (1997). The HADES wide-angle seismic profiles are shown as red lines and the RAPIDS 1-3 and COOLE profiles as blue lines. The PAD95 seismic reflection profiles are shown as the numbered black lines.

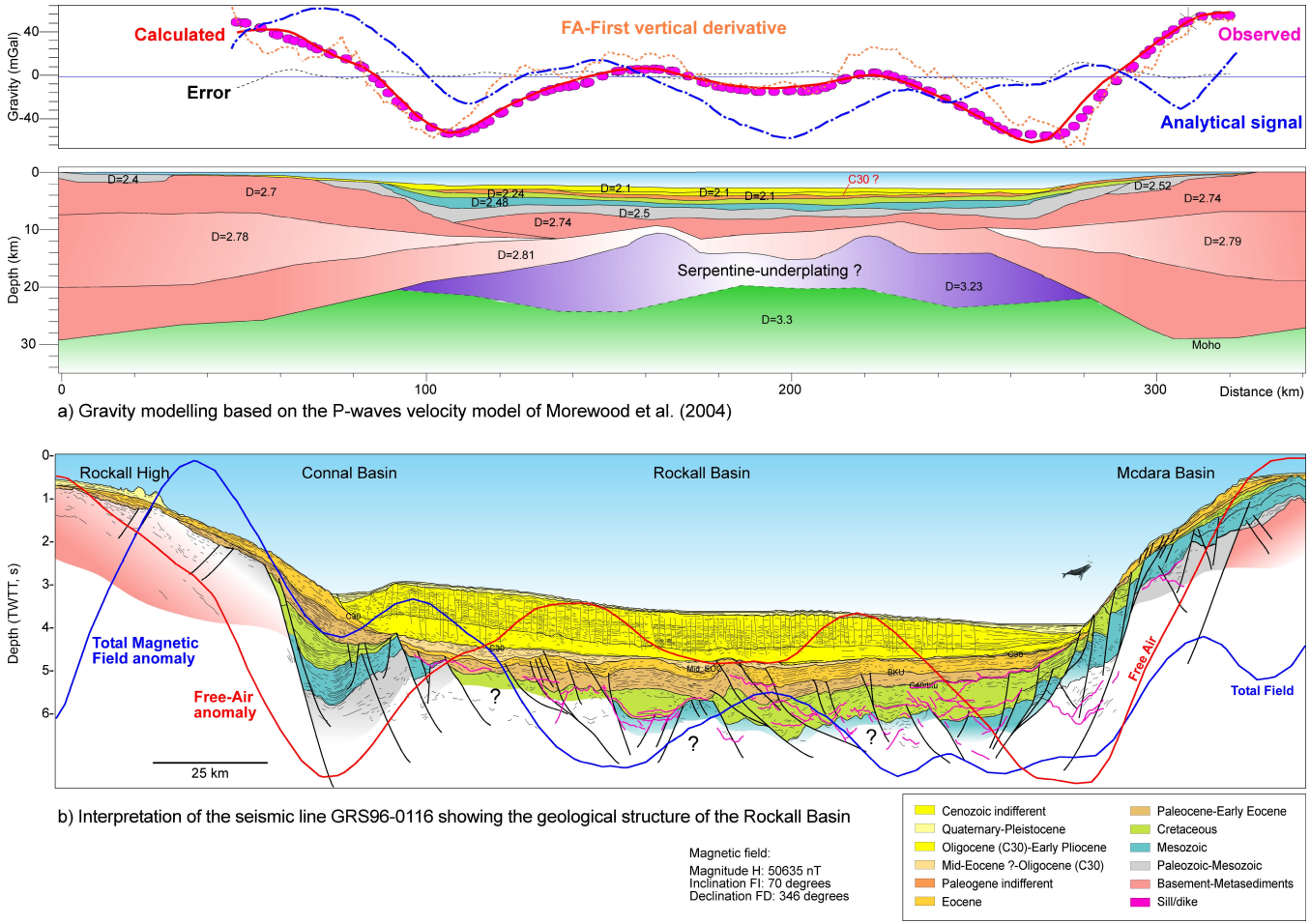

Figure 4: (a) Gravity modelling based on the P-wave velocity model of Morewood et al. (2004). Upper curves show the observed Free-Air anomaly (magenta dots), calculated anomaly (red line), first vertical derivative (dotted sand-colour line) and the analytic signal (blue line). See also Figure 5 for more details. (b) Interpretation of the seismic line GRS96-0116 across the Rockall Basin with geological interpretation. Also shown are the Free-Air gravity anomaly (red line) and the total magnetic field (blue line). See text for details.

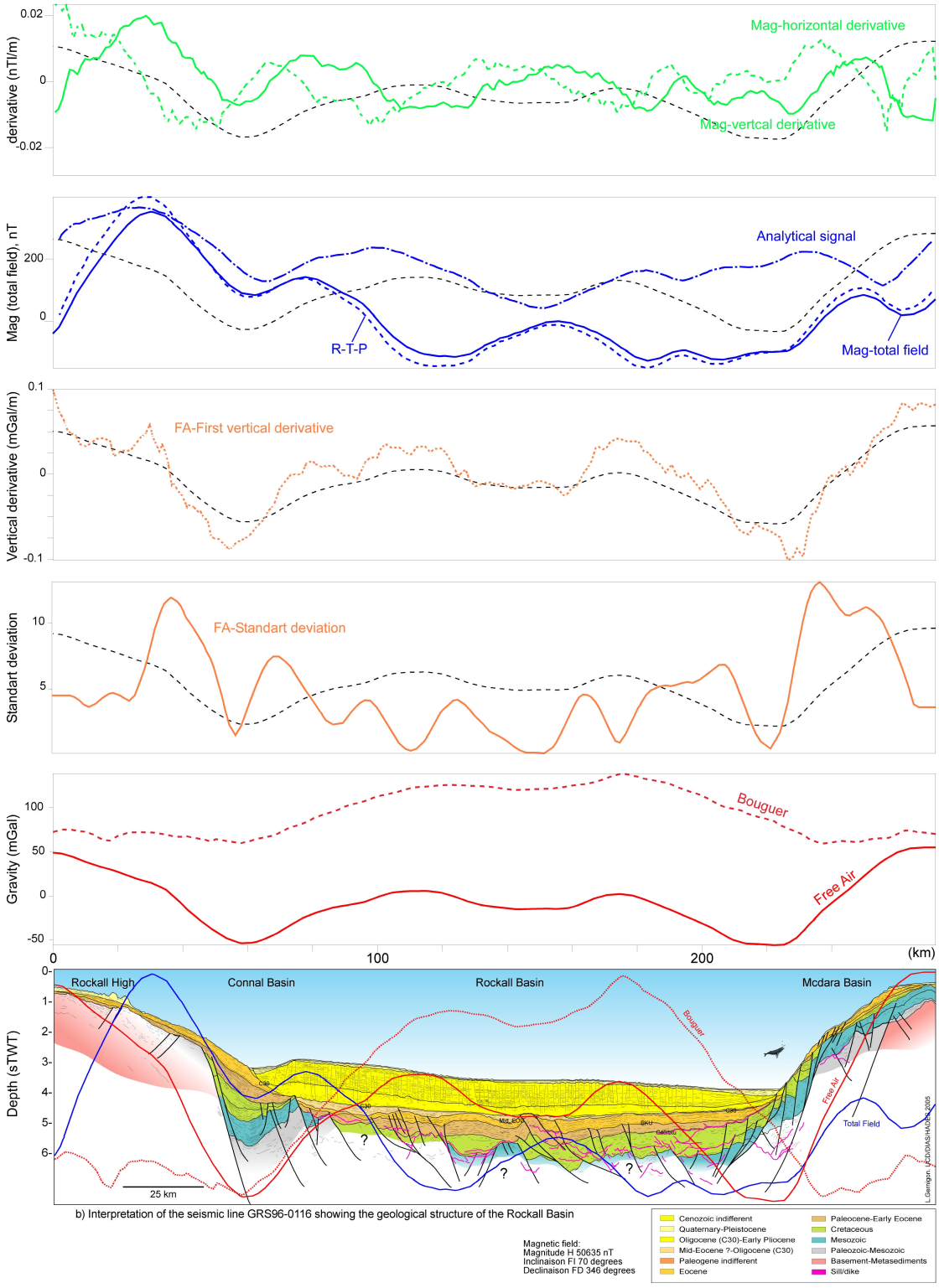

Figure 5: Geological transects and gravity magnetic signatures and filtering across the Rockall Basin along the GRS96-0116 seismic line.

Seismic reflection profiles clearly show that the Rockall Basin is a complex faulted system onlapped by thick Palaeogene-Neogene formations. For the most updated description and discussion of the Neogene succession and tectonics the reader is referred to the recent reviews by Praeg et al. (2005) and Stoker et al. (2005a, 2000b). Along the eastern and western flanks of the Rockall Basin, isolated and perched basins are clearly imaged on reflection data (Shannon et al., 1999; Corfield et al., 1999; Naylor et al., 1999; Walsh et al., 1999). In a regional context, the rotated fault block in the western part of the Rockall Basin is expected to be Permo-Triassic to Jurassic in age, similar to the nearby Slyne, Erris and Porcupine Basins (Corfield et al., 1999). The pre-Neogene strata and age of the syn-rift succession on the eastern flank of the Rockall Basin are poorly constrained, due largely to the lack of deep well data and regional seismic profiles in the Irish sector. Also, as observed on the GRS96-0116 profile (Figures 5 and 5), the deep (pre-Cenozoic) part of the basin is severely masked by the effects of sills and dykes.

Well 132/15-1, close to the Hebrides Terrace seamount penetrated Tertiary and bottomed in Albian strata, resting on granitic basement (Corfield et al., 1999; Musgrove and Mitchener, 1996). Well 164/7-1 to the north penetrated Late and Middle Eocene marine siltstones and Albian to Cenomano-Coniacian claystones beneath Palaeocene volcanics (Archer et al., 2005). Assuming that the Rockall Trough was already a significant depocenter before the Cretaceous, it is expected that the Mesozoic successions should thicken basin-wards. Therefore, Jurassic and probable Permo-Triassic sediments can be expected in parts of the Rockall Basin.

The RAPIDS 2 and RAPIDS 3 data provided new information about the deeper parts of the Rockall Basin (Shannon et al., 1994; Hauser, 1995; Mackenzie et al., 2002; Morewood et al., 2004, 2005). The models indicate that the sedimentary succession in the Rockall basin is typically 4.5 km thick and could be up to 7 km thick. Three main velocity packages have been proposed: (1) an upper package (1.8-3.1 km/s) with thickness of 1-1.5 km, interpreted to be Oligocene to Neogene in age; (2) a middle package (2.3-3.4 km/s) with a combined thickness of ca 1.5 km, interpreted as Cretaceous to early Cenozoic age; (3) a regionally extensive package (3.6-5.2 km/s), up to 4 km thick and interpreted as Palaeozoic to Jurassic in age.

3.1.2 Barra Volcanic Ridge System (BVRS)

Gravity and magnetic signatures of the Rockall Basin suggests that the structure of the Rockall Basin is quite homogeneous in the central part. A slight asymmetry is suggested between the western and the eastern margins of the basin, where the Feni Drift developed and forms a shallow marine province overlying a Palaeozoic to Mesozoic terrace. Gravity and magnetic signatures show that the geophysical pattern is more complex than in the central and northern parts of the basin. A system of ridges, the Barra Volcanic Ridge System (BVRS) (Bentley and Scutton, 1987), is observed and correlates with N10°E to N135°E magnetic trends, stretching from the Charlie-Gibbs Fracture Zone northwards to the Rockall-Hatton Plateau. Gravity and magnetic signatures suggest that the BVRS is different in the south compared to the north. To the north the total magnetic field anomalies are higher and the system is expressed as a single gravity high that is not observed to the south. The transition between the north

and south BVRS is also characterised by a sharp bathymetric change along a NE-SW lineament, defined as the Porcupine-Barra slope lineament in the following discussion.

Scrutton and Bentley (1988) noted the strong similarity between the trend of the ridges and the NW-SE magnetic lineation associated with the C34 anomaly (Early Campanian in age). They suggested that the BVRS coincides with seismic ridges that they interpreted as massive volcanic and magmatic features formed during the spreading of the Porcupine Abyssal Plain.

The PAD95-09 seismic line (Figure 7) provides a new look at the northern part of the BVRS. On line PAD 95-08, the top of the ridge is characterised by a high-amplitude surface, locally eroded, which delimits the top of a well-layered seismic package in the Feni Drift platform. Locally volcanic vent features are observed and are connected deeper with contemporaneous magmatic sills, intruding the lower packages. Usually vents are contemporaneous with the sills emplacement inside the sedimentary basin, as demonstrated in the Vøring Basin by Planke et al. (2005). This surface is interpreted to be late Palaeocene - Early Eocene in age. It is suggested that the main sill complex and the related vents are Palaeogene in age. The seismic package underlying this Early Cenozoic horizon pinches out onto the ridge to the north. At the end of the PAD 95-09 seismic line, well-layered sequences are also observed but are not clearly observed along the ridge. Sub-basalt imaging problems, related to local lava flows emplaced on top of the ridge, could also explain this. The transparent seismic facies observed beneath the lava do not necessarily represent a massive intrusion, but are probably due to the effects of seismic masking beneath basaltic layers. Layering, and some wedges intruded by sills and dykes are better observed locally along lava-free windows. The ridge may represent a sedimentary (?) horst affected by the magmatic injections and probably interbedded with mid to Late Cretaceous volcanics, which may explain the deep and high-amplitude reflection imaged beneath the sill complex to the south. According to our interpretation, the ridge was in a structurally high position during Cretaceous time and may represent the southern flank of a continental rift propagator. The close similarities with the oceanic magnetic lineations suggests that the ridge was likely uplifted and faulted during the onset of oceanic spreading in the Porcupine Abyssal Plain in mid-Cretaceous time (e.g. Corfield et al., 1999). It is suggested that the BVRS initiated before Campanian time but after the breakup of the Goban Spur in Aptian - Early Albian time.

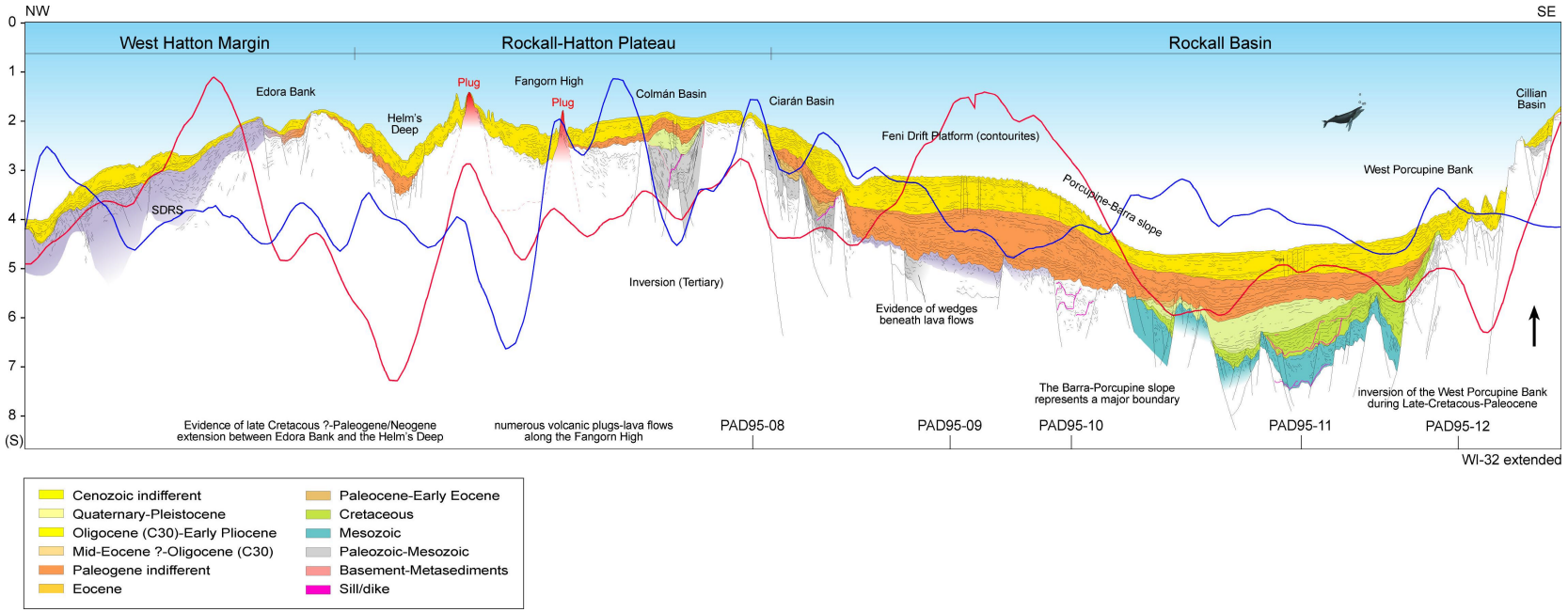

Figure 6: Geological transect from the Porcupine Bank to the West Hatton Margin crossing the southern part of the Hatton Basin.

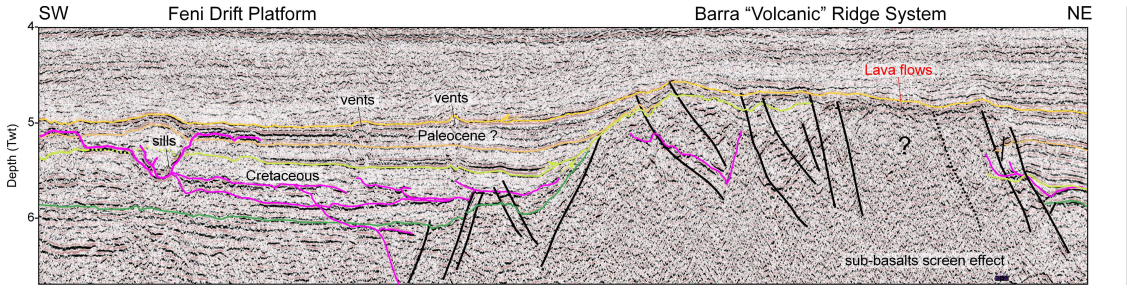

Figure 7: Seismic section across the Barra Ridge (northern part of the PAD95-09 line).

3.1.3 West Porcupine Bank Basin (WPBB)

East of the BVRS, the West Porcupine Bank Basin (WPPB) is defined in the western part of the Porcupine Bank. It represents a transition between the central Rockall Basin and the Charlie-Gibbs Fracture Zone / Clare Lineament to the south. With the BVRS, it forms the South Rockall Basin. To the north, the WPBB in bounded by the Porcupine Bank - Barra Lineament. Gravity and magnetic maps suggest a N-S axis for this basin, different from the NW-SE trends observed in the Porcupine Abyssal Plain and the NW-SE trends observed in the central part of the Rockall Basin. This structural setting is quite similar to the transition between the Viking Graben and the Møre Basin via the Møre-Trondelag Fault Zone in Norway. A transfer zone could be expected between the WPBB and the central Rockall.

To the southwest the continental/oceanic boundary between the WPBB and the Porcupine Abyssal Plain is highlighted by the C34 and C33 magnetic anomalies. However, 40 km northeast of C34, a N-S oriented magnetic anomaly is also identified (tentatively interpreted as M0). It may represent pre-Campanian oceanic crust or a highly magnetic transitional crust (continental). This transition zone is characterised by basement horsts and narrow grabens (10 km wide), smaller than both those observed in the oceanic crust and along the WPBB itself. Along the transition zone, the strong chaotic reflections observed in the deeper part of the WPBB at around 7-9 s TWTT disappear. These deep reflections may represent lower crustal or upper mantle fabrics.

The PAD95-09 profile (Figure 7) clearly illustrates the structural and sedimentary architecture of the WPBB. It is characterised by wide faulted panels (25-30 km wide) and half-grabens controlled by west-dipping normal faults. Syn-rift sequences have been interpreted as Early to Late Cretaceous sediments and post-rift formations represented by the Palaeogene-Neogene units. A migration of the deformation and active faulting to the south can also be observed on the PAD95-09 line. Older Mesozoic or Palaeozoic structures could be present in the deeper wedges observed in the basin.

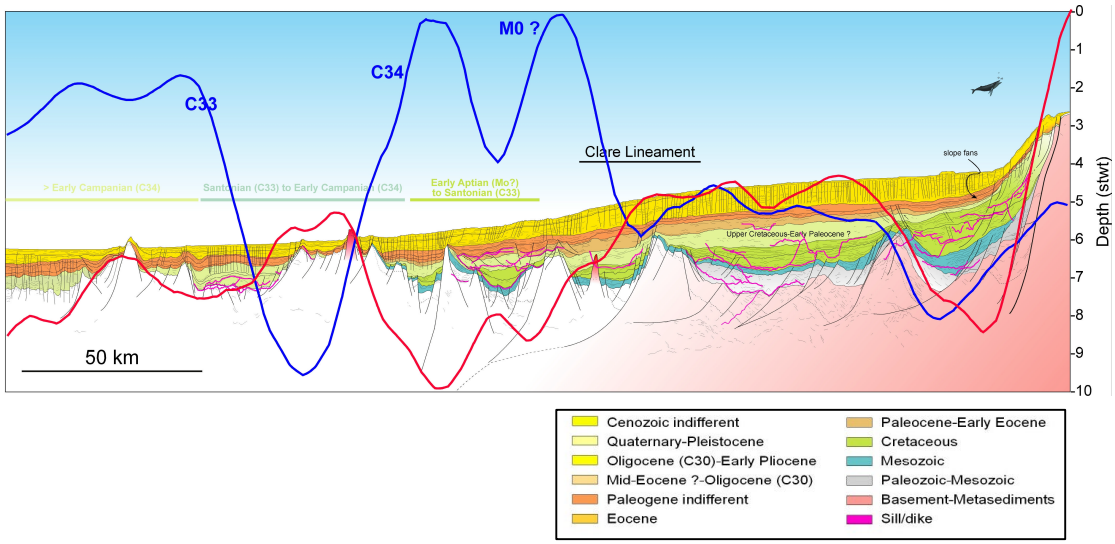

Figure 8: West Porcupine Bank and margin. Geological transect from the Porcupine Bank to the Porcupine Abyssal Plain (PAD95-11 line).

Close to the Porcupine Bank, slope fans and lensoid features have been identified and represent probably Palaeocene to Eocene formations emplaced during the regional uplift of the Porcupine Bank at this time. Numerous intrusions can be observed. Sills and dykes intruded the Cretaceous - Early Eocene sequences. Along the Clare Lineament, magmatic plugs can also be observed to have intruded the Cretaceous succession.

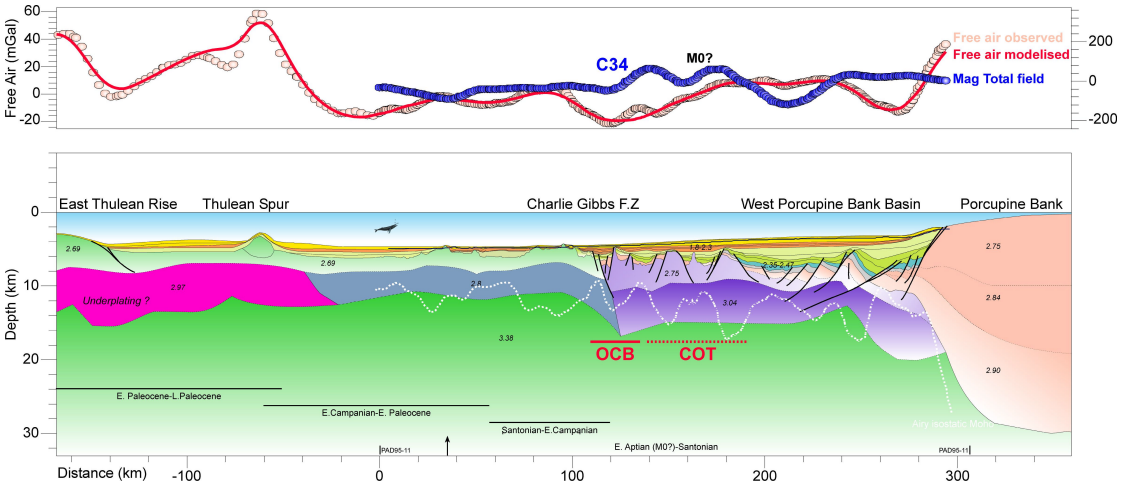

Figure 9: Crustal transect and gravity modelling from the Porcupine Bank (PAD95-11) to the East Thulean Rise, extended southwards using bathymetry from Sandwell and Smith (1997) and the sedimentary thickness map (Map 4). See also Figure 10.

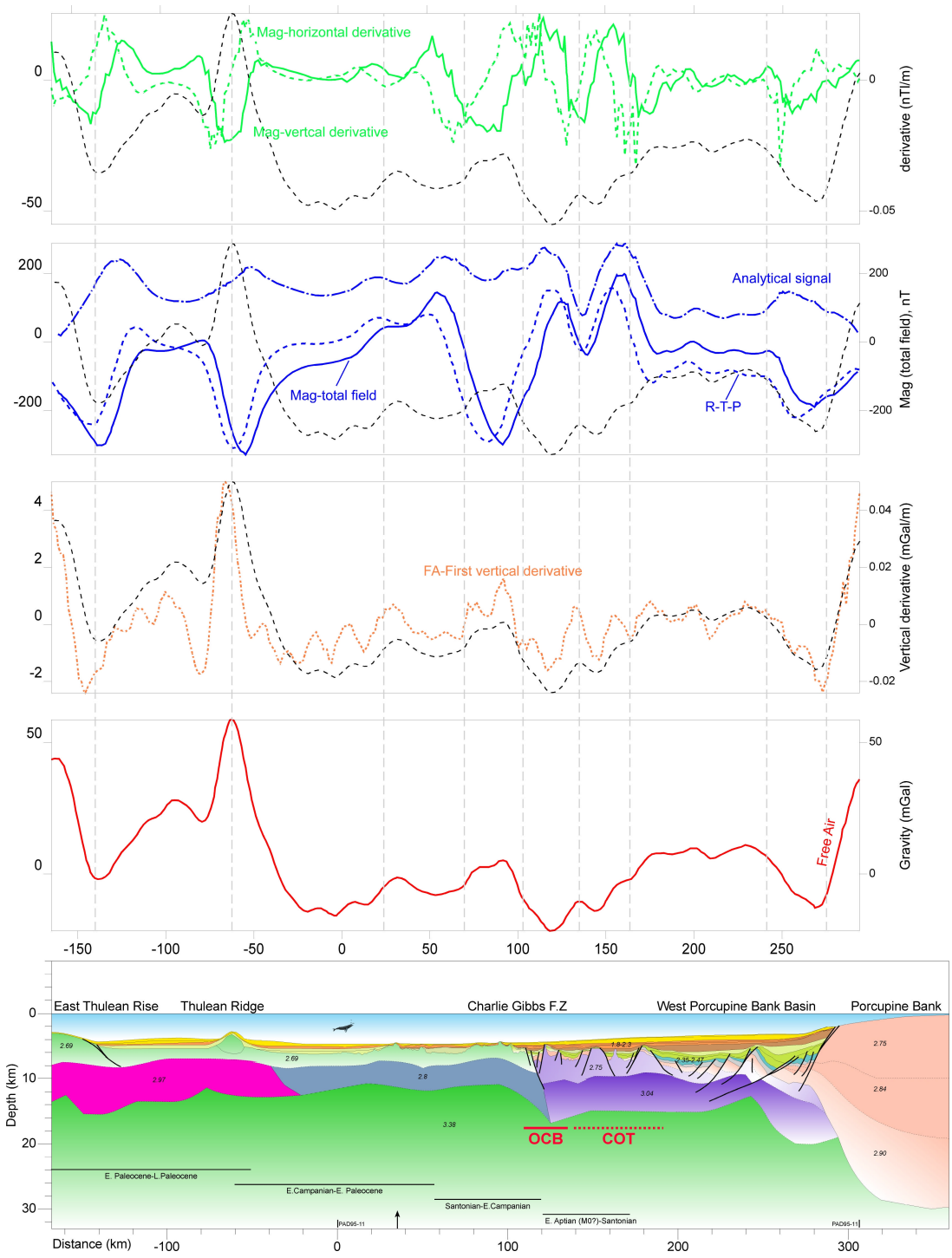

Figure 10: Crustal transect, potential field curves and filtering from the Porcupine Bank to the East Thulean Rise. Gravity and magnetic data are from Sandwell and Smith (1997) and Verhoef et al. (1996), respectively.

3.2 South Rockall Hatton Margin (SRHM)

3.2.1 Structure and stratigraphy

The southern Rockall-Hatton plateau has traditionally been considered to be a combination of a rifted and shear-rifted margin (Robert et al., 1979). We have defined the South Rockall Hatton Margin (SRHM) as the rifted segment lying from the Charlie-Gibbs Fracture Zone to the Edoras Bank between 52°N and 56°N.

Magnetic data show this area to be bounded to the west by the oceanic crust of the Iceland Basin formed after the C24 magnetic chron. As presented on the regional maps, the Iceland Basin is characterised by a distinctive sequence of linear magnetic anomalies continuing westwards toward the present day spreading axis (the Reykjanes Ridge). Chron C24 can be traced to the south until offset by the CGFZ. North of the Charlie-Gibbs Fracture Zone, another clear magnetic trend is indicated by chrons C34 and C33 (Robert et al., 1985). West of the Lorien High, these anomalies are clearly observed but, as suggested by Bull and Masson (1996), the northern prolongation of this anomaly south of the Edora Bank is more controversial because the linearity is not so obvious. West of C34, the Cretaceous oceanic crust was later intersected by the Cenozoic oceanic spreading centre (represented by C24). We refer to the oceanic fragment between C34 and C33, lying also between the Charlie-Gibbs Fracture Zone and the South Edora Transform Zone, as the North Thulean Oceanic Basin.

The South Edora Transform Zone (SETZ) marks a significant bathymetric change and a significant slope limit, south of the Edora Bank. The SETZ is characterised by a steep contrast between low free-air gravity anomalies (less than –30 mGal) and the dominant gravity anomaly observed along the Edora Bank (see Figures 11 and 12). This low anomaly extends NW-SE from the Eriador seamounts and seems to form a triple junction with similar anomalies observed along Helm’s Deep (HD) and the West Fangorn Basin (WFB).

DSDP sites 405 and 406 are located along the SETZ and provide a good calibration of the Cenozoic sequences as illustrated by the seismic line PAD95-06 (Figure 13b). It is currently the only well calibration available in this area.

Several reflectors can be identified in the SETZ. In agreement with Bull and Masson (1996), four prominent Cenozoic reflectors, mostly calibrated by the Well 405, can be observed on the PAD95-06 seismic section (Figure 14):

Reflector I mirrors the sea bed and onlaps Reflector II and older surfaces near site 405. Between reflectors I and II, sub-horizontal reflections of variable amplitudes are observed.

Reflector II occurs at ca 4.5s TWTT and onlaps Reflector III. Flat lying and semi continuous, high-amplitude reflections, with occasional sigmoidal and erosional seismic features, mark the sequence between reflectors II and III. All the reflections onlap the Reflector III unconformity.

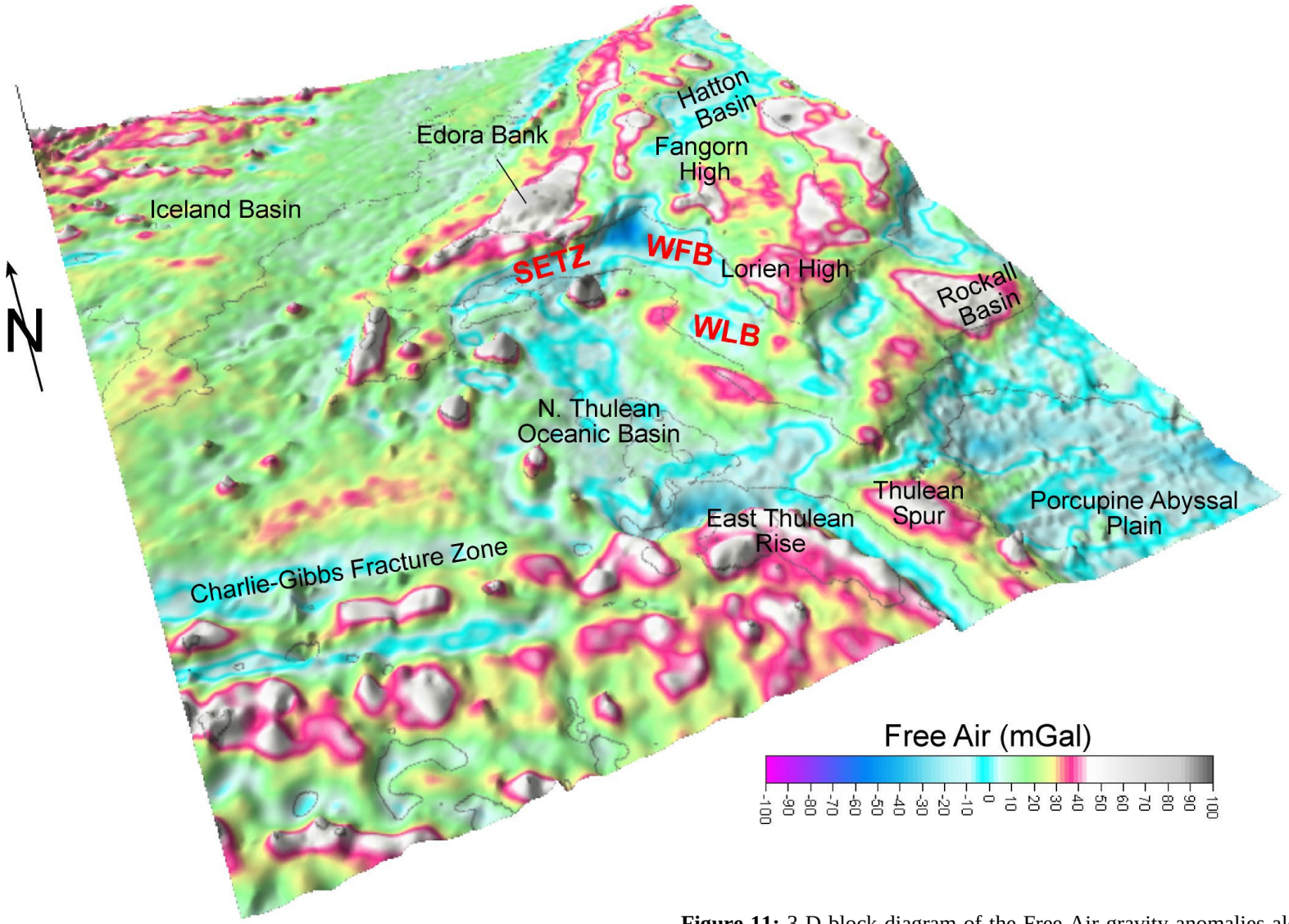

Figure 11: 3-D block diagram of the Free Air gravity anomalies along the South Rockall Hatton area draped on the satellite-derived bathymetry (Sandwell and Smith, 1997).

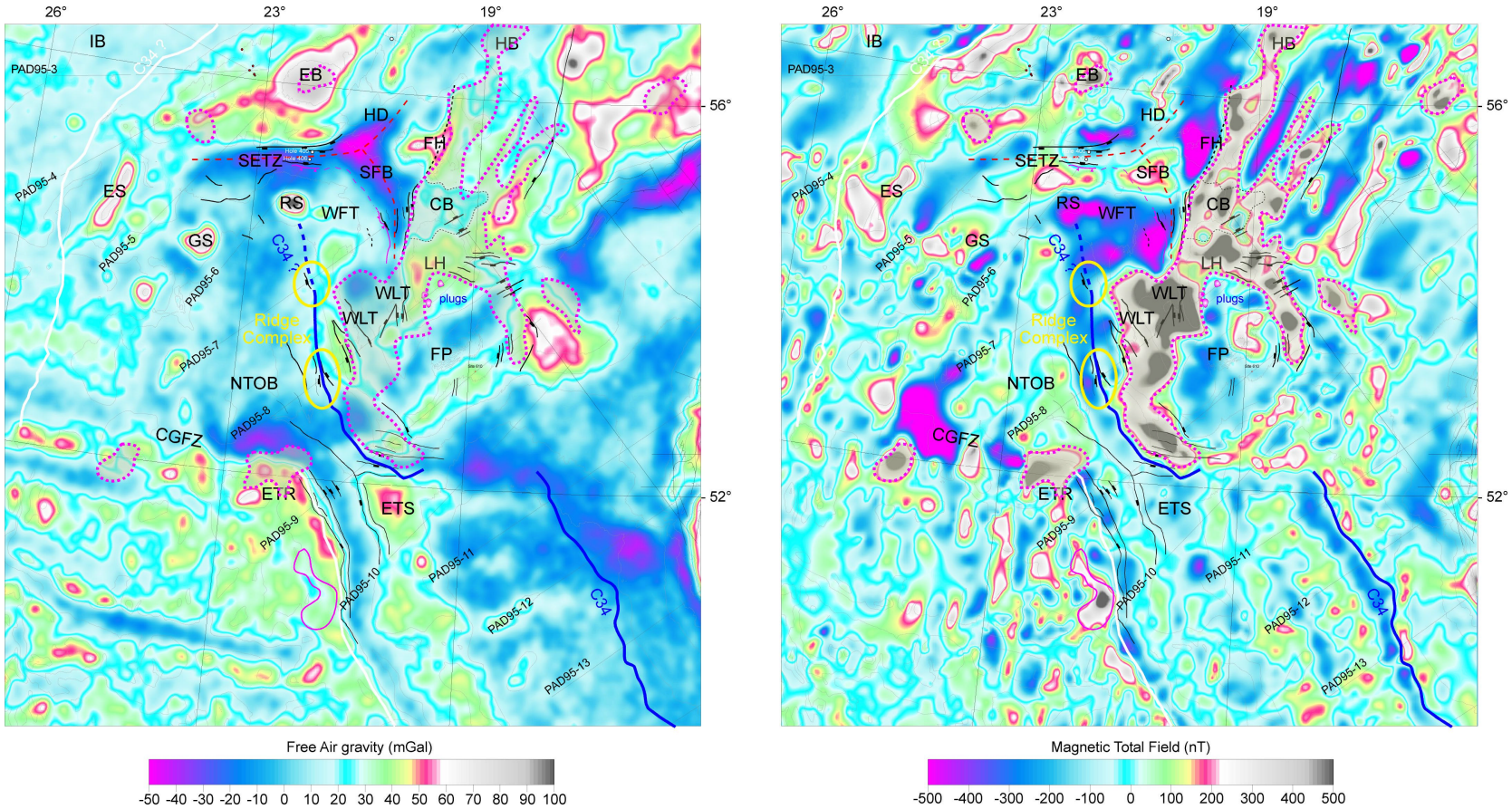

Figure 12: Free-air gravity and magnetic maps of the South Rockall Hatton. (a) Free-air gravity anomaly based on the satellite derived grid (v7.2) of Sandwell and Smith (1997). (b) Total magnetic field based on the regional data compilation of Verhoef et al. (1996). Abbreviation: CB:Cólmán Basin; CGFZ: Charlie-Gibbs Fracture Zone; EB: Edora Bank; ESt: Eriador Seamounts; ETR: East Thulean Rise; ETS: East Thulean Spur; FP: Feni Platform; FH: Fangorn High; GS: Gondor Seamount; HD: Helm's Deep; HB: Hatton Basin; IB: Iceland Basin; LH: Lorien High; NTOB: North Thulean Ocenic Basin; RS:; Rohan Seamount; SFB: South Fangorn Basin; WFP: West Fangorn Terrace; WLP: West Lorien Terrace.

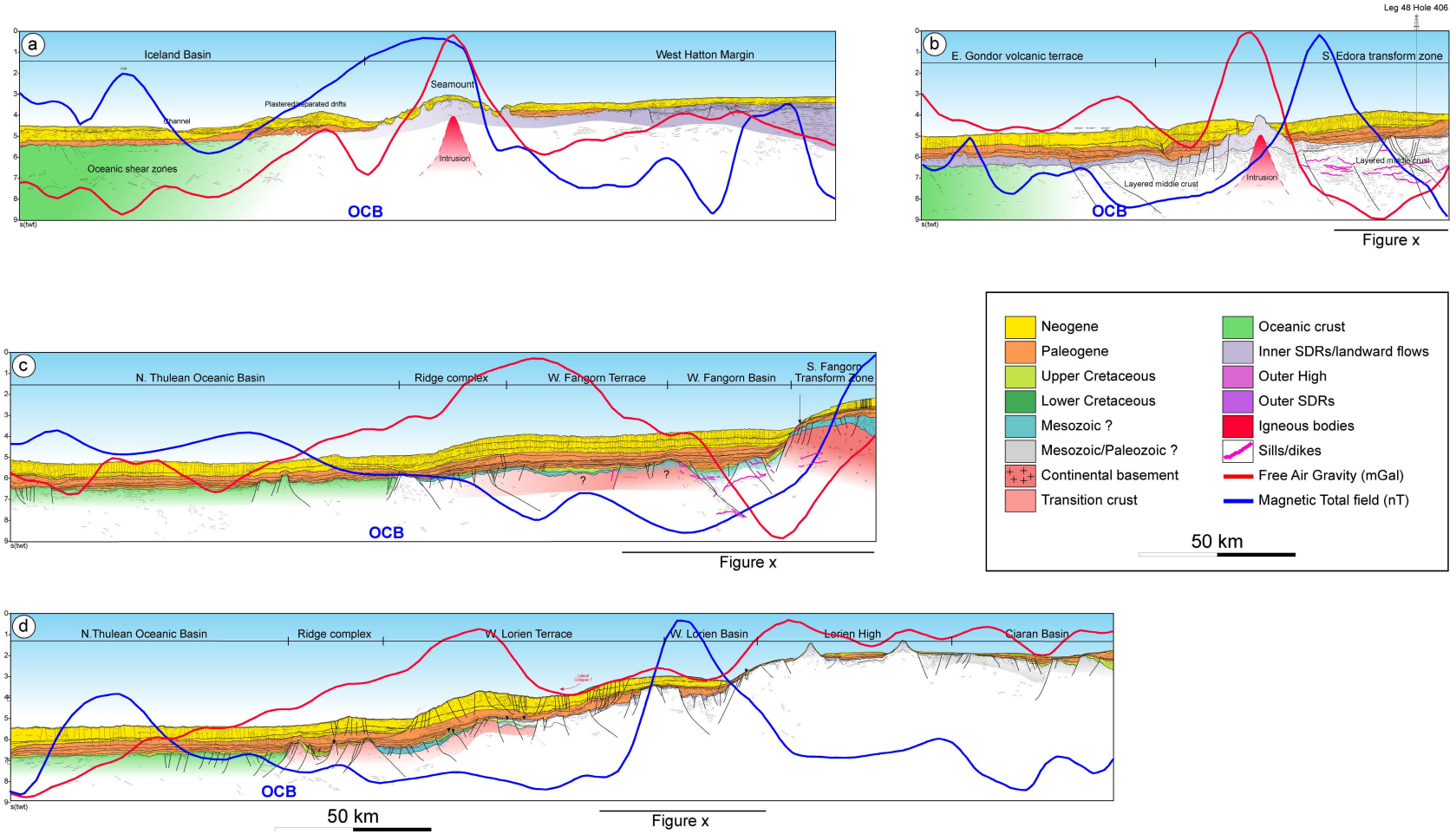

Figure 13: Geological transects and gravity and magnetic signatures along the South Rockall-Hatton Margin. (a) PAD95-04, (b) PAD95-06, (c) PAD95-07, (d) PAD95-08. The location of the seismic sections shown in Figures 14 - 16 is indicated on (b), (c) and (d) respectively.

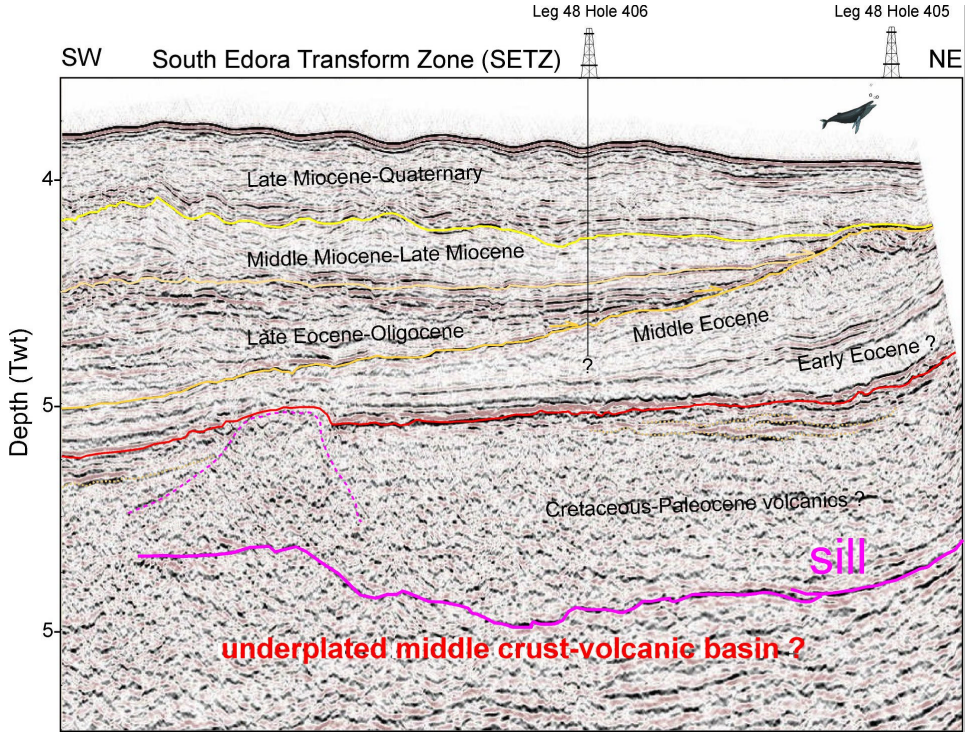

Figure 14: Migrated seismic section through DSDP Sites 405 and 406 (part of the line PAD95-06). The profile shows the stepped nature of the South Edora Transform Zone (SETZ) and the main reflections (I, II, III, IV) identified in the sub-basin.

Reflector III marks the top of a prograding fans/apron sequence and represents a significant seismic unconformity. The prograding sequence is mostly characterised by continuous low to high amplitude reflections downlapping Reflector IV. Near site 405, sigmoidal to chaotic reflections (slumps?) are observed.

Reflector IV defines the base of prograding wedge, thinning from 0.6 - 0.7s to 0.2 - 0.3 s TWTT away from the Edora Bank. Reflector IV is the uppermost of a series of high-amplitude reflectors mostly observed between 6 - 7 s TWTT. Few prograding high-amplitude reflections can be observed, however, near site 406. To the south, Reflector IV merges with the top basalt of the Rohan Seamount, imaged by the PAD95-6 seismic line.

Well 406 bottomed in middle Eocene strata but did not penetrate Reflector IV (see Figure 14), expected to be Early Eocene in age (Bull and Masson, 1996). Here, Reflector IV likely represents the top of a set of lava flows but the nature of the underlying sequences is uncertain. The well-layered seismic package observed in the middle crust between 6-7 s TWTT, from the SETZ to the southern part of the Rohan Seamount suggest a strong velocity contrast. Bull and Masson (1996) proposed that the transparent sequence just below Reflector IV may represent a thick volcanic layer (1 s TWTT) overlying a Cretaceous sedimentary sequence with a discontinuous appearance due to scattering by the overlying volcanics.

These sequences may also represent intruded crust (continental to oceanic?) or sedimentary sequences injected by high-velocity mafic sills. The gravity low observed on both side of the Rohan Seamount may favour the sub-basin hypothesis. The layered facies in the SETZ coincides with a strong NW-SE magnetic anomalies (20-40 nT) also observed in the southern part of the Helm's Deep. The SETZ was a direct eastern prolongation of the Labrador Sea spreading axis before the early Cenozoic breakup. Reactivation or second extension of the pre-existing crust is therefore expected in Late Cretaceous - Palaeocene time. A propagating graben in front of the spreading axis can be expected south of the Edora Bank in Late Cretaceous - Early Palaeocene time. Top basalt reflections, displaced by normal faults near the Helm's Deep suggest Palaeocene to Early Eocene extension.

Above Reflector IV, the prograding fan is Eocene in age and its top represents an unconformity between middle Eocene and late Eocene sediments. This distinct unconformity coincides with a long and complex hiatus which, on the flank of the SETZ, may represent several cycles of erosion (Montadert and Roberts, 1979; Bull and Masson, 1996). At site 406, this unconformity coincides with a sudden change from downslope sedimentation to pelagic basin infill. Elsewhere in the North Atlantic and offshore Ireland, this change has also been observed and explained in terms of a regional increase in abyssal circulation from Late Eocene to Oligocene leading to sediment drift formation (Stoker et al., 2005). As a consequence Reflector III represents an equivalent of the C30 unconformity described in the Rockall and Porcupine basins (Stoker et al., 2001; McDonnell and Shannon, 2001). However, the fan geometry suggests that this unconformity started to form earlier as a response to the local uplift of the Rockall-Hatton plateau from late Palaeocene to middle Eocene.

Reflector II correlates with a downward decrease in density as the sediments changed abruptly from chalks above to diatomites below (Montadert and Roberts, 1979; Masson and Kidd, 1996). This early Miocene event coincides with the onset of strong ocean circulation leading to the decrease of diatomite production (Montadert and Roberts, 1979).

Reflector I was interpreted as a late Miocene marker, which may represent a lithification boundary in calcareous sediments (Masson and Kidd, 1996).

The West Fangorn Basin (WFB) is also part of the low gravity set observed in the southern part of the Hatton Basin. The PAD95-07 line (Figures 13c and 15) illustrates the structure of this basin located and defined between the Fangorn High (FH) and a volcanic terrace, named the West Fangorn Terrace (WFT).

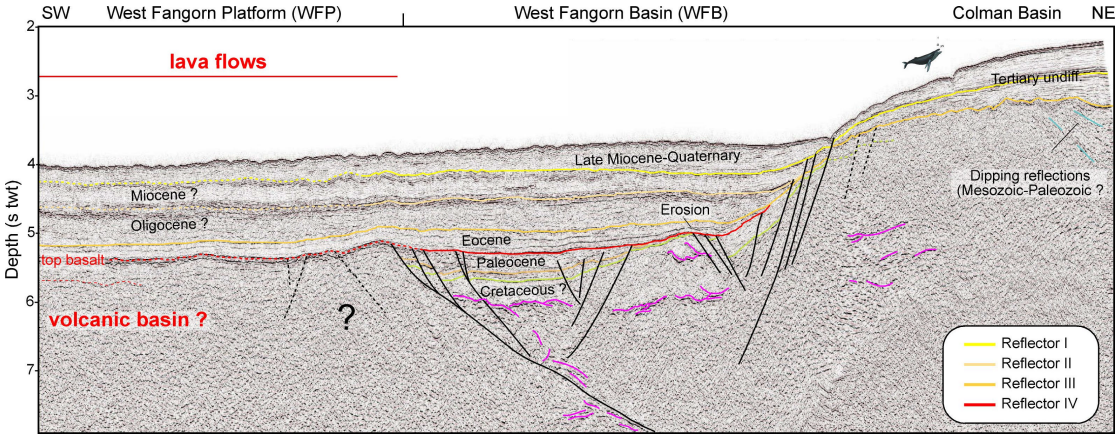

Figure 15: Migrated seismic section along the West Fangorn Basin. This section illustrates the western part of transect PAD95-07 near the slope of the Fangorn High. The section shows Mesozoic? - Palaeocene sediments imaged in a basalt-free window in the lava, located to the SW in the South Fangorn Terrace. Pre-Cenozoic formations are hidden by scattered lava flows. Locally, some windows allow imaging of deeper sedimentary basins injected by magmatic sills (Cretaceous and/or Palaeogene in age).

The WFB is imaged adjacent to the slope which represents the surface expression of an underlying fault zone. This fault zone coincides with a significant magnetic and gravity trend that extends from the north in the Fangorn High. This structural setting is similar to the SETZ but no prograding fan or obvious C30 are observed.

To the west, a high-amplitude, smooth and fairly continuous reflection bounds the basin. Beneath this marker, the seismic facies is poorly imaged and is mostly transparent and low-amplitude. This strong marker represents a high impedance contrast between the lava flows and overlying sedimentary rocks. We assume that these lava flows are Palaeogene in age and represent the continuity of the Reflector IV described in the SETZ. The basalts extend along the WFT linked with the Rohan Seamount to the northwest. In the WFB, the top basalt (i.e. Reflection IV) merges with a clear horizon, interpreted as a late Palaeocene - early Eocene unconformity. The limit of the gravity anomaly lows and can be used to map the lateral extension of the lava flows. Clear wedges and syn-rift sequences are observed beneath this unconformity. They probably represent Palaeocene and upper Cretaceous sediments, locally injected by magmatic sills. This interpretation suggests a Late Cretaceous-Palaeocene phase of extension in this part of the SRHM. This also suggests that extension along the WFT was still active in the area after the breakup of this margin segment initiated in Early Campanian time (C34). It is difficult to map these syn-rift sequences beneath the lava flows but some Cretaceous-Palaeocene sub-basins can be expected along the WFT.

Above the Reflector III, a well-layered, low-amplitude seismic sequence is observed. Its top is tentatively interpreted as the Reflector III, equivalent to the C30 in the Rockall Basin. This sequence (Eocene?) shows evidence of local erosion, which suggests a shallow marine or sub-aerial deposition during the Eocene.

The West Lorien Basin (WLB) (Figures 13d and 16) represents the southeastern prolongation of the WFB. It is a transition sub-basin between the Lorien High (LH) and the West Lorien Terrace (WLT). This system coincides with the prolongation of the WFT and WFB. WLB represents a narrow graben, 25 km wide, in the prolongation of the gravity low observed in the WFB. This graben is now in a high structural position (4s TWTT) compared to WFB (6 s TWTT). This suggests that there is a transfer zone between the WFT/WFB and WLB/WLT systems. This graben coincides with a strong magnetic anomaly which could be explained by the numerous sills and dykes observed in the basin.

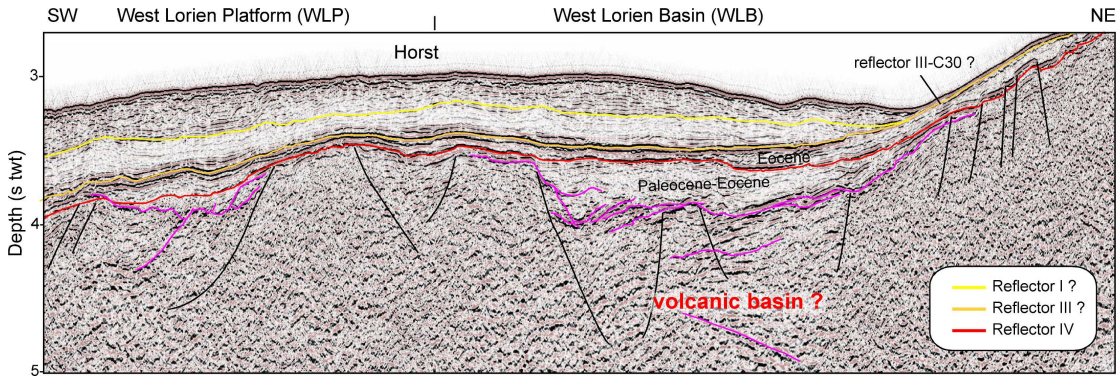

Figure 16: Migrated seismic section along the West Lorien Basin. This section illustrates the western part of transect PAD95-08 near the slope of the Lorien High. The section illustrates the West Lorien Basin, a narrow graben which represents the southeastern continuity of the South Fangorn Basin. This graben is heavily injected by magmatic sills. The deeper layered section is interpreted as a shallow Mesozoic (Cretaceous?) basin intruded by magmatic sills or interbedded with lava flows.

Along the WFT and WLT, the structures are poorly defined due to difficulties in sub-basalt imaging. Some wedges and syn-rift features are locally imaged but do not allow a clear vision of the system. Most of this area shows evidence of scattered lava flows and shallow intrusions. It is difficult to estimate the maximum thickness of the lava in this area but local basalt-free windows suggest that the basaltic flows are probably thin, except near the main intrusion characterised by circular, positive gravity anomalies.

3.2.2 Nature of the ocean continent-transition in the SRHM

The SHRM is a complex rifted zone linking the WHM segment with the Celtic and Iberian non-volcanic margins. The SHRM was influenced by an earlier Cretaceous phase of break-up and, compared to the WHM, the nature of the continent-ocean transition is different. The oceanic crust in the North Thulean Oceanic Basin is clearly identified by the transparent facies, with an absence of coherent intra-basement reflectors. The top of the oceanic crust is characterized by a high-amplitude, smooth reflections affected by normal faults that are most pronounced close to the C34 magnetic anomaly. This morphology suggests a fast oceanic spreading rate (~100 mm yr-1) between C34 and C25.

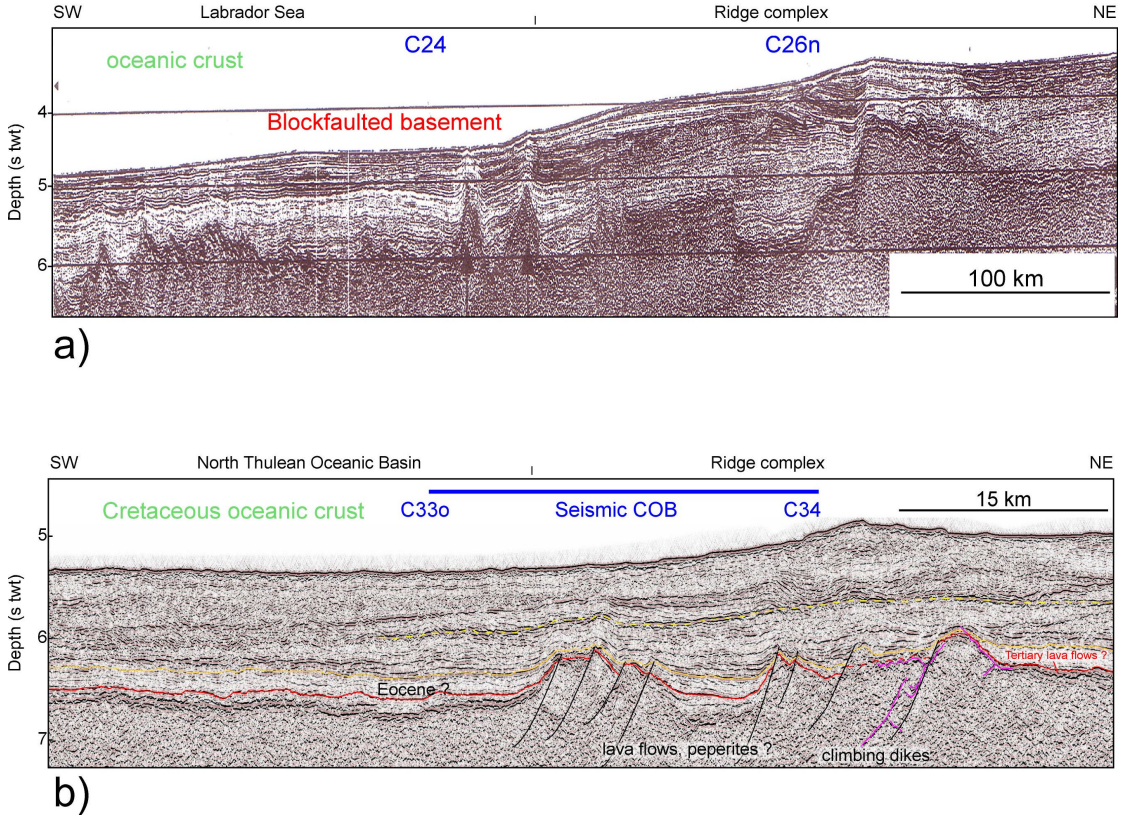

Figure 17: The ridge complex of the South Rockall Hatton Margin. (a) Seismic reflection line BGR/77-2 published by Nielsen et al. (2002). Structures close to the C24 magnetic anomaly are very similar to basement structures in age along the PAD95-08. Nielsen et al. (2002) suggest that this type of structure could represent mounds of tectonically-unroofed and serpentinised mantle. (b) Our seismic interpretation along the SHRM. Close to the C34 magnetic anomaly, the continent-ocean transition (COT) is defined by a sharp contrast between a smooth oceanic basement (in green) and the block-faulted structure that exhibit both syn- and post-breakup features. These are very similar to structures described along the adjacent (pre-drift) southwest Greenland margin described by Nielsen et al. (2002) and Chian and Louden (1994). They may represent severely intruded continental basement, faulted oceanic crust or mounds of tectonically-unroofed and serpentinised mantle that form in rift environments where little to no melting occurred.

Along the C34 magnetic anomaly, and west of the WFT and WLT, the ocean-continent transition (COT) is defined by a sharp contrast between a smooth oceanic basement and block-faulted ridge. The ridge complex is parallel and located near the positive elongate gravity anomalies observed in the WFT and WLT. The crust here is characterised by atypical basement features with transparent seismic facies. Syn-rift facies are observed between the rotated faulted blocks locally affected by sills and dykes. These are very similar to basement structures found along the COT further north along southwest Greenland (Chian and Louden, 1994; Nielsen et al., 2002, and Figure 17a) as well as on the Iberian margin (Pickup et al., 1996; Boillot and Froitzheim, 2001)

Close to the oceanic crust and C34, the succession may represent a combination of serpentinized peridotites and/or intruded continental basement. The SRHM could therefore be classified as a non-volcanic margin and could be very similar to the Galician Margin, where stretching of the lithosphere led to the progressive exhumation of the upper mantle just before the final break-up.

No seaward dipping reflectors (SDRs) are imaged as in the WHM (see later, section 3.3) but evidence of minor magmatism is identified. Thin lava flows and transgressive sill complexes, magmatic plugs and seamounts intruding the Cretaceous oceanic crust are observed in the vicinity of the ridge complex. Cretaceous syn-rift magmatism could be present along the SRHM but most of the volcanism seems to be linked with the main Palaeogene magmatic event. If this interpretation is correct, the precise age for the continent-oceanic transition in this area is Early Campanian (~80 Ma).

3.2.3 The conjugate system: the Canadian basins

Before the breakup and the opening of the Porcupine Abyssal Plain and the North Thulean Oceanic Basin, the Rockall-Hatton system was located adjacent to the northeast Newfoundland basins. Plate reconstructions (Figure 18) (e.g. Srivastava and Verhoef, 1992; Louden et al., 2004; Sibuet et al., 2005) suggest that the Orphan Basin was located at the southern prolongation of the Rockall Basin and the Rockall-Hatton Plateau was situated in front of the Cartwright Arch and St Anthony Basin. Similarity of the geological histories and correlation of major tectonic events in adjacent basins, (St Anthony, Orphan, Jeanne d'Arc and Flemish Pass basins) can be used to better constrain the geological context offshore Ireland.

The Orphan Basin represents an area of thinned and foundered continental crust with stretch factors greater than 0.5 over most of the area (Keen and Dehler, 1993; Chian et al., 2001). It formed during the period from the Late Triassic to Late Cretaceous, as a result of the opening of the North Atlantic Ocean. It is bounded to the west by the Bonavista Platform (Figure 19), to the south by a high block separating it from the Jeanne d'Arc and Flemish Pass basins (Enachescu, 1987; Grant and McAlpine, 1990; Enachescu, 2004; Sibuet et al., 2005), to the north by onlap of sediments onto a series of basement ridges and the Charlie-Gibbs Fracture Zone, and to the east by a high basement ridge that runs between the Orphan Knoll and the Flemish Cap.

Well control in the basin is extremely sparse. The Blue H-28 well was drilled on a basement high and encountered Cenozoic and only a thin Mesozoic formation (Lower and upper Cretaceous) before entering the Palaeozoic. The DSDP (Joides) 111 well drilled on the Orphan Knoll also provided some geologic data and indicates evidence of Jurassic rocks (Laughton et al., 1972).

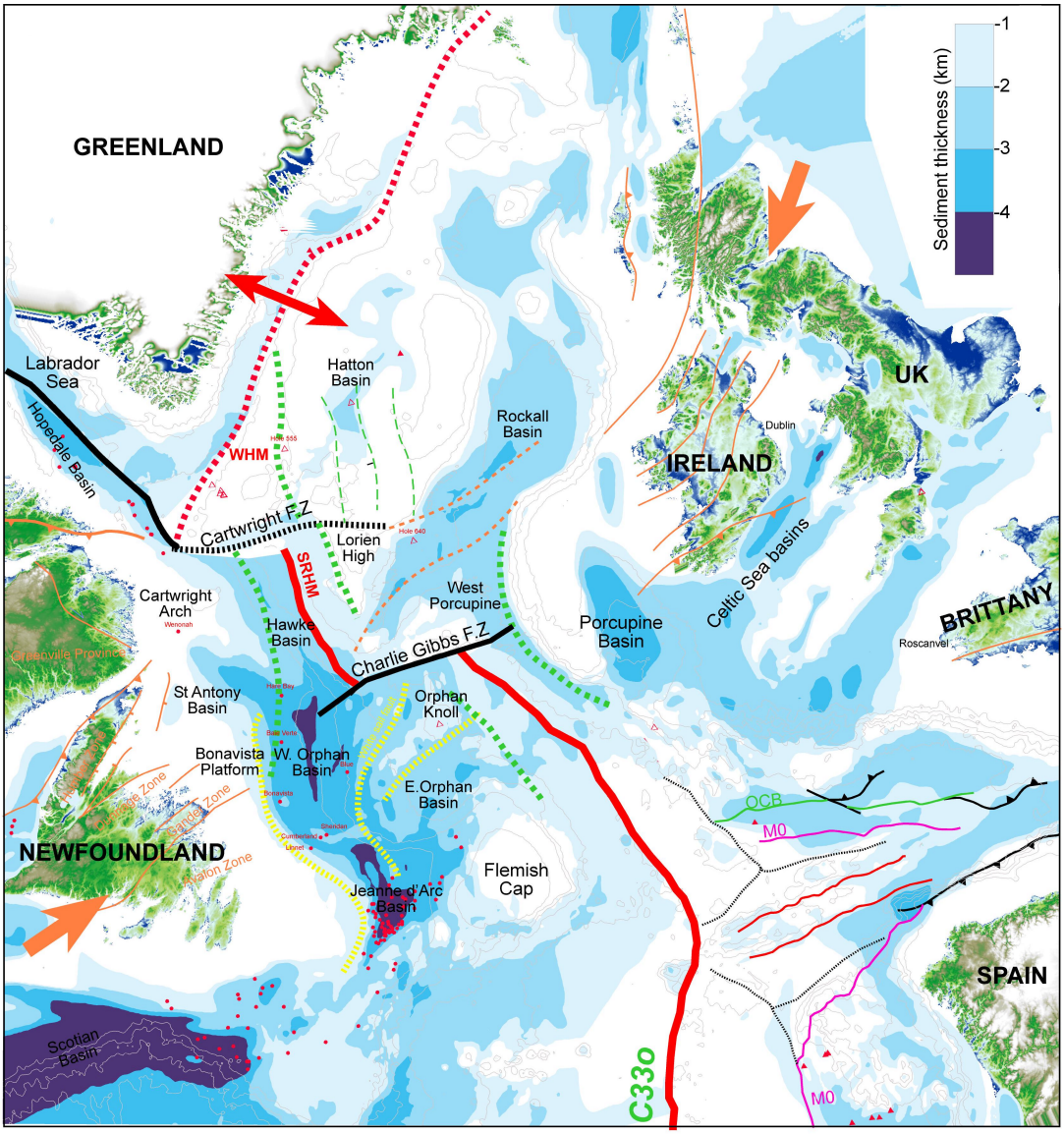

Figure 18: Plate reconstruction between the Irish and Canadian basin immediately after the breakup along the Porcupine Abyssal Plain (C34, Early Campanian). Red dots represent exploration wells drilled along the Canadian basins.

The geologic evolution of the basin is similar to that of the adjacent Jeanne d'Arc, and Flemish Pass basins, and is also similar to the history of the Porcupine Basin (Shannon et al., 1995). Intense tectonism during several extensional events, coupled with possible halokinesis, resulted in the Mesozoic section being structured into a number of anticlinal and tilted fault blocks. In a recent update Enaschescu et al. (2004) subdivided the Orphan Basin into the East and West Orphan Basins, divided by the White Sail Fault. A strong connection between the East Orphan Basin and the western Porcupine Basin is suggested. The West Orphan Basin could be linked with the Feni Drift Platform and the South Hatton Basin.

The East Orphan Basin represents a thick Mesozoic basin with Triassic to Jurassic strata overlying older sediments and a Palaeozoic basement (Enaschescu et al., 2004). Here the structural trends are NS-oriented, probably due to the Late Jurassic - Early Cretaceous rifting. A second rifting phase occurred in the eastern part of the West Orphan Basin where the oldest Mesozoic sediments are early Cretaceous in age to the west. Here, the trends are mostly 20° N. A late phase of rifting during late Cretaceous is also observed in the westernmost part of the West Orphan Basin and probably in the eastern part of the Orphan Knoll and Flemish Cap.

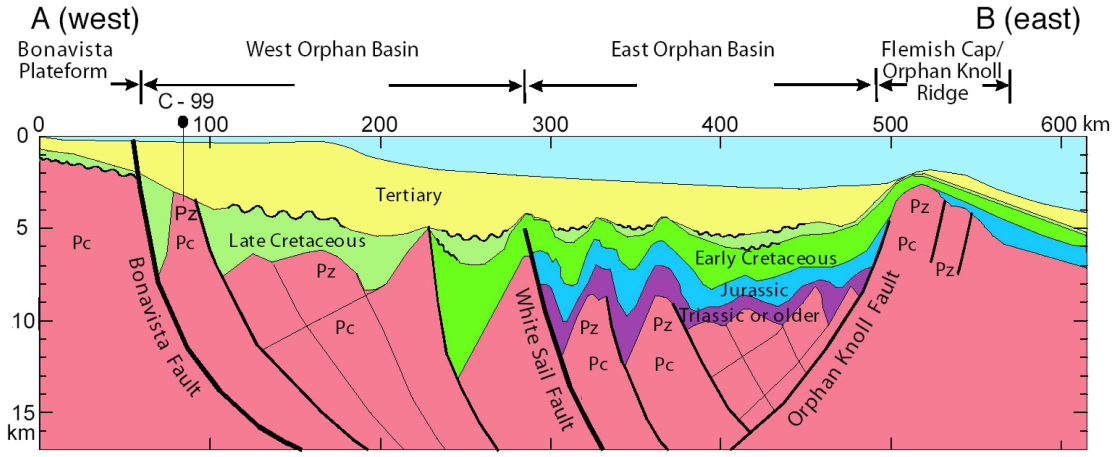

Figure 19: Schematic geological cross-section across the Orphan Basin from the Flemish Cap to the Bonavista platform showing that basins become younger westward (Figure from Enaschescu et al., 2004; also Sibuet et al., 2005).

There is little information for the area between the Cartwright Arch and the St Anthony Basin. The Mesozoic section in this area is poorly documented and only suggested along the break-up axis. A thick Cenozoic succession is recognised above a significant regional unconformity interpreted in the few transects published along this area (Grant and Mc Alpine, 1990). The Hare Bay E-21 well and other shallow drillholes suggest that the pre-Cenozoic sections north of the Charlie-Gibbs lineament are mostly Carboniferous overlying Precambrian and Palaeozoic basement (Grant and McAlpine, 1990). The oldest Mesozoic sediments, drilled by Hare Bay E-21, are Campanian in age but represent a condensed section.

Carboniferous rocks are expected in the vicinity of the Lorian High and Cólmán Basin and Campanian is expected along the SRHM. Evidence of Triassic-Jurassic strata is less obvious but could exist in the southern part of the Hatton Basin. With the exception of the Jurassic polymorphs and natural oil seep detected in the northern part of the Hatton Basin, there is no direct evidence of rock older than Cretaceous in the Hatton Basin and surrounding areas.

3.3 Hatton Basin and West Hatton Margin (WHM)

The Hatton Basin and the WHM are part of the Rockall-Hatton Plateau, which represents a continental fragment between the Rockall Basin and the oceanic crust, west of the C24 magnetic anomaly.

3.3.1 Structure and stratigraphy of the Hatton Basin

The Hatton Basin is located between the Rockall Bank and the Hatton Bank. The geology of the Hatton Basin is currently poorly constrained due to the scarcity of wells and little seismic coverage.

DSDP well 116 drilled the western part of the Hatton Basin and penetrated 808 m of Oligocene and Mio-Pleistocene ooze and chalk with cherts and 46 m of upper Eocene carbonate ooze (Naylor and Shannon, 1982). Well 117 penetrated 152 m of Oligocene cherty limestone and ooze overlying lower Eocene oozes, claystones and basalts. BGS wells in the UK part of the Hatton Basin (94/1, 94/2 and 94/3) encountered Jurassic and Cretaceous palynomorphs reworked into Eocene close to the Rockall Bank. Stoker et al. (2001) suggested the availability of a local Mesozoic source of reworked material on top of Rockall Bank. Carboniferous palynomorphs were recorded in the BGS shallow cores, while Albian paralic sediments are present beneath the thin Cenozoic section in the western part of the Hatton Basin (Hitchen, 2004). These bore-holes drilled wedges described by Neish (1993) and Hitchen (2004). These seismic successions represent Mesozoic formations (Jurassic? - Cretaceous) onlapped by Cenozoic lava flows sourced from kilometric igneous centres, clearly characterised by circular gravity anomalies. These intrusive centres were defined by Edwards (2002) and Hitchen (2004) and were named as Aramassa, Mammal, Lyonesse, Owlsgard, Sandarro, Sandastre and Swithin.

In the Irish sector of the Hatton Basin, the structure of the basin is relatively poorly documented. The gravity and magnetic signatures (Figures 20 and 21) are different from the UK sector. The gravity lows observed to the north are less uniform in the southern part of the Hatton Basin and the gravity highs are less dominant. Instead, linear N10°E and N30°E gravity trends are observed near the Fangorn High and south of the Owlsgard intrusive centre. Between the Cólmán Basin and the Aramassa intrusive centre, the gravity signature shows a N10°E orientation. The same trend is observed on the magnetic map which shows significant positive and negative anomalies. This pattern might reflect major underlying faults; shear zone, dykes swarms, fault-controlled lava flows or volcanic ridges.

Interpretation of the PAD95 seismic lines along the West Hatton Margin (PAD95-01 to 04) is shown in Figure 22. The interpreted structures (SDRS, Outer High, dyke swarm, seamounts) suggest that the WHM falls into the category of a volcanic margin. Along the Hatton Bank, sedimentary wedges, previously imaged by Neish (1993), have been drilled recently by the British Geological Survey and are proved to be Early Cretaceous in age (Aptian proved in boreholes 99/1 and 99/2A).

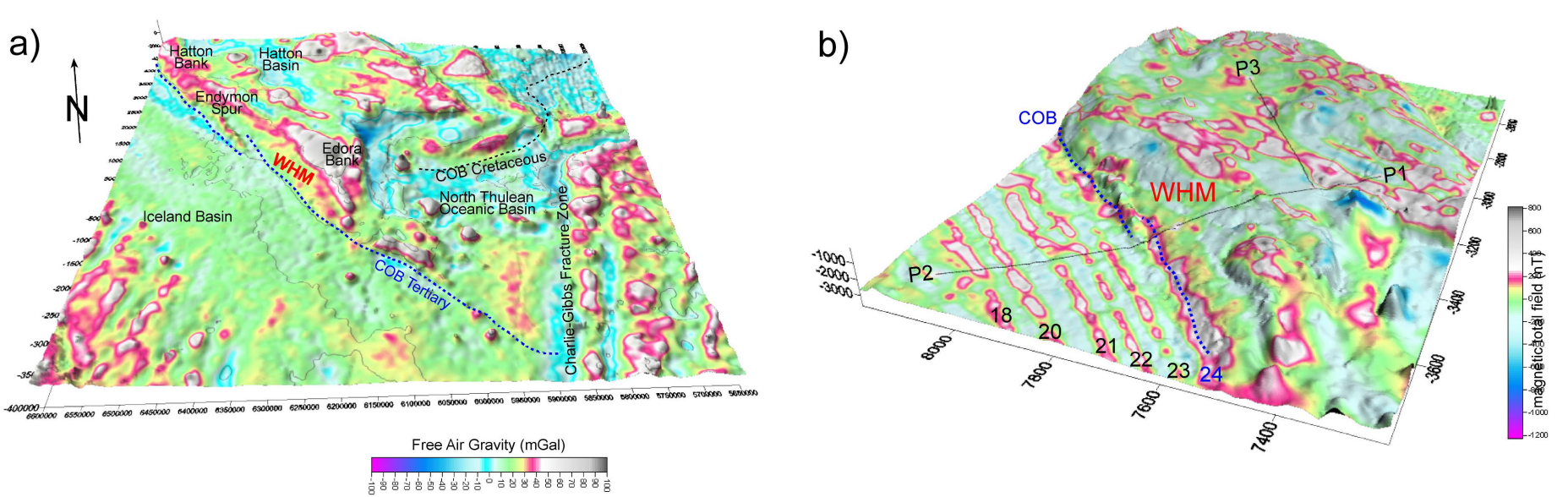

Figure 20: 3-D block diagrams of (a) the Free-air gravity anomaly, and (b) the total magnetic field anomaly along the Hatton Basin and West Hatton Margin (WHM), both draped on the satellite-derived bathymetry (Sandwell and Smith, 1997). The diagram illustrates the location of the Hatton Deep Seismic (HADES) transect along the continent-ocean transition. The continental-oceanic boundaries are marked by a change in magnetic character. Location of the HADES wide-angle transects in indicated.

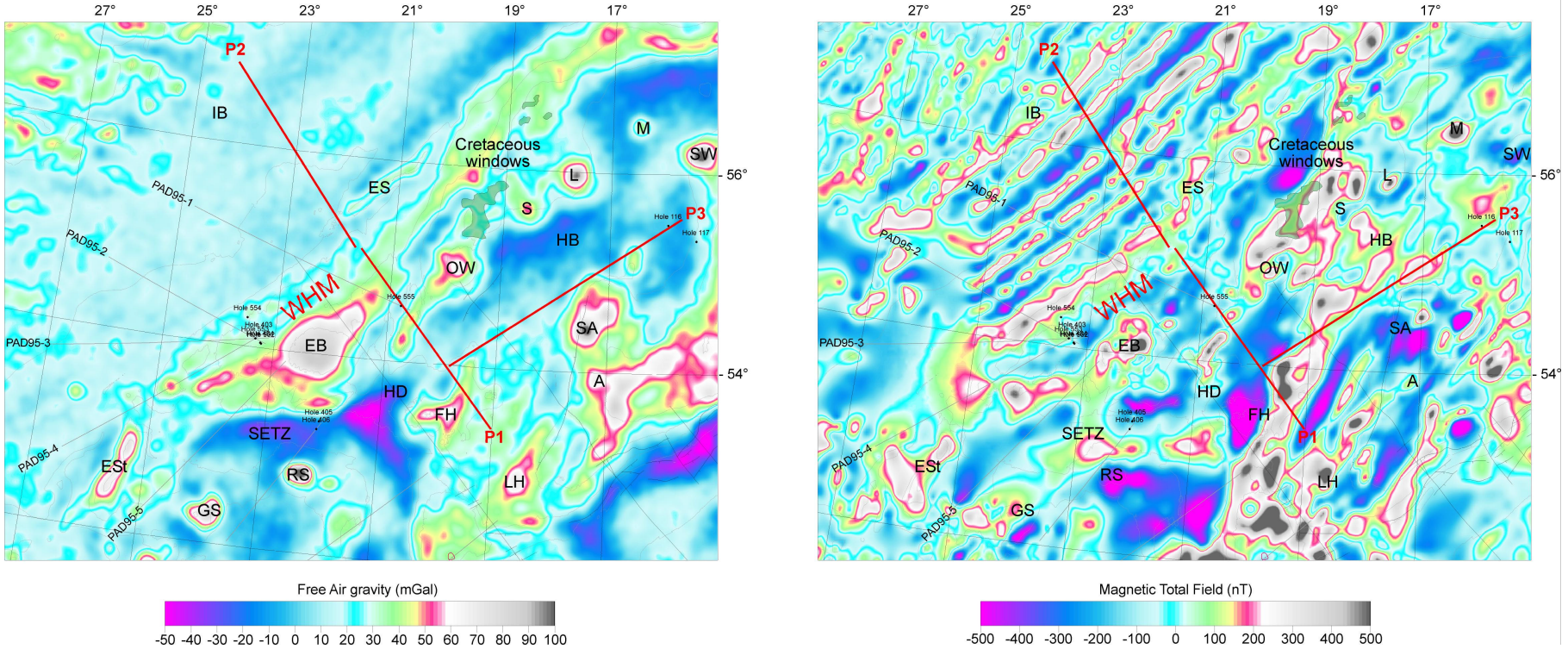

Figure 21: (a) Free-air gravity anomalies and (b) total magnetic field anomaly along the South Rockall Hatton area draped on the satellite-derived bathymetry (Sandwell and Smith, 1997). A: Aramassa; CB:Cólmán Basin; CGFZ: Charlie-Gibbs Fracture Zone; EB: Edora Bank; ESt: Eriador Seamount; ES: Endymion Spur; ETR: East Thulean Rise; ETS: East Thulean Spur; FP: Feni Platform; FH: Fangorn High; GS: Gondor Seamount; HD: Helm's Deep; HB: Hatton Basin; IB: Iceland Basin; LH: Lorien High; L:Lyonesse; M: Mammal; NTOB: North Thulean Oceanic Basin; OW: Owlsgard; RS: Rohan Seamount; S: Sandarro; SA: Sandastre; SFB: South Fangorn Basin; SW:Within; WFP: West Fangorn Terrace; WLP: West Lorien Terrace.

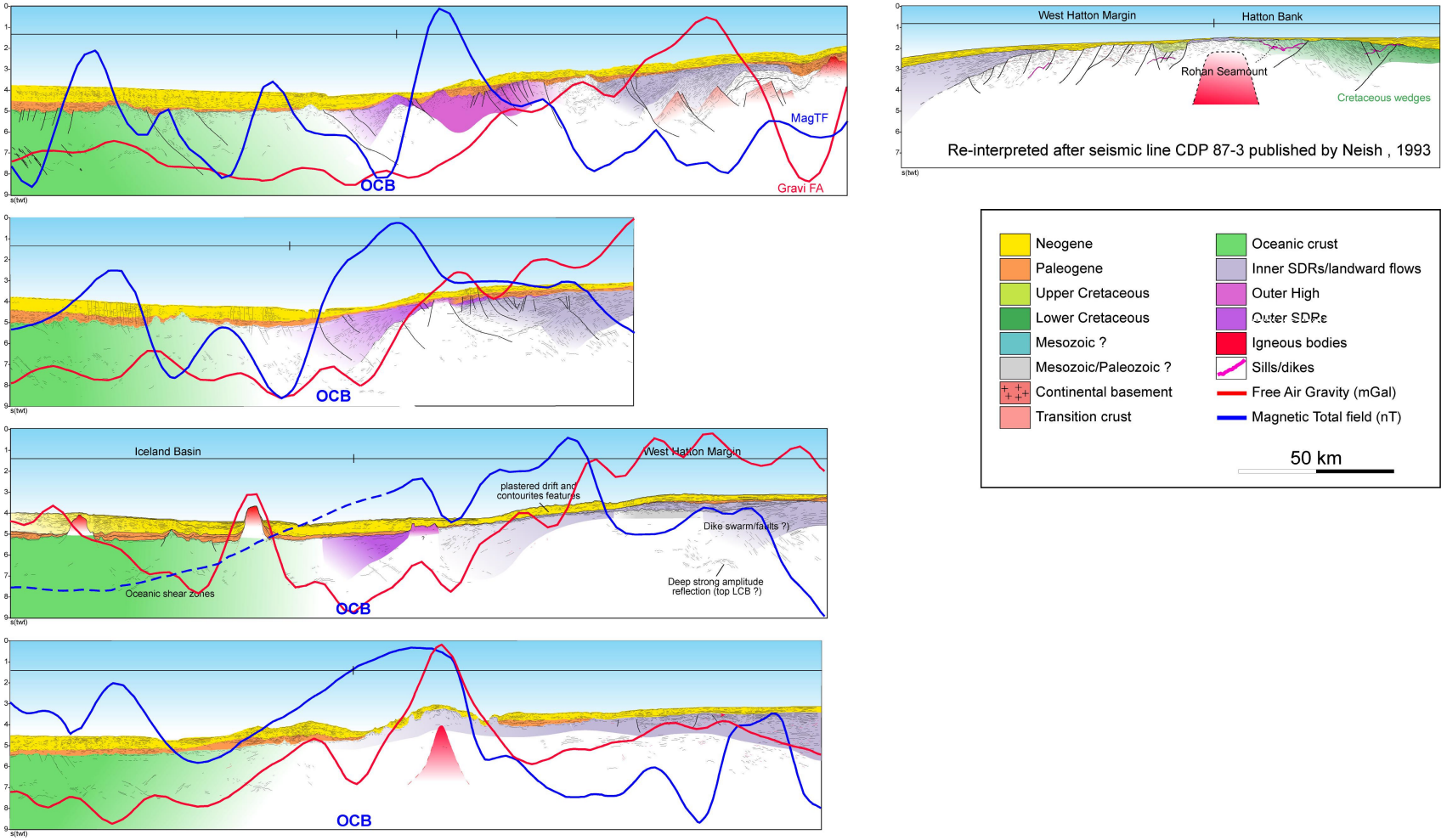

Figure 22: Interpretation of the PAD seismic lines along the WHM. The interpreted structures (SDRS, Outer High, dyke swarm, seamounts) suggest that the WHM falls into the category of a volcanic margin. Along the Hatton Bank, sedimentary wedges, previously imaged by Neish (1993), have been drilled recently by the British Geological Survey and are proved to be Early Cretaceous in age (Aptian proved in boreholes 99/1 and 99/2A).

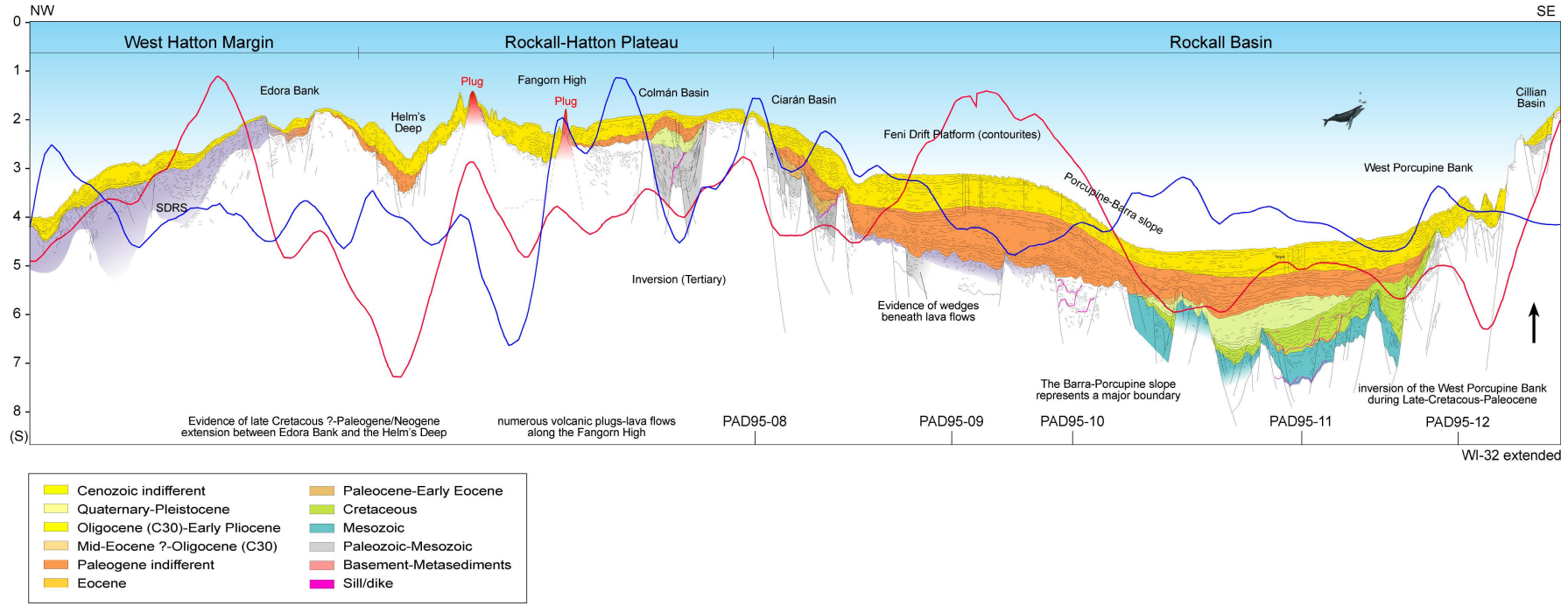

Figure 23: Geological transect along WI-32 across the Rockall basin extended to the West Hatton Margin.

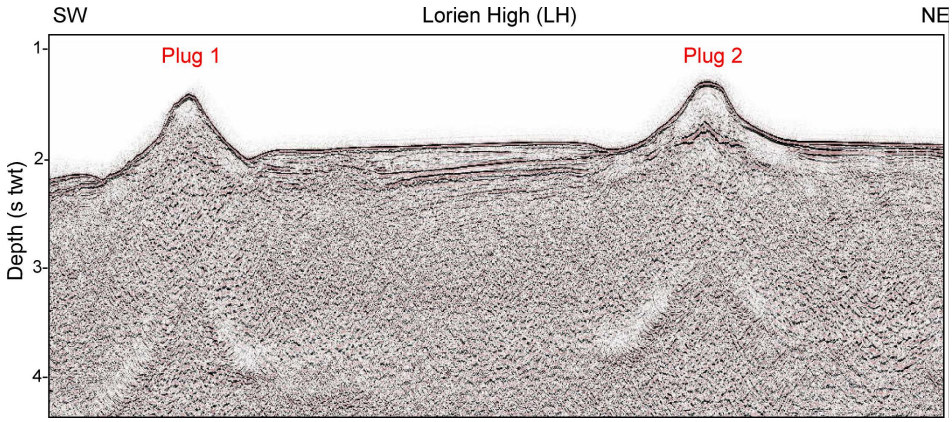

Figure 24: Mound-shaped features are observed in the Lorien High. Such features, ~ 10 km wide, have been interpreted as magmatic plugs.

On the WI-32 seismic profile (Figure 23), some of the 10°E gravity and magnetic trends (see above) coincide with features on the upper surface, clearly observed in the Fangorn High area. They represent linear magmatic plugs quite similar to those observed in the Lorien High (Figure 24). These plugs are also similar to those observed in the Ciarán Basin to the east (e.g. PAD 95-08) (see Figure 13d).

Close to DSDP well 555, the linear gravity and magnetic trends coincide with a volcanic ridge observed on seismic profiles. It represents the southern prolongation of the Owlsgard intrusive centre, which is part of the Hatton Bank. It is likely that these volcanic ridges intrude a pre-existing depocenter. This is also supported by the fact that sedimentary wedges are observed between Owlsgard and Sandaro. Such a magmato-tectonic interaction between sedimentary strata, lava flows and intrusions has been observed in Skye Island (Scotland) and in Namibia where huge intrusive complexes intrude and the pre-existing sedimentary layers.

3.3.2 Structure and volcano-stratigraphy of the West Hatton Margin

The shallow structure of the WHM has been previously discussed by Barton and White (1997) who described SDRs and deep structures along the Edora Bank. The basalts of the southern Rockall Plateau/Hatton Bank were sampled at three sites (553, 554, and 555) during DSDP Leg 81. DSDP Leg 81 drilled tholeiitic basalt lava flows, extruded under subaerial or very shallow marine conditions. The lavas at these sites are all consistently MORB-like in composition (Harrison and Merriman, 1984). The age of the lavas is at least Late Palaeocene/Early Eocene based on the age of the overlying sediments (Roberts et al., 1984) and identification of oceanic magnetic anomalies (Vogt and Avery, 1974). A more direct method of dating the lavas was attempted by interpreting the dinoflagellate cyst assemblages in sediments intercalated with lava flows at Site 555. These sediments, like those associated with the Vøring lavas, are correlated to Zone NP9 (Brown and Downie, 1984). K-Ar dating of the DSDP Leg 81 lavas gave a range of ages, although two from Site 555 which gave 52.3 ± 1.7 Ma and 54.5 ± 2.0 Ma are the most reliable, according to Macintyre and Hamilton (1984). Using Ar-Ar methods, Sinton and Duncan (1998) revealed a good four-step plateau

age of 57.6 ± 1.3 Ma and a concordant but imprecise isochron age of 51.6 ± 9.0 Ma for basalts on Site 555.

3.3.3 Rockall Plateau/Hatton Bank: new observations

In order to refine our knowledge of the tectonics involving the magmatism, an initial volcano-stratigraphic interpretation of the section PAD95-01 (Figure 25) was made to constrain the probable nature (lava flows, lava breccias, pillow lavas, tuffs, sills, peperites) and environmental setting (subaerial, submarine) of the different seismic facies interpreted as volcanic. This interpretation uses terminologies and concepts proposed by Planke et al. (2000) and Berndt et al. (2001).

The WHM represents a late Palaeocene - early Eocene volcanic margin as suggested by a typical volcano-stratigraphic sequence (Inner SDRs, Outer High, Outer SDRs, oceanic crust) observed near the breakup axis.

The Landward Flows unit is identified on the PAD95-01 seismic line. The top reflection is a strong, smooth event and the internal reflections of these sequences are disrupted, hummocky or sub-parallel.

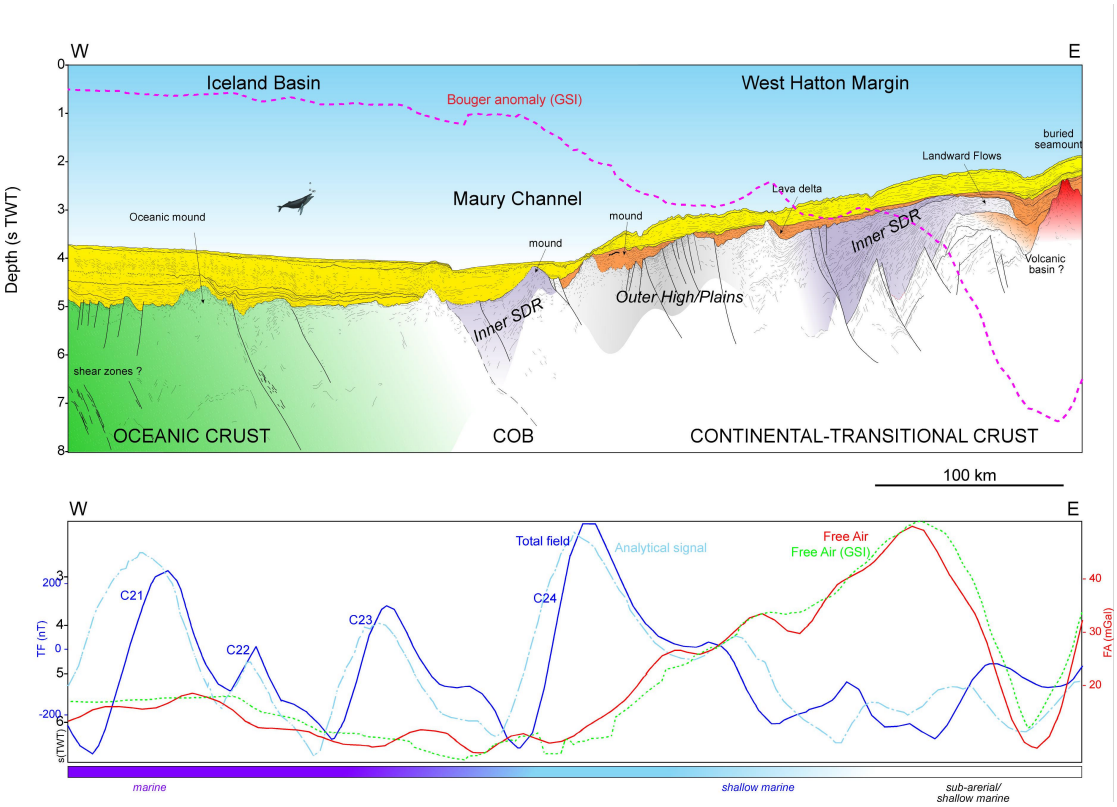

Figure 25: Example of volcano-seismic facies and sequences observed along the PAD seismic line PAD95-01. We use the volcano-stratigraphic nomenclature of Planke et al. (2000). The transect shows the changing seismic expressions from the Inner SDR wedges to the Outer SDR wedge, located oceanward, close to the oceanic crust and the C24 magnetic anomaly.

The Inner SDRs represent a wedge-shaped unit in the oceanward prolongation of the Landward Flows. The inner SDRs observed in most of the PAD lines along the WHM are characterised by a strong, continuous, smooth or wavy top basement reflection. Locally the reflection is truncated or includes small escarpments or erosional features. Intra-wedge reflections are fairly weak and discontinuous with a divergent-arcuate or sometimes a divergent planar pattern. Internal sub-sequences can be observed in the inner SDR wedges, with small angular disconformities (e.g. PAD95-01). In the deeper part or the Inner SDRs, high-amplitude continent-ward dipping reflections are observed. They could represent artefacts, deep rotated faulted blocks or dyke swarms. This unit is associated with high gravity anomalies and low magnetic anomalies, except near the Edora Bank.

The Outer Highs contain mounded features with a chaotic internal reflection configuration. Usually they are observed between the Inner and Outer SDRs. Locally faults can be interpreted and clinoforms, which may represent lava delta, are imaged along the WHM.

Two main sets of SDR units are observed along the WHM. The seismic characteristics of both seismic wedges are relatively similar. However the Outer SDRs are smaller with weaker, less prominent internal reflections. Along the WHM, the Outer SDRs are located along the C24 magnetic anomalies close to the oceanic crust characterised by transparent internal seismic facies. The Outer SDRs usually coincide with the C24 magnetic anomaly and correlates with low gravity anomalies.

The nature of the characteristic seismic units identified within the volcanic seismic response may represent variation in volcanic morphology and emplacement conditions (Planke et al., 2004).

The Inner SDRs likely represent flood basalts and fluvial sediment emplaced in a subaerial setting. Erosional features observed on the PAD lines, between the Inner SDR and the Landward Flows, confirm the shallow setting of the Inner SDR. The Outer High probably represents hyaloclastic flows and volcano-clastics and fragmented basalts emplaced in a shallow marine to subaerial environment. Hole 554A drilled ~82 m into the Outer High, recovering volcano-clastic conglomerates and sandstones, interbedded with sub-marine lava flows, emplaced just below wave base. The Outer SDRs represent flood basalts mixed with pillow basalts, sediments and sills emplaced in a deeper marine environment.

A model for the formation of the volcano-stratigraphic sequences ascribes their shape to lava extrusion from an oceanward source with the seaward dip resulting from the progressive subsidence of the extruded lava.

Planke et al. (2000) propose several volcanic stages to explain the development of these shallow structures, imaged along the WHM:

- The onset of explosive volcanism including the development of the Landward Flows.

- The onset of effusive subaerial volcanism, rapidly infilling the rift system along the break-up and forming the inner SDR wedge.

- Explosive shallow marine volcanism occurring during the subsidence of the margin, forming shallow marine (surtseyan-type) deposits, imaged as the Outer SDRs.

The development of vertical and lateral feeder dykes of the Inner SDR volcanic system resulting in a steep, landward-dipping reflection.

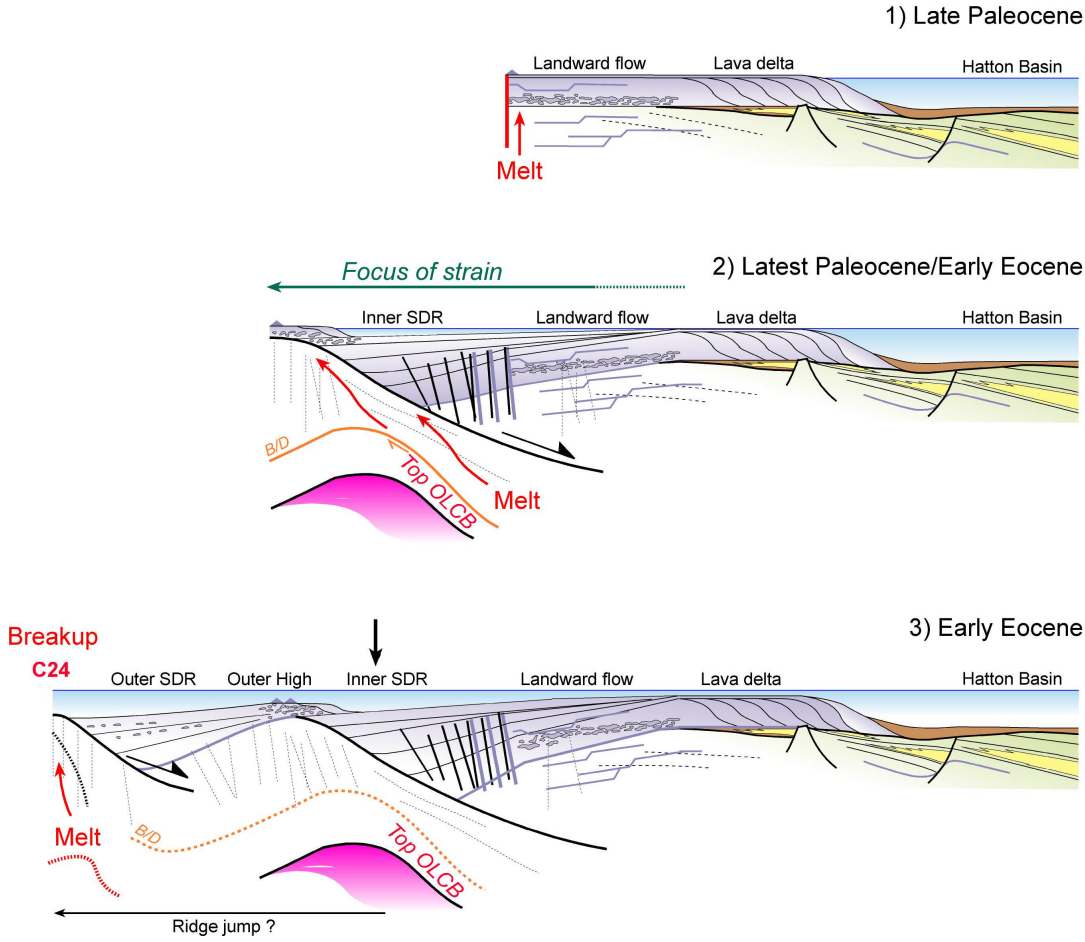

Figure 26: Schematic emplacement model for the formation of the shallow volcanic structures on volcanic margins. (After Planke et al., 2000).

Thin and intruded sediments and continental crust typically underlie the Inner SDR wedges. In our structural interpretation, the transition between the continent and the oceanic crust is estimated to span 25 - 30 km if it is assumed that the SDRs are built on oceanic crust, or roughly 40 - 50 km if the crust beneath seaward-dipping reflector sequences is continental. In non-volcanic “Galician”-type margins, crustal stretching is usually marked in the upper crust by arrays of continent-ward tilted blocks limited by seaward-dipping normal faults (Figure 27a). Stretching over distances of up to 200 km

accommodates the progressive crustal thinning towards the continent-ocean boundary. In the case of the WHM, the distance over which stretching exists is less than 200 km.

The thick volcanic system has been mapped. The Inner SDRs and Landward Flows are wider in the southern part of the WHM, where the lava plateau merges with the Edora Bank, which is interpreted here as the main feeder complex of the WHM (probably a shield-volcano). It is also pertinent to note that this main volcanic complex fits with a triangular bathymetric depression in the southwestern spur of the Rockall Plateau, which could represent the northern prolongation of the SRHM. In other words, the distribution of the Inner SDRs could therefore be controlled by reactivated grabens formed earlier in Cretaceous time.

3.3.4 Deep Structures

A literature review, combined with a reinterpretation of previously published data suggest that the margin located in the western part of the Rockall Plateau can be classified as a volcanic-type margin. Seismic sequences interpreted as SDRs along the Hatton margin, the huge amount of magmatic bodies observed and drilled in the area and the low post-breakup subsidence recorded along the WHM strongly confirm the volcanic nature of this margin (White, 1992; Barton and White, 1997).

Volcanic margins are part of large igneous provinces, characterised by massive occurrences over a short time interval of mafic extrusives and intrusive rocks (Robert and Montadert, 1979; White and McKenzie, 1989; Holbrook and Keleman, 1993; Eldholm et al., 2000). Volcanic margins differ from classical passive margins by a number of characteristics (Figure 27), such as (a) the huge volume of magma formed during the early stages of accretion along the future spreading axis, typically as seaward-dipping reflector sequences (SDRs) (Mutter et al., 1982), (b) the lack of strong passive margin subsidence during and after break-up, and (c) the presence of underplating (Planke et al., 1991; Eldholm et al., 2000).

Geophysical evidence of underplating is usually linked with anomalously high lower crustal seismic P-wave velocities (7.1 - 7.8 km s^{-1}), defining lower crustal bodies (LCBs) (Mutter et al., 1984; Planke et al., 1991; Holbrook and Keleman, 1993; Eldholm et al., 2000).

LCBs are recognised in several parts of the Hatton Basin and along the WHM. Massive and scattered LCBs are observed beneath the volcanic complexes imaged along the WHM. Other LCBs are located beneath the Hatton Basin and between the Fangron and the Lorien Highs. The location of LCBs is usually in good agreement with potential field anomalies suggesting that they represent also high density and locally highly magnetic features. The deep structures of the Outer High and outer SDR features are underlain by massive LCBs interpreted as breakup underplating previously suggested by the RAPIDS 2 results (Vogt et al., 1996; Shannon et al., 1999).

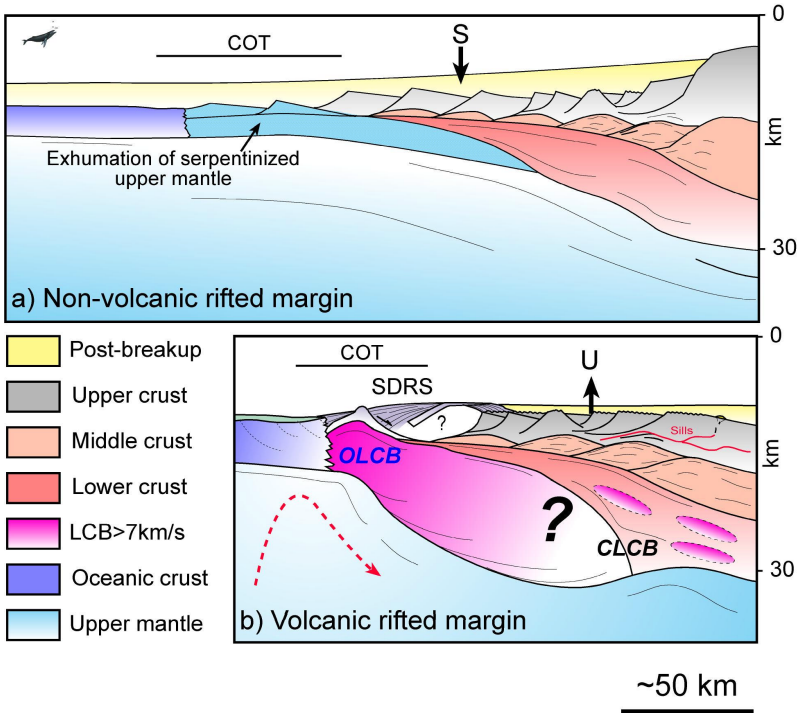

Figure 27: Main characteristic of volcanic margins versus non-volcanic passive margin. (a) Schematic crustal section of a wide non-volcanic "Galician type" margin characterised by the progressive exhumation of the underlying serpentinized mantle. (b) Structure and main characteristics of a narrow volcanic "Norwegian type" margin. CLCB: Continental lower crustal body; OLCB: Oceanic lower crustal body; SDRs: Seaward Dipping Reflectors. (S) The post-break-up subsidence of the non-volcanic margin, (U) the relative uplift recorded along the volcanic margin as an isostatic consequence of thick high velocity underplating observed along the continent-ocean transition (COT).

Gravity modelling using the PAD95-01 seismic line for the shallow structure suggests that a deep, high density body is required to explain the long wavelength gravity anomaly observed along the WHM (see Figure 28a). This density anomaly fits very well with the LCB identified by the RAPIDS 2 transect (Figures 28 and 29) (Shannon et al., 1999) located in the trend of the PAD95-01 line. Compared to the previous interpretation of the RAPIDS 2 profile, the new PAD line suggests that the wedge indicated by the wide-angle model represents the Inner SDR wedge of the line PAD95-01. It was previously interpreted as a sedimentary wedge during the first RAPIDS experiment (O'Reilly et al., 1996).

Preliminary results of the inversion along the HADES profile P1 (Figure 30) suggest that the deeper part of the margin is more complex than resolved by the older and less dense RAPIDS 2 data. The model suggests the existence of several separate LCBs beneath the SDRs wedge (see also report for HADES project P1). LCBs are also observed in the Hatton Basin itself and along the Cólmán Basin.

The most popular idea is to interpret the LCBs as magmatic underplating that represents both ponded magmatic material trapped beneath the Moho and magmatic sills injected into the lower crust (White and McKenzie, 1989; Cox, 1993; Rutter et al., 1993; Thybo et al., 2000).

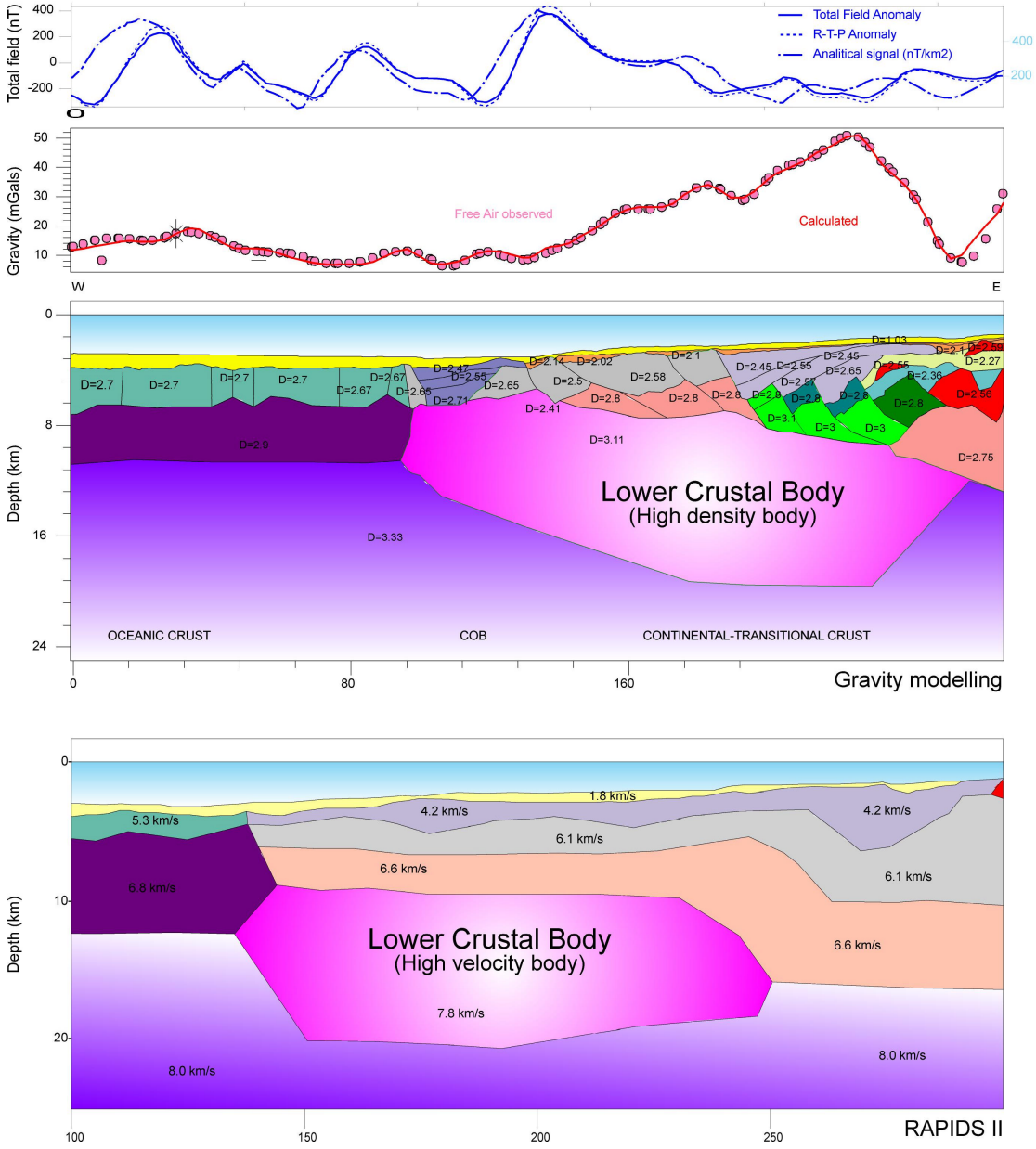

Figure 28: (a) Crustal structure of the WHM derived from gravity modelling. The deeper crustal structure is constrained by the RAPIDS 2 data while the shallow structures is refined by the higher resolution seismic reflection dataset of the coincident and recent PAD95-01 profile. The model is quite similar to the velocity model obtained during the RAPIDS 2 experiment. (b) Velocity model of the West Hatton Margin (RAPIDS 2).

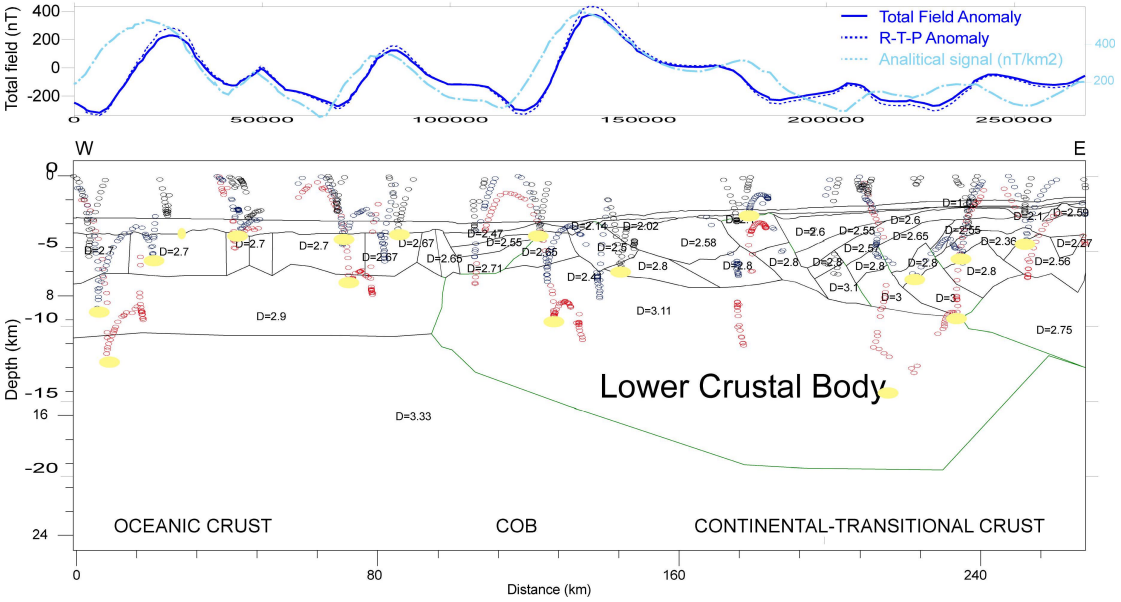

Figure 29: Magnetic signature, filtering and Euler deconvolution along the PAD95 line 01. Results from the Euler deconvolution are not very convincing.

The high velocities (Vp > 7 km s^{-1}) and the thickness of the LCBs are often used to support a mantle plume effect, leading to the formation of huge amount of magmatic rocks (White and McKenzie, 1989; Eldholm and Grue, 1994). The potential temperature of the mantle is obviously one factor that may explain the geophysical characteristics of the LCBs, but alternative models involving high extension rates, or small-scale convection in the upper mantle may however explain significant melt production (McKenzie and Bickle, 1988; Wilson, 1993; Boutillier and Keen, 1999; Korenaga, 2004; Bick and Pamentier, 1986, Pedersen and van der Beek, 1994; Van Wijk et al., 2001; Nielsen and Hopper, 2004; Foulger et al., 2005).

For the LCBs located along the continental-ocean transition of the WHM, breakup-related underplating is reasonable since there is a close temporal and spatial relationship between them and the SDRs, dated as Palaeocene - Eocene in age. In the other parts of the Hatton Basin, the nature and timing of the formation of the LCBs is probably more complex. Underplating is one possibility, but, as discussed by Gernigon et al. (2003, 2004), high Vp values in the lower crust may be better explained as serpentinized upper mantle (as suggested in the Rockall Basin by Hauser et al.,1995) or as high velocity metamorphic rocks like HP-HT eclogites.

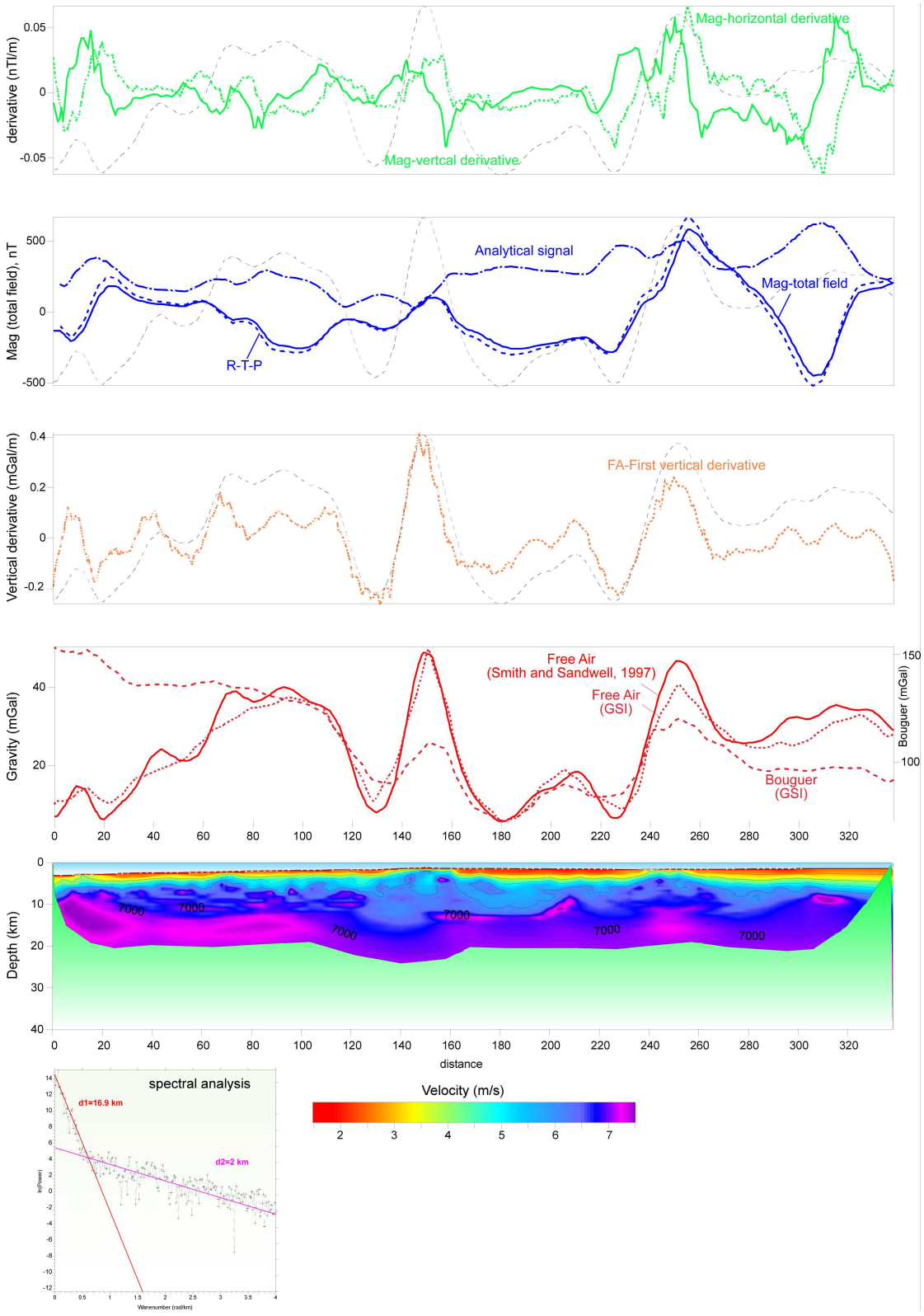

Figure 30: Gravity and magnetic variations (from Sandwell and Smith, 1997) and Verhoef et al., 1996, respectively) along the HADES Profile 1 (see Report for Project P1). Note the structure in the lower crustal high velocity body between distances ~0-100 km suggesting the possibility of two distinct lower crustal bodies, and the high velocity lower crust beneath the SRDS wedges.

3.3.5 Conjugate system: the SE Greenland margin

Shallow structure

Before the breakup and the opening the Iceland Basin, the WHM system was the conjugate system of the southeast Greenland margin. The conjugate margin is characterized by well-developed SDRs (Figure 31) in a wide zone across the shelf and in the adjacent offshore region. A more complete tectonic and magmatic sequences from pre-rift to post-rift is now better constrained by the results from the DSDP Legs 152 and 163 drilling transect (Larsen et al., 1999; Larsen and Saunders, 1998). The results showed that the SDRs were formed by subaerial or shallow marine lavas produced from a fairly narrow, Iceland-type spreading centre. A smooth, basement reflector steps down to the northwest between sites 989 and 917 along the inner part of the primary transect (Planke and Alvestad, 1999). The position of this reflector beneath and landward of the SDRs indicates that it relates to the lower continental succession (Landward Flows). A weak basal reflector, drilled at site 917, occurs at the base of this volcanic complex. Reflection profiles and gravity models indicate significant thinning of the continental crust within a narrow 25 km-wide continent-ocean transition zone seaward from site 917 (Larsen et al., 1999). Seaward of the continent-ocean boundary (COB), two well-defined SDR units, similar to those of the WHM, have been observed, separated by a 20-km-wide zone with more disrupted reflectivity. Drilling during Legs 152 and 163 sampled the feather edge and the central part of the SDRs, recovering mainly basaltic lavas that were exclusively subaerially-erupted (Larsen et al., 1988; Larsen et al., 1994; Duncan et al., 1996). Site 918 drilled 121 m into the volcanic basement, recovering 21 basaltic lava flows, and site 917 penetrated 779 m of basalts and dacites of Late Palaeocene age (61 Ma). The four shallow basement sites along the inner part of the transect (sites 915, 916, 989, 990) all terminated within the Inner SDRs and numerous subaerially-emplaced basaltic lava flows were recovered (Figure 31). Drilling results indicate that the SDRs comprise a lowermost (innermost) continentally-contaminated lava sequence followed by an upper series of picrites (MgO rich rocks) and tholeiites with minor continental contamination. These drilling results allowed the refinement of the evolution of the WHM conjugate system (Larsen and Saunders, 1998; Tegner et al., 1999). The tectono-magmatic calendar includes a continental-type volcanism at ~61-60 Ma, a syn-breakup volcanism beginning at ~57 Ma, and a post-breakup volcanism at ~49.6 Ma. There is an apparent time gap of ~3-4 m.y. between the Middle Series of Landward Flows and the main seaward SDR series.

Deep structure

In the deeper part of the margin, published results of the SIGMA project (Seismic Investigation of the Greenland Margin) (see Figures 32 - 34) facilitates an insight into the conjugate margin architecture (Korenaga et al., 2000; Holbrook et al., 2001, Hooper et al., 2003). P-wave velocity models were derived by inverting travel times of refractions and wide-angle reflections recorded by the ocean-bottom instruments and onshore seismometers (Korenaga et al., 2000).

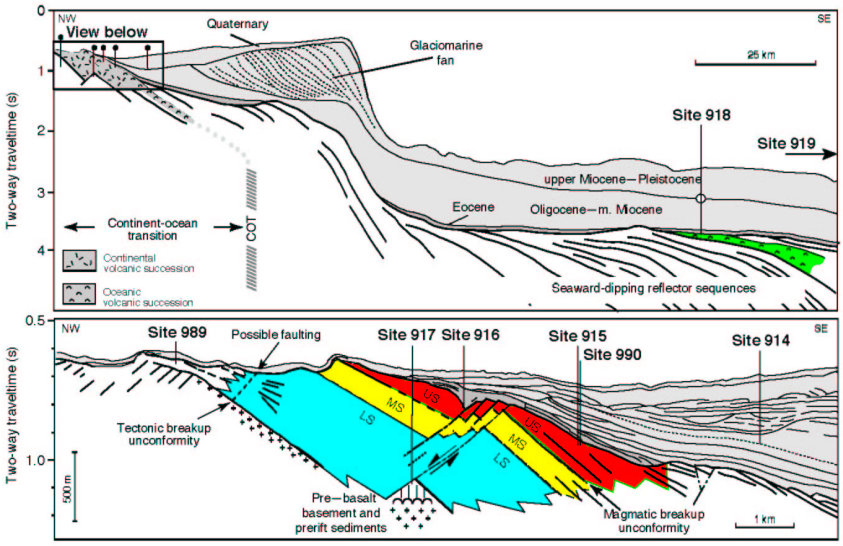

Figure 31: Interpreted cross-section along the EG63 transect (after Duncan et al., 1996).

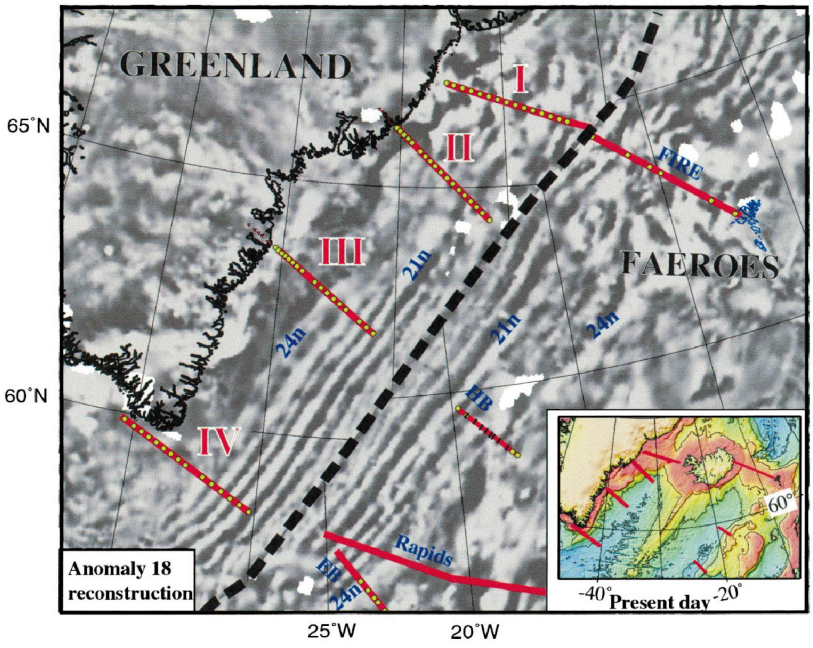

Figure 32: Location of SIGMA seismic profiles 1 - 4 and profiles on the conjugate Faroe-Hatton-Rockall margins, on anomaly 18 (~40 Ma) reconstruction of the North Atlantic. Shading represents positive (light) and negative (dark) magnetic anomalies. Anomalies 21n and 24n are labelled. FIRE, Faroe-Iceland Ridge Experiment (Smallwood, 1999); HB, Hatton Bank (White et al., 1987); EB, Edoras Bank (Barton and White, 1997); Rapids (Vogt et al., 1986). Inset shows profile locations on present-day bathymetry. Circles represent ocean-bottom seismic instruments; short solid lines represent expanding spread profiles on the HB transect. (Map from Holbrook et al., 2001).

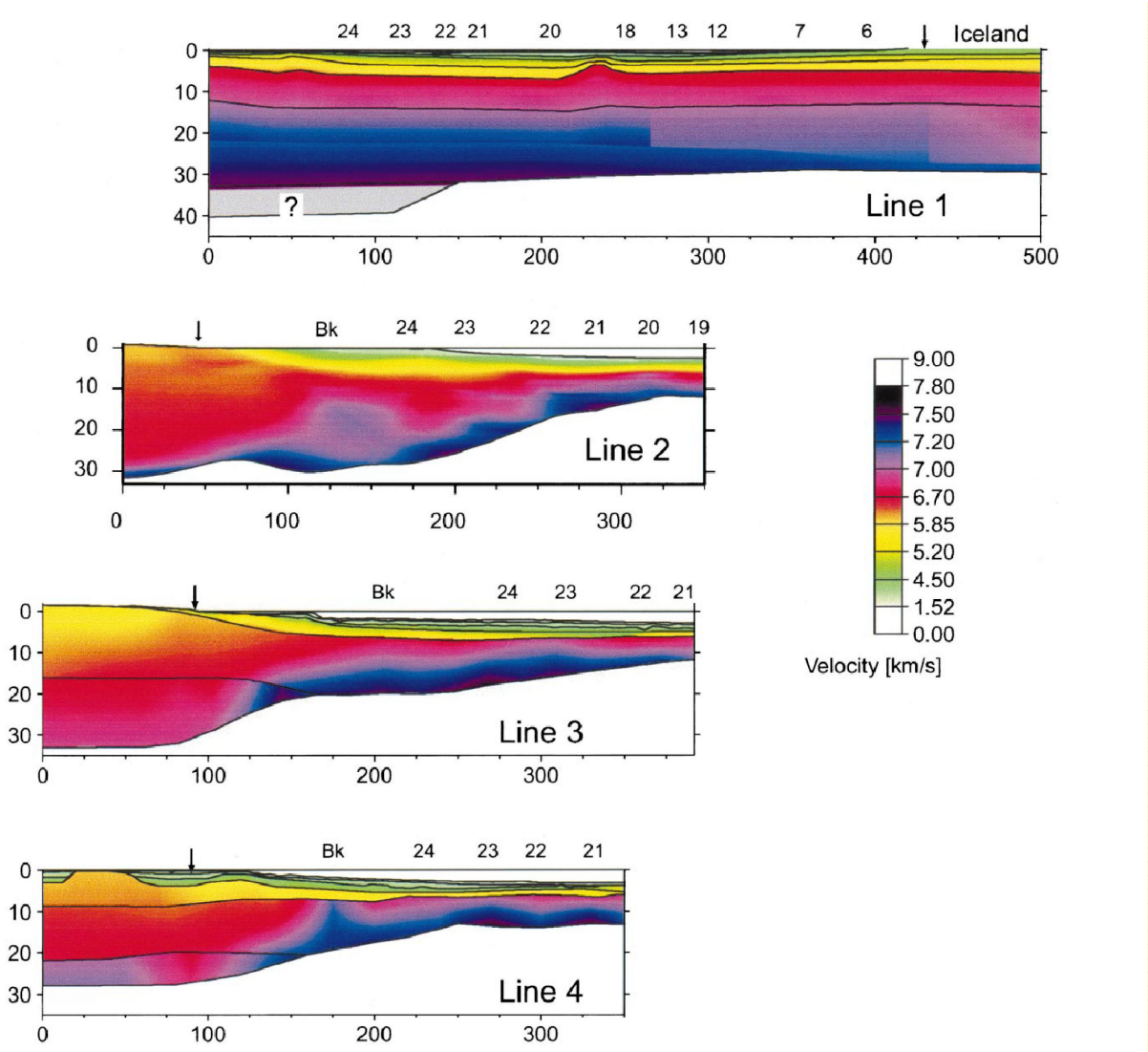

Figure 33: P-wave velocity models for the four SIGMA transects (Holbrook et al., 2001). Horizontal and vertical scales in km. Arrows show coastlines (projected on Line 4). Numbers along top of models (e.g., 24, 23, etc.) are magnetic anomalies; Bk, interpreted breakup position (100% igneous crust). Colour bar shows P-velocity values in km/s. Transect 2 also published as Plate 1 in Korenaga et al. (2000).

Along the conjugate system, the wide occurrence of thick igneous crust, including high-velocity lower crust (LCB) and a thick extrusive layer with the SDRs and onshore lava flows, confirms that the southeast Greenland margin is volcanic along its entire length. Along the SE Greenland margin the four SIGMA transects image high-velocity lower crust (LCBs). Two crustal zones have been defined (Holbrook et al., 2001):

- A hotspot-proximal zone (SIGMA 1) with consistently thick (~30 - 33 km) crust and LCB.

- A distal zone (SIGMA 3 and 4) with more modest LCB thickness (10 - 20 km).

- A transition zone characterised by SIGMA 2. Its maximum crustal thickness (~ 30 km) is initially close to that of SIGMA 1 but decreases over 10 - 12 Myr just after the C24 magnetic anomaly to only 8 - 9 km, similar to SIGMA 3 and 4.

Comparison of the SIGMA profiles with profiles in approximately conjugate positions on the Irish and UK margins along Rockall are relevant for our understanding of volcanic margin evolution. The SIGMA-3 profile (Figure 34) shows a 150-km-wide zone of thick igneous crust, in contrast to a 50 km-wide zone on the conjugate WHM profiles published by Fowler et al. (1989), Morgan et al. (1989) and Smith et al. (2005) in the UK sector (the iSIMM experiment). Smith et al. (2005) and Hooper et al. (2003) suggested an asymmetric vision of the conjugate Rockall-Greenland system. Hooper et al. (2003) suggested major ridge jumps after spreading which could be ruled out by the lack of dip reversals in SDRs on the profile (Holbrook et al., 2001). An apparent asymmetry in the timing of peak magmatism may be illusory, because magnetic anomaly identification is uncertain at that latitude seaward of the WHM. SIGMA transects and the WHM profiles, together with the RAPIDS and HADES profiles, may not be perfectly conjugate. It should be noted that the existing data used for the margin symmetry have limited resolution beneath the axis of the Hatton/Edoras Bank. Results of the HADES experiment show a different picture since it images a more complex LCB system at depth. Preliminary results along the HADES profile P1 also show a thin LCB in the oceanic domain located west of the C24. This oceanic LCB could coincide with similar features observed along most of the conjugate transect between C24 and C21 (Holbrook et al., 2001).

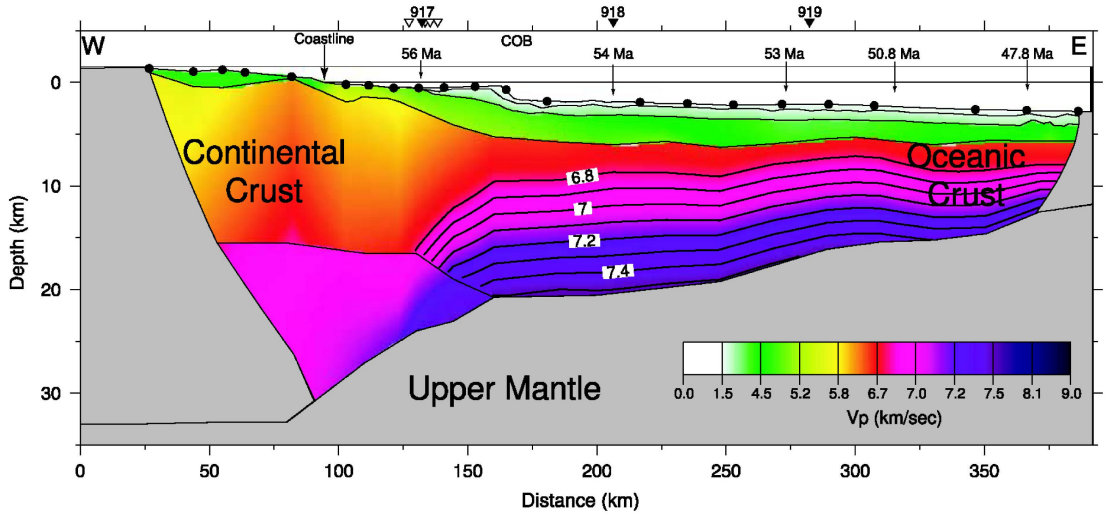

Figure 34: Cross-section along the SIGMA 3 profile from Hopper et al. (2003). Colours are seismic velocities derived from travel time modelling of wide-angle data. Triangles along the top are Ocean Drilling Program Legs 152 and 163 coring locations. Times labelled along the top are from ^{39}Ar-^{40}Ar dating of basalts and from well-defined magnetic anomalies (not shown). This transect shows that the conjugate volcanic margin displays also high velocity lower crust.

3.4 East Thulean Rise (ETR)

The East and West Thulean Rise (Vogt and Avery, 1974) formed just south of the Charlie Gibbs-Fracture Zone between the North Thulean Basin and the Porcupine Abyssal Plain. The same bathymetric feature is observed in the Canadian conjugate system. Although formed in the inside corner of the fracture zone, the ETR and its conjugate are much wider than the typical inside corner highs on transform faults. The ETR and WTR are shorter and wider than the Reykjanes V-shaped ridges but surprisingly seem to present the same kind of steep outward-facing slopes. For the first time, the PAD line 95-09 (Figure 35) allows us to image the WTR. Seismic data show that the WTR represents an oceanic plateau affected by steep west dipping faults. From the bathymetry and the magnetic anomalies, we suggest that these features began to form ca 58 Ma near the fracture zone and then at around 55 Ma in the southern part. The average propagation rate was thus 10mm/year.

Two seismic units are clearly observed, separated by a high-amplitude reflection displaced by the faults. The upper units likely represent Palaeocene and/or Neogene sediments and the lower unit is interpreted as a volcanic plateau, formed during Palaeocene time. Compared to the volcanic system mapped along the WHM, no dipping wedges and SDRs are observed, at least in the eastern part of the rise. The WTR is interpreted to be part of the same igneous province and could have formed in the southern prolongation SDR system, probably influenced by an elongated mantle source of high fertility. However, it is surprising than such volcanic plateau are not observed in the North Thulean Oceanic Basin. Instead, numerous seamounts including the Eriadors, Gondor and Rohan seamounts are observed. They represent scattered feeder systems. The bathymetric expression also suggests that the North Thulean Oceanic Basin subsided more than the WHM and ETR. While there is little information about the deepest part of the WTR, the gravity modelling suggests that the deeper part of the WTR could be denser (2.9 - 3.0 Mg m^{-3}) that a normal oceanic crust (2.7 - 2.8 Mg m^{-3}) in order to explain the gravity highs observed in this area. This may reflect a higher MgO content and partial melting in the oceanic crust.

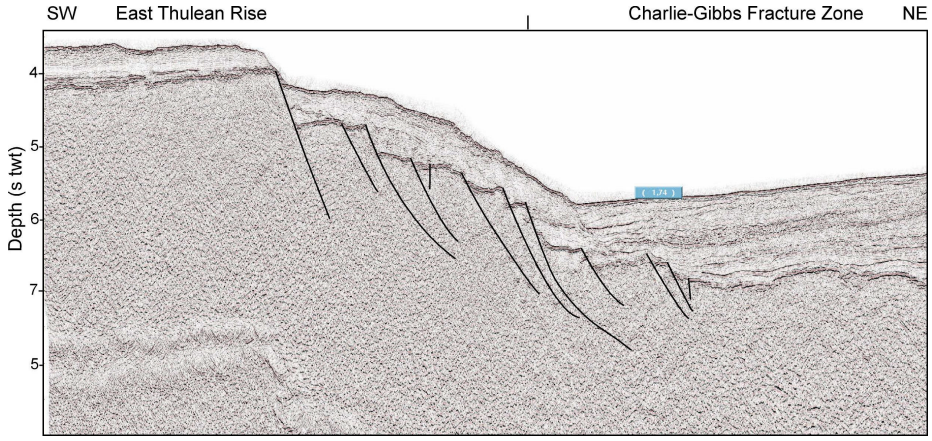

Figure 35: Seismic section across the East Thulean Rise (from PAD95 line 09).

East of the WTR, another bathymetry high is observed and is called the West Thulean Spur (WTS). A deep trough, characterised by low-gravity anomalies, separates the WTR and the WTS. Compared to the WTR, the WTS does not have any conjugate in the Canadian area. It may reflect a dissymmetry between the two systems. Ridge jump is also expected during the formation of the WTR and ETR. The deep through could represent an aborted spreading ridge of the North Thulean Oceanic Basin, shifted to west during the Late Palaeocene breakup.

4 MAGMATISM ALONG THE IRISH MARGINS

4.1 Age of the magmatism

Magmatism is a crucial element for understanding the geodynamic and stratigraphic setting of the Rockall-Hatton area. Due to the lack of calibration, the seismic characteristics of the basalts, sills and volcanic vents were used to constrain the age of the seismic sequences. In this report, we assume that the main magmatic phase is earliest Cenozoic in age. Our calibration therefore suggests that post-lava sequences are Cenozoic in age and pre-lava are most likely Mesozoic in age.

A regional picture emerges of widespread Palaeogene magmatism (Figure 36), stretching from West Greenland through East Greenland to the British Isles and Ireland, which covers a distance of over 2000 km. Large volumes of flood basalts were extruded over the northern half of the Rockall Basin close to the Palaeocene-Eocene boundary. These basalts are the lateral equivalents of the Faroe Plateau Lava. The emplacement of large volumes of volcanic and crustal igneous rocks caused regional tectonic uplift and was associated with changes in sedimentary depositional environments. This was accompanied by a dramatic increase in volcanism prior to breakup and led to the formation of seaward-dipping reflectors (SDRs) in the latest Palaeocene-Early Eocene (Ypresian). Close to the Charlie-Gibbs Fracture Zone, the WTR probably represents a thick Palaeocene oceanic volcanic plateau, uplifted and block faulted during Cenozoic time. It might represent the southern prolongation of the thick volcanic sequences described in the WHM.

The earliest evidence for volcanism related to the Iceland mantle anomaly is the Anton Dohrn Seamount, which is of Maastrichtian age (based on Ar-Ar isotopic dating of dredge samples in the northern part of the Rockall Basin (O'Connor et al., 2000) and dating of calcareous nanoplankton from the chalky infill of lava vesicles (Stoker et al., 1993)). By the end of the Palaeocene, the northern Rockall Trough was "plumbed" with seamounts and underlying or adjacent intrusive complexes. Once again theses huge intrusive complexes, emplaced along pre-existing Caledonian trends, have a much more complex magmatic history since several magmatic pulses from Cretaceous to Palaeocene have been identified by geochronology (O'Connor et al., 2000).

Samples of igneous rocks have been recovered in the Rockall Bank area by the British Geological Survey. They comprise basaltic rocks, gabbro and andesites (Hitchen et al., 2004). The British Geological Survey has also sampled Sandastre but no firm age has been published. However, Hitchen (2004) suggested an early Cenozoic age, similar to that for the Mammal and Swithin centres. The Rockall Islet granite has been also dated at 54.5 Ma (Ritchie and Hitchen, 1996).

The nearly simultaneous timing and duration of widely separated locations of flood basalt magmatism suggests that a mantle plume may have ascended and spread out at velocities 10-100 times faster than the observed crustal spreading rates of several cm/yr. Convection models within a temperature and depth-dependent mantle rheology are consistent with this model, especially if viscous heating of the fast rising plume is included (White and McKenzie, 1989; Larsen et al., 1999).

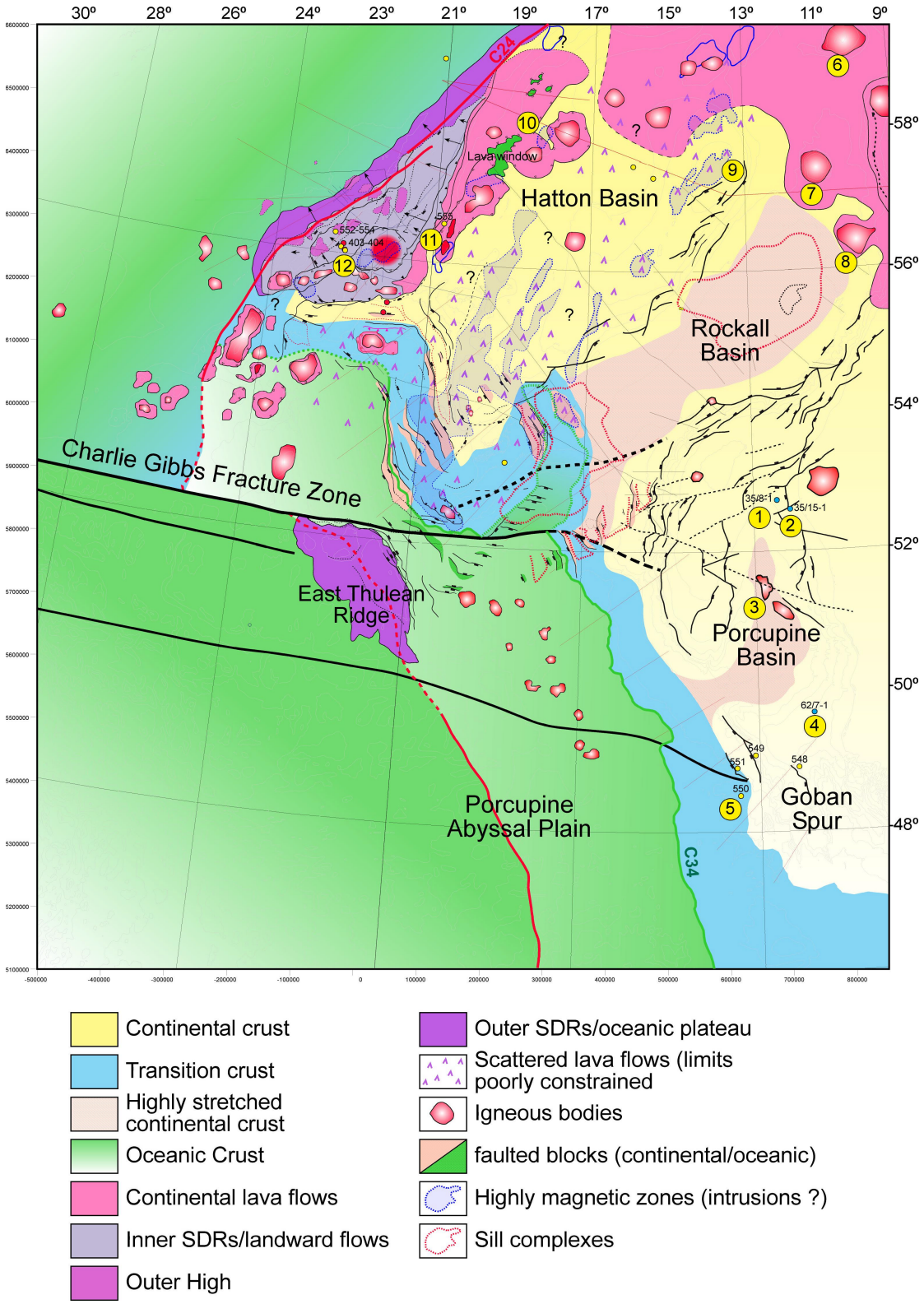

Figure 36: Age of the magmatism along the Rockall-Hatton area. See legend on page 64 or details.

Studies suggest that plume and high mantle temperature are not required to explain the volcanic margin formation. Some geodynamic models can easily explain significant magmatic production without involving any mantle plume effect. The most recent seismic velocity profile across the conjugate SE Greenland margin (Korenaga et al., 2000) indicates an approximately constant mean velocity of 6.9-7.0 km/s within the transitional crust generated by the plume, while its thickness reduces from 25 to 10 km. Melt models require a constant mantle potential temperature of ~1300°C in order to fit the constant mean crustal velocity, coupled with a drastic 8-fold decrease in the ratio of vertical upwelling rate to spreading rate in order to fit the variation in thickness.

Melting of hot plume mantle is then irreconcilable with the crustal structure of the East Greenland margin (Holbrook et al., 2001). Hotter mantle produces a larger amount of melt, with increasing MgO content (due to a larger olivine component in the melt). In general the seismic velocity of igneous crust is mainly controlled by the MgO content, with higher MgO leading to higher crustal seismic velocity. Therefore, there should be a correlation between crustal volume and crustal velocity, if melting anomalously hot mantle produces thick igneous crust (Korenaga et al., 2002). This is not observed on the East Greenland margin part of the North Atlantic igneous province (Holbrook et al., 2001). Clearly something other than the melting of hot mantle plume must also have been involved.

Figure 36, legend: Age of the magmatism along the Rockall-Hatton area.

Numbers refer to numbered locations shown as yellow circles.

1. Albo-Aptian* and Hauterivian-Barremian* tuffs drilled by well 35/8-1 (Tate and Dobson, 1988)
2. Campanian-Maastrichtian* volcanics drilled by well 35/15-1 (Tate and Dobson, 1988)
3. Seismic evidence of Early Cretaceous volcanic ridges, later injected by Cenzoic sills (e.g. Tate and Dobson, 1988)
4. Valanginian** basaltic lavas drilled by well 62/7-1 (Tate and Dobson, 1988)
5. Albian* pillow-lavas drilled by well DSDP 550 (Bailey, 1985)
6. Tertiary volcanic event (52.3-42.5 Ma***) dated on dredged samples along Rosmary Bank (O'Connors et al., 2000)
7. Maastrichtian-Palaeogene volcanic event (70.5-47.7 Ma***) dated on dredged samples from Rosmary Bank (O'Connors et al., 2000)
8. Cenozoic volcanic event (51.2-48.2 Ma***) dated on dredged samples from Hebride Terrace (O'Connors et al., 2000)
9. Sea-bed samples of Late Palaeocene-E. Eocene trachytes/basalts (57.03-52.8 Ma***) (Hitchen, 2004)
10. Seismic evidence of Cenozoic igneous complexes (Hitchen, 2004)
11. Palaeocene-E. Eocene** lavas, hyaloclatites and tuffs drilled during Leg DSDP 81 (Roberts et al., 1981)
12. SDRs imaged and Palaeocene - Early Eocene** volcanics drilled during Leg DSDP 81 (Roberts et al., 1981)

Methods: * biostratigraphy, ** K-Ar, *** Ar-Ar

The limit of the main volcanic province seems to be controlled by the pre-breakup rift architecture. It is very surprising that the SDRs stop along the South Edora Bank area, which is clearly a pre-existing boundary formed before a putative plume impingement beneath the lithosphere expected to be Maastrichtian in age. It is surprising that a mantle plume should stop, by coincidence, exactly at this level. From this observation we can deduce mantle anomalies are only one factor involved in the process of volcanic margin formation. Alternative models to the plume exist. Moderate temperature (1250-1300°C), fertile mantle patches (e.g. eclogites) in the upper mantle, and small-scale convection may explain such melt production without a plume (e.g. Boutillier and Keen, 1999; Anderson et al., 2000; van Wijk et al., 2001; Korenaga, 2002, 2004; Anderson & Natland, 2005; Foulger et al., 2005; Lundin and Doré, 2005).

The Early Cenozoic magmatic event is very significant in the Irish Atlantic Margin and all along the NE Atlantic margin system. Morrissey (2003) presented seismic and geochemical evidence of Early to mid-Cretaceous magmatism in the region and its conjugate margins. However, the magnitude and geographical extent of magmatism in the region are still unclear. Scrutton and Bentley (1988) interpreted a major volcanic event characterised by the Barra Volcanic Ridges System (BVRS). They interpreted the BVRS as volcanic features that were first formed in earliest Cretaceous time prior to significant syn-rift deposition and later affected by volcanics interfingered sediments. After re-interpretation, the possibility cannot be discounted that the seismic reflections, interpreted as volcanics by Scrutton and Bentley (1988), may be sill injections. Sill complexes and acoustically-layered intervals exhibiting seismic velocities of 5.7 - 6.3 km s^{-1} have also been observed throughout the Rockall Basin (Joppen and White, 1990). This layer has been interpreted as massive syn-rift lava flows intercalated with sediments since the velocity is too high for sediments alone (Joppen and White, 1990). Evidence of Palaeogene magmatism (lava flows) is also interpreted along the BVRS. The Barra Volcanic Ridge is a much more complex area, re-interpreted here as a structural horst cut by Early Cretaceous extrusives and intrusives, and subsequently affected by Palaeogene volcanics. In the northern part of the system, there is no clear evidence to support massive magmatic intrusion. The chaotic seismic facies in this area are due to a sub-basalt imaging problem and do not represent any intrusive complex.

The Porcupine Median Volcanic Ridge in the Porcupine Basin has been interpreted to have a similar age, and exhibits clear volcano-stratigraphic features. The ridge has been interpreted as volcanic vents and ridges emplaced in the central part of the rift in early Cretaceous time (Tate and Dobson, 1988; Tate, 1993). However, this interpretation has recently been challenged by Reston et al. (2004) who interpreted the ridge as a “diapiric mud serpentine” structure. We, however, believe that this interpretation is probably incorrect. The seismic facies of the ridge exhibit a chaotic lower unit onlapped by clear, flat, well-layered markers that are not indicative of a diapiric feature, which by definition should be chaotic. The ridge may represent a seamount feature emplaced first in a submarine, then in a subaerial environment (e.g. Tate and Dobson, 1988; Tate, 1993). Magmatic sills and related vents are also observed in the Porcupine Basin. Due to the fact that the events are located close to the C30 horizon, the sills are expected to be Cenozoic in age. This suggests two distinct magmatic events in the Porcupine Basin.

Morrissey (2003) suggested that the highest magnetic anomalies (up to 800 nT) observed along the SRHM and Hatton Basin may represent the lateral distribution of this Early Cretaceous magmatic episode, probably connected with the mantle. Morrissey (2003) noted that these highest magnetic anomalies coincide with similar anomalies observed along the Canadian conjugate margin, located close to the Rockall-Hatton plateau before the breakup. Between the Charlie-Gibbs and Cartwright Fracture zones, a series of similar large positive magnetic anomalies follow the shelf edge (Haworth and Miller, 1982). Most of the shelf region here exhibits positive magnetic anomalies, which appear to connect to the south with linear highs in the Appalachian Dunnage Zone of Newfoundland. This might suggest Palaeozoic mafic to ultramafic rocks as the magnetic source (Haworth and Miller, 1982). However, Pe-Piper et al. (1990) and Balkwill et al. (1990) showed that along the Cartwright Arch the main magnetic anomalies might reflect the geophysical signature of shallow volcanic rocks, drilled along these area and proved to be lower Cretaceous in age.

In the Rockall-Hatton area, the source of the high magnetic anomalies is probably more complex as the last one coincides locally with the presence of Early Cenozoic lava flows (magnetic anomalies along the north BVRS). However, the striking symmetry with the Canadian system is still surprising and we come to the conclusion that the Palaeogene volcanics might develop in the same location as older magmatic terranes (early Cretaceous). Balkwill et al. (1990) showed that on seismic evidence it is also difficult to distinguish this volcanic formation (Alexis Formation) from later Upper Cretaceous - Palaeocene basalts observed in this area and proven to the northwest in the Labrador Sea. This could suggest a kind of localised “magmatic migration pathway”, which is apparently controlled by deep shear zones.

4.2 Petroleum Implications

Exploration in the Rockall-Hatton area is likely to encounter potential targets influenced to some degree by volcanism. This is already occurring to the north in the Faroes-Shetland Basin, the UK Rockall area (Archer et al., 2005) and in the Vøring Margin, off Norway where the sedimentary basins have been strongly affected by volcanic margin processes (Gernigon et al., 2004; Planke et al., 2004). There is certainly a clear need to understand volcanic margin formation and its petroleum implications (e.g. Skogseid, 2001). There are a variety of significant linked effects that arise from volcanic margin formation. The age of the magmatism and its crustal expression are also important points in the Rockall-Hatton area.

4.2.1 Effect 1: Vertical buoyancy forces

Upwelling of the asthenosphere has the potential to produce uplift, partial melting, crustal deformation, movement and emplacement of melts through the lithosphere. This can result in underplating, intrusion and lava flows emplacement, and palaeogeographical changes. Therefore, size, distribution and timing of the magmatism needs to be better constrained.

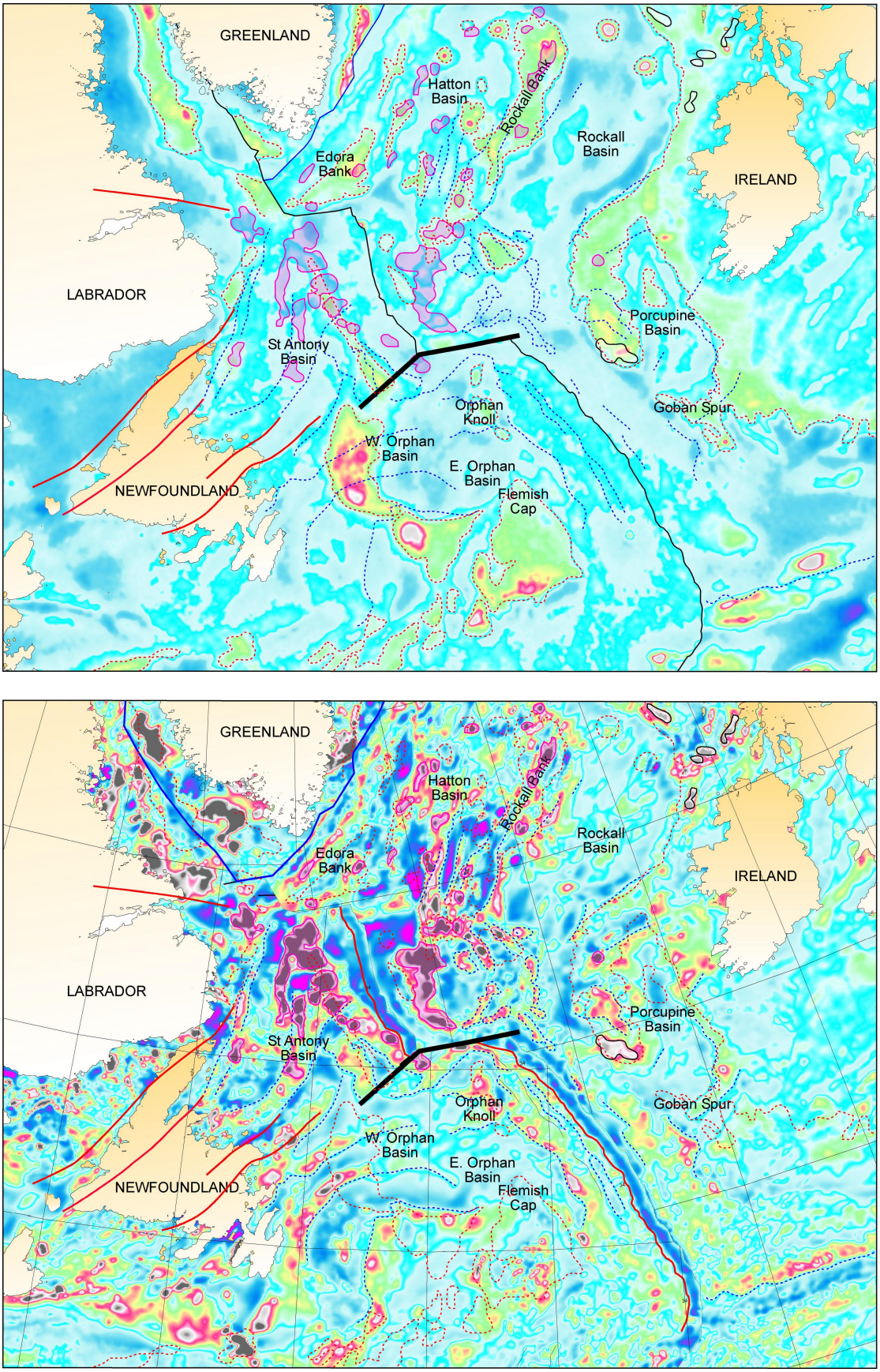

Figure 37: Free-air (upper) and magnetic (lower) anomalies plotted on suggested configuration of Irish and Canadian basins prior to breakup. The main magnetic anomalies are overlain on both maps.

Changes in vertical motion are caused by upwelling of the asthenospheric mantle (small-scale convection) or plume emplacement and can result in regional transport and palaeo-environmental changes that can significantly influence the lithofacies development. When combined with underplating, which is expected along the WHM, the effect can be even more widespread. By analogy with other parts of the North Atlantic margin two main phases of uplift could be expected in the Rockall-Hatton area. A regional uplift during late Maatrichtian - early Palaeocene time, associated with the regional onset of the Iceland mantle anomaly, and a second phase associated with the breakup processes and underplating emplacement in late Palaeocene - early Eocene time.

Modification of the vertical motion is also caused by magmatic underplating, which increase the crustal thickness, causing a permanent buoyancy forces that significantly reduce the post-rift and post-breakup subsidence of the margin (Brodie and White, 1995; Skogseid et al., 1992, 2000). Strong evidence of underplating during rifting comes from petrological indications of both fractionation at lower crustal pressures, temperatures, and crustal contamination occurring during the melt migration into shallow or deep magma chambers. Dynamic evidence of underplating is often proposed to explain surface uplift, massive sand influx and sea level variations and the low subsidence rate that occurs during and after the breakup along volcanic margins and their adjacent areas. A typical thickness of 2 - 5 km of underplating can cause uplift in the range of 0.5 - 1.5 km.

Subaerial basalts drilled by DSDP wells, erosional features and prograding wedges observed on the PAD seismic reflection survey lines suggest that a land-bridge probably stretched along the incipient breakup axis of the WHM. This probably influenced factors such ocean circulation, drainage patterns and the depositional environments in the Rockall-Hatton area. Hitchen et al. (2004) suggest that an uplift of 1500 - 1600 m may have occurred in the Hatton Basin during these periods.

4.2.2 Effect 2: Thermal implications - maturity

Thermal effects and the lack of subsidence of the volcanic margin need to be taken into account in heat flow and hydrocarbon modelling of associated basins. At non-volcanic margins with high extension factors, the crustal heatflow will increase substantially over a relatively long period of time and a simple correlation with the post-rift subsidence (McKenzie 1987) can be used to easily approximate the background heat flow. However, if significant underplating exists, the crustal heat flow can increase significantly over a relatively short period of time (Pedersen et al., 1996). For example, if massive and instantaneous (few Ma) underplating is emplaced at the base of the crust, it can cause a three-fold increase of the heat flow at the base of the basin. This intrinsic thermal effect cannot be predicted with the McKenzie model. Due to the low post-rift subsidence, the McKenzie model predicts, on the contrary, low stretching factors, and as a consequence, low heat flow values. Therefore maturity values for the basin and the petroleum prediction can be significantly different.

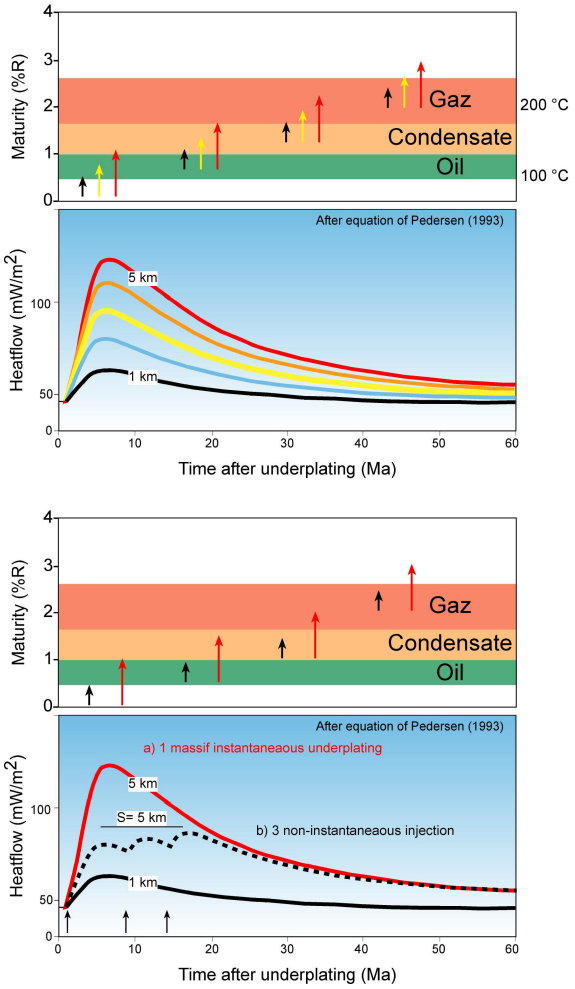

Figure 38: If significant underplating exists, crustal heat flow is greatly increased over a relatively short period of time (Pedersen et al., 1996). Massive and instantaneous (few Ma) underplating at the base of the crust can cause a three-fold increase of the heat flow, otherwise progressive cooling of individual magmatic bodies reduce the thermal effects. Therefore maturity values for the basin and the petroleum prediction can be significantly different.

Other thermal effects related to the sills or other shallow intrusions could be important and can locally increase the level of maturation of organic matter. These effects have been proved in the Vøring Basin (Utgard Well, Norway), where vitrinite reflectance increases near the sill injection. A local example is the well 164/7-1 drilled in the NE Rockall Basin which shows extremely high % Ro values, explained by the thermal effect of a plutonic body intruded in depth (Archer et al., 2004). Svensen (2004) and Planke et al. (2004) have shown that intrusions can also produce heating of host-rock fluids, possibly leading to the formation of hydrothermal vent complexes and fluid escape, locally observed in the Porcupine Basin and near the BVRS. These kinds of pipe-like complexes, locally observed in the Rockall and Porcupine basins can have long-term effects, including differential compaction, oil/gas remigration and compartmentalisation of sedimentary sequences.

5 SUMMARY AND CONCLUSION

5.1 Results

1. A large volume of geophysical data (wide-angle seismic, seismic reflection, gravity and magnetic) have been synthesized to produce an updated regional synthesis. Regional maps have been produced in order to allow comparison to be made. The compilation includes maps of the Irish offshore region and maps at a bigger scale including the conjugate systems (Canada and Greenland).

2. The initial HADES model has been tested with independent data from other datasets (e.g. RAPIDS 2, reflection seismics, gravity and magnetics) which indicate that the model is robust.

3. The Barra Volcanic Ridge System has been re-examined. In the north, the BVRS may represent a structural horst intruded by Cretaceous and Cenozoic sills and dykes.

4. Contrasting margins segments (volcanic and non-volcanic) have been identified and information on their structure, timing and mode of formation has been provided.

5. The South Rockall Hatton Margin segment represents a shear-rifted margin with the characteristics of a non-volcanic margin. Exhumed upper mantle may represent the continental-oceanic transition zone. Compared to the WHM, the volcanism is along this area is moderate.

6. To the west, the volcanic system of the West Hatton Margin has been mapped in detailed and was probably controlled by the pre-breakup configuration of the margin, probably connected to the South Rockall Hatton Margin.

7. Gravity modelling, comparison with previous seismic refraction profiles, the new PAD seismic reflection lines and the preliminary result of the HADES wide-angle seismic profiles confirm the presence of high-density, high-velocity bodies in the deeper part of the margin. The HADES projects bring significant new imaging of the deep crust along the Hatton Basin.

5.2 Suggestions for future work in the region

1. A global tectonic setting, including the Canadian basins, would be a significant step for understanding the geodynamics of the Irish margins and adjacent basins. Accurate plate reconstruction and a better quantification of the regional extension along the conjugate system is desirable.

2. Acquisition of a long-offset reflection line along the HADES transect would be extremely relevant to refine the preliminary results based on tomography.

3. Acquisition of new regional lines along the Hatton Basin and the South Rockall Hatton Margin are required in order to confirm some of our interpretations.

4. Extension of Irish National Seabed Survey gravity and magnetic database from the Goban Spur to the West Hatton Margin would provide valuable regional information to constrain the structure of the southern part of the Irish Atlantic margin.

5. One or two wide-angle transects along the South Rockall Hatton Margin and the East Thulean Rise would help to constrain the melt distribution in this area, which represent the southernmost expression of the North Atlantic Igneous Province.

6. Sampling and dating of some plugs in the southern part of the Hatton Basin (e.g. the Lorien High).

Acknowledgements

This project uses data and survey results acquired during a project undertaken on behalf of the Geological Survey of Ireland (GSI) and the Porcupine Studies Group (PSG) of the Irish Petroleum Infrastructure Programme Group 3. The PSG comprised: Agip Ireland BV, Chevron UK Ltd, Elf Petroleum Ireland BV, Enterprise Energy Ireland Ltd, Marathon International Hibernia Ltd, Phillips Petroleum Company United Kingdom Ltd, Statoil Exploration (Ireland) Ltd and the Petroleum Affairs Division (PAD) of the Department Communications, Marine and Natural Resources. The PAD kindly provided the 2-D seismic data used for this interpretation.

References

Anderson, D. 2000. The Thermal State of the Upper Mantle: No Role for the Mantle Plumes. *Geophysical Research Letters*, **27**, 3623-3626.

Anderson, D.L. and Natland, J.H. 2005. A brief history of the plume hypothesis and its competitors: Concept and controversy. *In*: Foulger G.R., Natland, J.H., Presnall D.C. and Anderson D.L. (eds) Plates, Plumes & Paradigms. *Geological Society of America*, 119-145.

Archer, S.G., Bergman, S.C., Iliffe, J., Murphy, C.M. and Thornton, M. 2005. Palaeogene igneous rocks reveal new insights into the geodynamic evolution and petroleum potential of the Rockall Trough, NE Atlantic Margin. *Basin Research*, **17**, 171-201.

Balkwill, H., McMillan, H., MacLean, B., Williams, G. and Srivastava, S. 1990. Geology of the Labrador Shelf, Baffin Bay and Davis Strait. *In*: Keen, M.J. and Williams, G.L. (eds) *Geology of the Continental Margin of Eastern Canada*. Geological Society of America, **I-1**, 293-348.

Bentley, P.A. and Scutton, R.A. 1987. Seismic investigations into the basement structure of southern Rockall Trough. *In*: Brooks, J and Glennie, K.W. (eds) *Petroleum Geology of North-West Europe*, 667-675.

Blakely, R. 1996. *Potential Theory in Gravity and Magnetic Applications*. Cambridge University Press, 461pp.

Blystad, P., Brekke, H., Faerseth, R., Larsen, B., Skogseid, J. and Tørudbakken, B., 1995, Structural elements of the Norwegian continental shelf, Part II. The Norwegian Sea Region. *Norwegian Petroleum Directorate Bulletin*, **8**, 0-45.

Boillot, G. and Froitzheim, N. 2001. Non-volcanic rifted margins, continental break-up and the onset of sea-floor spreading: Some outstanding questions. *in*: Wilson, R.C.L., Whitmarsh, R.B., Taylor, B. and Froitzheim, N. (eds) *Non-volcanic rifting of continental margins; a comparison of evidence from land and sea*. Geological Society, London, Special Publications, **187**, 9-30.

Boutillier, R.R. and Keen, C.E. 1999. Small-scale convection and divergent plate boundaries. *Journal of the Geophysical Research*, **104**, 7389-7403.

Boutillier, R.R. and Keen, C.E. 1999. Small-scale convection and divergent plate boundaries. *Journal of the Geophysical Research*, **104**, 7389-7403.

Brodie, J. and White, N. 1994. Sedimentary basin inversion caused by igneous underplating: Northwest European continental shelf. *Geology*, **22**, 147-150.

Buck, W. and Parmentier, E. 1986. Convection beneath young oceanic lithosphere: implications for thermal structure and gravity. *Journal of Geophysical Research*, **91**, 1961-1974.

Bull, J.M. and Masson, D.G. 1996. The southern margin of the Rockall Plateau: Stratigraphy, Tertiary volcanism and plate tectonic evolution. *Journal of the Geological Society, London,* **153**, 601-612.

Chalmers, J.A. and Pulvertaft, T.C., 2001. Development of the continental margins of the Labrador Sea: a review. *In*: Wilson, R.C.L., Whitmarsh, R.B., Taylor B. and Froitzheim, N. (eds) *Non-volcanic rifting of continental margins; a comparison of evidence from land and sea*. Geological Society Special Publications, **187**, 77-105.

Chapman, T., Brooks, T., Corcoran, D., Duncan, L. and Dancer, P.N. 1999. The structural evolution of the Erris Trough, offshore northwest Ireland, and implications for hydrocarbon generation. *In*: Fleet, A.J. and Boldy, S.A.R. (eds) *Petroleum geology of northwest Europe: Proceedings of the 5th conference*, The Geological Society, London, 455-469.

Chian, D., I. Reid, I. D. and Jackson, H.R. 2001. Crustal structure beneath Orphan Basin and Crustal structure beneath Orphan Basin and implications for nonvolcanic continental rifting. *Journal of Geophysical Research,* **106**, 10923-10940.

Chian, D. and Louden, K.E. 1994. The continent-ocean crustal transition across the Southwest Greenland margin. *Journal of Geophysical Research*, **99**, 9117-9135.

Cole, J.E. and Peachey, J. 1999. Evidence for pre-Cretaceous rifting in the Rockall Trough: an analysis using quantitative plate tectonic modelling. *In*: Fleet, A.J. and Boldy, S.A.R. (eds) *Petroleum Geology of Northwest Europe: Proceedings of the 5th Conference*. The Geological Society, London, 359-370.

Cooper, G. 2002. An improved algorithm for the Euler deconvolution of potential field data. *The Leading Edge,* **21**, 1197-1198.

Corfield, S., Murphy, N. and Parker, S. 1999. The structural and stratigraphic framework of the Irish Rockall Trough. *In*: Fleet, A.J. and Boldy, S.A.R. (eds), *Petroleum geology of northwest Europe: Proceedings of the Fifth Conference*. The Geological Society, London, 407-420.

Coward, M. 1995. Structural and tectonic setting of the Permo-Triassic basin of northwest Europe. *In*: Boldy, S.A.R. (ed) Permian and Triassic Rifting in Northwest Europe. *Geological Society, London, Special Publications,* **91**, 7-39.

Croker, P. and Shannon, P.M. 1987. The evolution and hydrocarbon prospectivity of the Porcupine Basin, Offshore Ireland. *In*: Brooks, J. and Glennie, K.W. (eds) *Petroleum Geology of North West Europe*. Graham and Trotman, London, 633-642.

Cunningham, G.A. and Shannon, P.M. 1997. The Erris Ridge: a major geological feature in the NW Irish offshore basins. *Journal of the Geological Society, London,* **154**, 503-508.

Dancer, P., Algar, S. and Wilson, I. 1999. Structural evolution of the Slyne Trough. *In*: Fleet, A.J. and Boldy, S.A.R. (eds) *Petroleum Geology of Northwest Europe: Proceedings of the 5th Conference*, Geological Society, London, 445-453.

De Graciansky, P.C. and Poag, C.W. 1985. Geologic history of Goban Spur, Northwest Europe continental margin. Initial Reports DSDP Leg 80, Brest to Southampton. US Government Printing Office (UK distributors, IPOD Committee, NERC, Swindon), 1187-1216.

Dean, K., McLachlan, K. and Chambers, A. 1999. Rifting and the development of the Faeroe-Shetland. *In*: Fleet, A.J. and Boldy, S.A.R. (eds) *Petroleum Geology of Northwest Europe: Proceedings of the 5th Conference*. Geological Society, London, 533-544.

Doré, A., Lundin, E., Jensen, L.N., Birkeland, Ø., Eliassen, P. and Fichler, C. 1999. Principal tectonic events in the evolution of the northwest European Atlantic margin. *In*: Fleet, A.J. and Boldy, S.A.R. (eds) *Petroleum Geology of Northwest Europe: Proceedings of the 5th Conference*. Geological Society, London, 41-61.

Eldholm, O. and Grue, K. 1994. North Atlantic volcanic margins: dimensions and production rates. *Journal of the Geophysical Research*, **99**, 2955-2968.

Enachescu, M.E. 1987. Tectonic and structural framework of the Northeast Newfoundland continental margin. *In*: Beaumont, C. and Tankard, A.J. (eds) *Sedimentary basins and basin-forming mechanisms*. Atlantic Geoscience Society Special Publication, **5**, 117-146.

Enachescu, M., Kearsey, S., Einarsson, P. and Nader, S. 2004. Orphan Basin offshore Newfoundland, Canada: Structural and tectonic framework, petroleum systems and exploration potential. *74 SEG Annual Meeting and Exposition*, expanded abstract, 4pp.

Erratt, D., Thomas, G. and Wall, G. 1999. The evolution of the Central North Sea Rift, *in*: Fleet, A. J. and Boldy, S.A.R. (eds) *Petroleum Geology of Northwest Europe: Proceedings of the 5th Conference*. Geological Society, London, 63-82.

Foulger, G., Natland, J. and Anderson, D. 2005. A source for Icelandic magmas in remelted Iapetus crust. *Journal of Volcanology and Geothermal Research*, **141**, 23-44.

Fowler, S., White, R., Spence, G. and Westbrook, G. 1989. The Hatton Bank continental margin-II. Deep structure from two-ship expanding spread seismic profiles. *Geophysical Journal*, **96**, 295-310.

Funck, T., Larsen, H.C., Louden, K.E., Tucholke, B.E. and Holbrook, S. 2004. Crustal structure of the northern Nova Scotia rifted continental margin (eastern Canada). *Journal of Geophysical Research*, **109**, B09102, 1-19.

Geoffroy L., Callot, J.P., Scaillet, S., Skuce, A., Gélard, J.P., Ravilly, M., Angelier, J., Bonin, B., Cayet, C., Perrot, K. and Lepvier, C. 2001. Southeast Baffin volcanic

margin and the North American-Greenland plate separation. *Tectonics*, **20**, 566-584.

Gernigon, L., Ringenbach, J.C., Planke, S., Gall B.L. and Jonquet-Kolst, O.H. 2003. Extension, crustal structure and magmatism at the outer Voring Basin, Norwegian margin. *Journal of the Geological Society, London*, **160**, 197-208.

Gernigon, L., Ringenbach, J.C., Planke, S. and Le Gall, B. 2004. Deep structures and breakup along volcanic rifted margins: Insights from integrated studies along the outer Vøring Basin (Norway). *Marine and Petroleum Geology*, **21**, 363-372.

Grant, A. and McAlpine, K. 1990. The continental margin around Newfoundland. *In*: Keen, M.J. and Williams, G.L. (eds) *Geology of the Continental Margin of Eastern Canada*. Geological Survey of Canada, Geology of Canada, vol. 2, 239-292.

Grant, S., van der Hilst, R. and Widiyantoro, S. 1997. Global seismic tomography: A snapshot of convection in the Earth. *GSA Today*, **7**, 1-7.

Gunn, P. 1975. Linear Transformations of Gravity and Magnetic Fields. Geophysical Prospecting, **23**, 300-312.

Hauser, F., O'Reilly, B.M., Jacob, A.W.B., Shannon, P.M., Makris, J. and Vogt, U. 1995. The Crustal Structure of the Rockall Trough: Differential Stretching Without Underplating. *Journal of Geophysical Research*, **100**, 4097-4116.

Haworth, R. and Miller, H. 1982. The structure of Paleozoic oceanic rocks beneath Notre Dame Bay, Newfoundland, *In*: St Julien, P. and Beland, J. (eds) *Major Structural Zones and Faults of the Northern Appalachians*. Geological Association of Canada, Special Paper, **24**, 149-173.

Hitchen, K. 2004. The geology of the UK Hatton-Rockall margin. *Marine and Petroleum Geology*, **21**, 993-1012.

Holbrook, W., Larsen, H., Korenaga, J., Dahl-Jensen, T., Reid, I., Kelemen, P., Hopper, J., Kent, G., Lizarralde, D., Bernstein, S. and Detrick, R. 2001. Mantle thermal structure and active upwelling during continental breakup in the North Atlantic. *Earth and Planetary Science Letters*, **190**, 251-266.

Hood, P. 1965. Gradient measurement in aeromagnetic surveying. *Geophysics*, **30**, 891-902.

Hopper, J.R., Lizarralde, D., Korenaga, J., Kent, G.M., Kelemen, P.B., Dahl-Jensen, T., Holbrook, W.S. and Larsen, H.C. 2003. Structure of the SE Greenland margin from seismic reflection and refraction data: Implications for nascent spreading center subsidence and asymmetric crustal accretion during North Atlantic opening. *Journal of Geophysical Research*, **108**, 13-22.

Jackson, H.R., Keen, C.E., Falconer R.K. and Appleton K.P. 1979. New geophysical evidence for sea-floor spreading in central Baffin Bay. *Canadian Journal of*

Earth Sciences, **16**, 2122-2135.

Jansen, E., Kringstad, L., Sejrup, H. and Lang, K. 1986. Paleo-oseanografiske endringer i Norskehavet og Nord-Atlanteren i Neogene og Kvartaer; DSDP Leg 94 and ODP Leg 104 (Translated Title: Palaeo-oceanographic alteration of the Norwegian North Atlantic Neogene and Quaternary; DSDP Leg 94 and ODP Leg 104), 62.

Johnston, S., Doré, A.G. and Spencer, A.M. 2001. The Mesozoic evolution of the Southern North Atlantic region and its relationship to basin development in the South Porcupine Basin, offshore Ireland. *In*: Shannon, P.M., Haughton, P.D.W. and Corcoran, D.V. (eds) *The Petroleum Exploration of Ireland's Offshore Basins*. Geological Society Special Publication, **188**, 237-263.

Oppen, M. and White, R.S. 1990. The structure and subsidence of Rockall Trough from two-ship seismic experiments. *Journal of Geophysical Research*, **95**, 19,821-19,837.

Keen, C.E. and Dehler, S.A. 1993. Stretching and subsidence; rifting of conjugate margins of the North Atlantic region. *Tectonics*, **12**, 1209-1229.

Kittilsen, J.E., Olsen, R., Marten, R., Hansen, E. and Hollingsworth, R. 1999. The first deepwater well in Norway and its implications for the Upper Cretaceous Play, Vøring Basin, *In*: Fleet, A.J. and Boldy, S.A.R. (eds) *Petroleum Geology of Northwest Europe: Proceedings of the 5th Conference*. Geological Society, London, Special Publications, 276-280.

Koch, J. and Heum, O., 1995, Exploration trends of the Halten Terrace. *In*: Hanslien, S. (ed) *Petroleum Exploration and Exploitation in Norway*. Norsk Petroleums Forening/NPF, Special Publications, **4**, 235-251.

Korenaga, J. 2004. Mantle mixing and continental breakup magmatism. *Earth and Planetary Science Letters*, **218**, 463-473.

Korenaga, J., Holbrook, W.S., Kent, G.M., Kelemen, P.B., Detrick, R.S., Larsen, H.C., Hopper, J.R. and Dahl, J.T. 2000. Crustal structure of the Southeast Greenland margin from joint refraction and reflection seismic tomography. *Journal of Geophysical Research*, **105**, 21,259-21,614.

Larsen, H.C. and Saunders, A. 1998. Tectonism and volcanism at the southeast Greenland rifted margin: A record of plume impact and later continental rupture, *In*: Saunders, A.D., Larsen H.C. and Wise S.R. (eds) *Proceedings of the Ocean Drilling Program, Scientific Results, College Station, TX (Ocean Drilling Program)*, 152, 503-533.

Larsen, H.C., Duncan, R.A., Allan, J.F. and Brooks, C.K. 1999. Proceedings, Scientific Results, Ocean Drilling Program, Leg 163, southeast Greenland Margin. *Proceedings of the Ocean Drilling Program: Scientific Results*, **163**, 1-173.

Laughton, A.S., Berggren, W.A. et al., 1972, Initial Reports of the Deep Sea Drilling Project 12. US Government Printing Office, Washinghton, DC, **12**, 395-671.

Lawver, L. and Müller, R. 1994. Iceland hotspot track. *Geology*, **22**, 311-314.

Louden, K.E., Tucholke, B.E. and Oakey, G.N. 2004. Regional anomalies of sediment thickness, basement depth and isostatic crustal thickness in the North Atlantic Ocean. *Earth and Planetary Science Letters*, **224**, 193-211.

Ludwig, W., Nafe, J. and Drake, C. 1970. Seismic refraction. *In*: Maxwell, A.E. (ed) *The Sea, Volume 4*. Wiley-Interscience, New York, 53-84.

Lundin, E. R. and Dore, A.G. 2005. Fixity of the Iceland "hotspot" on the Mid-Atlantic Ridge; observational evidence, mechanisms, and implications for Atlantic volcanic margins, *In*: Foulger, G.R., Natland, J.H., Persnall, D.C. and Anderson, D.L. (eds) *Plates, plumes, and paradigms*. Special Paper, Geological Society of America, **388**, 627-651.

Mackenzie, G.D., Shannon P M., Jacob, A.W.B., Morewood, N.C., Makris, J., Gaye, M. and Egloff, F. 2002. The velocity structure of the sediments in the southern Rockall Basin: Results from new wide-angle seismic modelling. *Marine and Petroleum Geology*, **19**, 989-1003.

Martinius, A., Kaas, I., Næss, A., Helgesen, G., Kjærefjord, J. and Leith, D. 2001. Sedimentology of the heterolithic and tide-dominated Tilje formation (Early Jurassic, Halten Terrace, offshore mid-Norway), *In*: Martinsen, O. and Dreyer, T. (eds) *Sedimentary Environments Offshore Norway-Palaeozoic to Recent*. Norsk Petroleums Forening, Special Publications, **10**, 103-144.

Masson, D.G. and Kidd, R., 1986, Revised Tertiary seismic stratigraphy of the Southern Rockall Trough. *Initial Reports, Deep Sea Drilling Project*. US Government Printing Office, Washinghton, DC, **44**, 1117-1126.

McDonnell, A. and Shannon, P.M. 2001. Comparative Tertiary stratigraphic evolution of the Porcupine and Rockall basins. *In*: Shannon, P.M., Haughton, P.D.W. and Corcoran, D.V. (eds) *The Petroleum Exploration of Ireland's Offshore Basins*. Geological Society, London, Special Publications, **188**, 323-344.

McKenzie, D. and Bickle, M. 1988. The volume and composition of melt generated by extension of the lithosphere. *Journal of Petrology*, **29**, 625-679.

Montadert, L., Roberts, D.G. 1979. *Initial Reports of the Deep Sea Drilling Project*, **48** U.S. Governement Printing Office, Washington, 0-1183.

Morewood, N., Shannon, P.M. and Mackenzie, G.D. 2004. Seismic stratigraphy of the southern Rockall Basin: a comparison between wide-angle seismic and normal incidence reflection data. *Marine and Petroleum Geology*, **21**, 1149-1163.

Morgan, J.V., Barton, P.J. and White, R.S. 1989. The Hatton Bank continental margin: III, Structure from wide-angle OBS and multichannel seismic refraction profiles.

Geophysical Journal International, **98**, 367-384.

Morris, P. 1989. A composite magnetic map of Ireland. *Communications of the Dublin Institute for Advanced Studies, Series D, Geophysical Bulletin*, **42**.

Morrissey, T. 2003. *Cretaceous and early Tertiary igneous activity and the geological evolution of the North Atlantic region*. PhD thesis, University College Dublin, Ireland.

Morton, N. 1989. Jurassic sequence stratigraphy in the Hebrides Basin, NW Scotland. *Marine and Petroleum Geology*, **6**, 243-260.

Murphy, C. 1993. Report on the compilation, processing and preliminary interpretation of magnetic data for both onshore and offshore Ireland. *Report AGP 91/4*, Applied Geophysics Unit, University College, Galway, Ireland.

Musgrove, F. and Mitchener, B. 1996. Analysis of the pre-Tertiary rifting history of the Rockall Trough. *Petroleum Geosciences*, **2**, 353-360.

Nabighian, M.N. 1972. The Analytic Signal of Two-Dimensional Magnetic Bodies with Polynomial Cross-Sections: Its Properties and Use for Automated Anomaly Interpretation. *Geophysics*, **37**, 505-517.

Nadin, P.A., Kusznir, N.J. and Cheadle, M.J. 1997. Early Tertiary uplift of the North Sea and Faeroe-Shetland Basins. *Earth and Planetary Science Letters*, **148**, 109-127.

Naylor, D. and Shannon, P.M. 2005, The structural framework of the Irish Atlantic margin, *In*: Doré, A.G. and Vining, B. (eds) *Petroleum Geology: North-West Europe and Global Perspectives: Proceedings of the 6th Petroleum Geology Conference*. Geological Society, London, 1009-1021.

Naylor, D., Shannon, P.M. and Murphy, N. 1999. Irish Rockall region - a standard structural nomenclature system. *Petroleum Affairs Division. Special Publication*, **1/99**, 42pp.

Neish, K. 1993. Seismic structure of the Hatton-Rockall area: an integrated seismic/modelling study from composite datasets. *In*: Parker J.R. (ed), *Petroleum Geology of Northwest Europe: Proceedings of the Fourth Conference*. The Geological Society, London, 1047-1056.

Nielsen, T.K. and Hopper, J.R. 2004. From rift to drift; mantle melting during continental breakup. *Geochemistry, Geophysics, Geosystems - G3*, **5**, 1-24.

Nielsen, T.K., Larsen, H.C. and Hopper, J.R. 2002. Contrasting rifted margin styles south of Greenland: implications for mantle plume dynamics. *Earth and Planetary Science Letters*, **200**, 271-286.

O'Reilly, B.M., Hauser F., Jacob, A.W.B. and Shannon, P.M. 1996, The lithosphere below the Rockall Trough: wide-angle seismic evidence for extensive

serpentinisation. *Tectonophysics*, **225**, 1-23.

O'Connor, J., Stoffers, P., Wijbrans, J.R., Shannon, P.M. and Morrissey, T. 2000. Evidence from episodic seamount volcanism for pulsing of the Iceland plume in the past 70 Myr. *Nature*, **408**, 954-958.

Pedersen, T. and van der Beek, P. 1994. Extension and magmatism in the Oslo Rift, SE Norway: No sign of a mantle plume. *Earth and Planetary Science Letters*, **123**, 317-329.

Pedersen, T., Heeremans, M. and Van der Beek, P. 1996. Models of crustal anatexis in volcanic rifts: applications to southern Finland and the Oslo graben, southeast Norway. *Geophysical Journal International*, **132**, 239-255.

Pe-Piper, G., Piper, D.J.W., Keen, M.J. and McMillan, N. 1990. Igneous rocks of the continental margin. *In*: Keen, M.J. and Williams, G.L. (eds) *Geology of the Continental Margin of Eastern Canada*. Geological Survey of Canada, Geology of Canada, vol. 2, 75-85.

Pickup, S., Withmarsh, R.B., Fowler, C.M.R. and Reston T.J. 1996. Insight into the nature of the ocean-continent transition off the West Iberia from a deep multichannel seismic reflection profile. *Geology*, **24**, 1079-1086.

Planke, S. and Alvestad, E. 1999. Seismic volcanostratigraphy of the extrusive breakup complexes in the northeast Atlantic: implications from ODP-DSDP drilling. *In*: Saunders, A., Larsen, H. and Wise, S. (eds) *Proceedings of the Ocean Drilling Program, Scientific Results, College Station, TX (Ocean Drilling Program)*, **163**, 3-16.

Planke, S., Symonds, P., Alvestad, E. and Skogseid, J. 2000. Seismic volcano-stratigraphy of large-volume basaltic extrusive complexes on rifted margins. *Journal of Geophysical Research*, **105**, 19335-19351.

Planke, S., Rasmussen, T., Rey, S. and Myklebust, R. 2005. Seismic characteristics and distribution of volcanic intrusions and hydrothermal vent complexes in the Vøring and Møre basin, *In*: Doré A.G. and Vinning B.A. (eds) *Petroleum Geology: North-West Europe and Global Perspectives - Proceedings of the 6th Petroleum Geology*. Geological Society, London, 833-844.

Reid, A., Allsop, J., Granser, H., Millet, A. and Somerton, I. 1990. Magnetic interpretation in three dimensions using Euler deconvolution. *Geophysics*, **55**, 80-91.

Reston, T.J., Gaw, V., Pennell, J., Klaeschen, D., Stubenrauch, A. and Walker, I. 2004. Extreme crustal thinning in the south Porcupine Basin and the nature of the Porcupine Median High: implications for the formation of non-volcanic rifted margins. *Journal of the Geological Society, London*, **161**, 783-798.

Ritchie, J.D. and Hitchen, K. 1996. Early Paleogene offshore igneous activity to the northwest of the UK and its relationship to the North Atlantic igneous province,

In: Knox R.W., Corfield R.M. and Dunay, R.E. (eds) *Correlation of the early Paleogene in Northwest Europe*. Geological Society Special Publications, **101**, 63-78.

Roberts, D.G., Masson, D.G. and Miles, P.R. 1981. Age and structure of the southern Rockall Trough; new evidence. *Earth and Planetary Science Letters*, **52**, 115-128.

Roberts, D.G., Montadert, L., Roberts, D.G., Auffret, G.A., Bock, W.D., Dupeuble, P. A., Hailwood, E.A., Harrison, W.E., Kagami, H., Lumsden, D.N., Muller, C.M., Schnitker, D., Thompson, R.W., Thompson, T.L. and Timofeev, P.P. 1979. Evolution of passive rifted margins: perspective and retrospective of DSDP Leg 48. Initial reports of the Deep Sea Drilling Project covering Leg 48 of the cruises of the Drilling Vessel Glomar Challenger, Brest, France to Aberdeen, Scotland, May-July, *Initial reports of the Deep Sea Drilling Project*, **48**, 1143-1153.

Roberts, D.G., Schnitker, D., Baldauf, J.G., Desprairies, A., Homrighausen R., Huddlestun, P.F., Kaltenback, A.J., Krumsiek, K.A., Morton A.C., Murray J. W., Westberg S.J., Zimmerman H.B. and Keene, J.B. 1984. Evolution of volcanic refited margins: synthesis of Leg 81 results on the west margin of the Rockall Plateau. *Initial Reports of the Deep Sea Drilling Project*, **81**, 31-233.

Roberts, D.G., Thompson, M., Mitchener, B., Hossack, J. and Carmichael, S. 1999. Palaeozoic to Tertiary rift and basin dynamics: mid-Norway to the Bay of Biscay - a new context for hydrocarbon prospectivity in the deep water frontier. *In*: Fleet, A.J. and Boldy, S.A.R. (eds) *Petroleum Geology of Northwest Europe: Proceedings of the 5th Conference*, Geological Society, London, 7-40.

Roberts, D.G. 1975. Marine Geology of the Rockall Plateau and Trough. *Philosophical Transactions of the Royal Society of London*, **A278**, 447-509.

Roest, W. and Srivastava, S. 1989. Sea-floor spreading in the Labrador Sea: a new reconstruction. *Geology*, **17**, 1000-1003.

Saalmann, K., Tessensohn, F., Piepjohn, K., Gosen, W. von and Mayr, U. 2005, Structure of Palaeogene sediments in east Ellesmere Island: Constraints on Eurekan tectonic evolution and implications for the Nares Strait problem. *Tectonophysics*, **406**, 81-113.

Sandwell, D.T. and Smith, W.H.F. 1997. Marine gravity anomaly from Geosat and ERS1 satellite altimetry. *Journal of Geophysical Research*, **102**, 10039-10054.

Saunders, A., Fitton, J., Kerr, A., Norry, M. and Kent, R. 1997. The North Atlantic Igneous Provinces, *In*: Mahoney, J.J. and Coffin, M.F (eds) *Large Igneous Provinces: Continental, Oceanic, and Planetary Flood Volcanism*. American Geophysical Union, Geophysical Monograph, **100**, 45-93.

Schwartz, A. 1974. *Calculus and Analytic Geometry, 3rd edition*. Holt, Rinehart, and Winston, New York, 1140pp.

Scrutton, R.A. and Bentley, P. 1988. Cretaceous volcanic province in southern Rockall Trough. *Earth and Planetary Science Letters*, **91**, 198-204.

Scrutton, R.A. and Roberts, D.G. 1971. Structure of Rockall Plateau and Trough, north-east Atlantic. *In*: Delany, F.M. (ed) *The Geology of the East Atlantic Continental Margin*. Institute of Geological Sciences Report, **70/14,** HMSO, 77-87.

Shannon, P.M. and Spencer, A.M. 1999. Atlantic margin, offshore Norway to offshore Ireland: introduction and review. *In*: Fleet, A.J. and Boldy, S.A.R. (eds) *Petroleum Geology of Northwest Europe: Proceedings of the 5th conference*, 229-230.

Shannon, P.M., Jacob, A.W.B., Makris, J., O'Reilly, B.M., Hauser, F. and Vogt, U. 1994. Basin evolution in the Rockall region, North Atlantic. *First Break*, **12**, 515-522.

Shannon, P.M. 1991. Tectonic framework and petroleum potential of the Celtic Sea, Ireland. *First Break*, **9**, 107-121.

Shannon, P.M. 1995. Permo-Triassic development of the Celtic Sea region, offshore Ireland. *In*: Boldy, S.A.R. (ed) *Permian and Triassic Rifting in Northwest Europe*. Geological Society, London, Special Publication, **91**, 215-237.

Sibuet, J.-C., Sirastava, S., Enachescu, M. and Karner, G. 2005. Early Cretaceous motion of Flemish Cap with respect to North America: Implications on the formation of Orphan Basin and S-E Flemish Cap/Galician Bank congugate margins. IMEDL proceedings volume.

Sibuet, J.-C., Srivastava, S. and Spakman, W., 2004, Pyrenean orogeny and plate kinematics. *Journal of Geophysical Research*, **B08104**, doi:10.1029/2003JB00.

Skogseid, J. 2001. Volcanic and exploration aspects. *Marine and Petroleum Geology*, **18**, 457-461.

Skogseid, J., Pedersen, T., Eldholm, O. and Larsen, B. 1992. Tectonism and magmatism during NE Atlantic continental break-up: the Vøring basin. *In*: Storey, B.C., Alabaster, T. and Plankhurst, R.J. (eds) *Magmatism and the Causes of Continental Break-up*. Geological Society, London, Special Publications, **68**, 305-320.

Smallwood, J. and White, R.S. 2002, Ridge-plume interaction in the North Atlantic and its influence on continental breakup and seafloor spreading, *In:* Jolley, D.W. and Bell, B.R. (eds) *The North Atlantic Igneous Province: Stratigraphy, Tectonic, Volcanic and Magmatic Processes*. Geological Society of London, Special Publications, **197**, 15-37.

Smallwood, J.R., Staples, R., Richardson, K., White, R. and Group F.W. 1999. Crust generated above the Iceland mantle plume: from continental to oceanic spreading center. *Journal of Geophysical Research*, **104**, 22885-22902.

Smellie, D.W. 1956. Elementary approximations in aeromagnetic interpretation. *Geophysics*, **21**, 1021-1040.

Smith, L.K., White, R.S., Kusznir, N.J. and the iSIMM Team. 2005. Structure of the Hatton Basin and adjacent continental margin, *In*: Doré, A.G. and Vining, B. (eds), *Petroleum Geology: North-West Europe and Global Perspectives - Proceedings of the 6th Petroleum Geology Conference*. Geological Society, London, 733-737.

Spector, A. and Grant, F.S. 1970. Statistical Models for Interpreting Aeromagnetic Data. *Geophysics*, **35**, 293-302.

Srivastava, S. and Verhoef, J. 1992. Evolution of Mesozoic sedimentary basins around the north Central Atlantic: a preliminary plate kinematic solution. *In*: Parnell, J. (ed) *Basins on the Atlantic seaboard: petroleum geology, sedimentology and basin evolution*. Geological Society, Special publications, London, **62**, 397-420.

Stoker, M.S., van Weering, T.C.E. and Svaerdborg, T. 2001. A mid- to late Cenozoic tectonostratigraphic framework for the Rockall Trough, *In*: Shannon, P.M. Haughton, P.D.W. and Corcoran, D.V. (eds) *The Petroleum Exploration of Ireland's Offshore Basins*. Geological Society, London, Special Publications, **188**, 411-438.

Stoker, M.S. 1993. Glacial sediments off NW Britain. *Earthwise (Keyworth)*, **3**, 10.

Stoker, M.S., Praeg D., Shannon P.M., Hjelstuen, B., Laberg, J., van Weering, T.C.E., Sejrup, H. and Evans, D. 2005. Neogene evolution of the Atlantic continental margin of NW Europe (Lofoten Islands to SW Ireland): anything but passive. *In*: Doré, A.G. and Vining, B. (eds) *Petroleum Geology: North-West Europe and Global Perspectives - Proceedings of the 6th Petroleum Geology Conference*. Geological Society, London, 1057-1076.

Surlyk, F. 1990. Timing, style and sedimentary evolution of Late Palaeozoic-Mesozoic extensional basins of East Greenland. *In*: Hardman, R.F.P. and Brooks, J. (eds) *Tectonic Events Responsible for Britain's Oil and Gas Reserves*. Geological Society, London, Special Publications, **55**, 107-125.

Svensen, H., Planke, S., Malthe-Sørenssen, A., Jamtveit, B., Myklebust, R., Rasmussen Eidem, T. and Rey, S. 2004. Release of methane from a volcanic basin as a mechanism for initial Eocene global warming. *Nature*, **429**, 542-545.

Talwani, M. 1973. Computer Usage in the Computation of Gravity Anomalies. *Methods in Computational Physics*, **13**, 343-389.

Tate, M.P. and Dobson, M.R. 1988. Syn- and post-rift igneous activity in the Porcupine Seabight Basin and adjacent continental margin west of Ireland. *In*: Morton, A.C. and Parson, L.M. (eds) *Early Tertiary volcanism and the opening of the NE Atlantic*. Geological Society Special Publications, **39**, 309-334.

Tate, M. and Dobson, M. 1989. Late Permian to early Mesozoic rifting and

sedimentation, offshore NW Ireland. *Marine and Petroleum Geology*, **6**, 59.

Tate, M. 1993. Structural framework and tectonostratigraphic evolution of the Porcupine Seabight Basin offshore western Ireland. *Marine and Petroleum Geology*, **10**, 95-123.

Tegner, C., Duncan, R.A., Larsen, H.C., Duncan, R.A., Allan, J.F., Aita, Y., Arndt, N.T., Buecker, C.J., Cambray, H., Cashman, K.V., Cerney, B. P., Clift P.D. and Fitton, J.G. 1999. ^{40}Ar- ^{39}Ar chronology for the volcanic history of the Southeast Greenland rifted margin. Proceedings of the Ocean Drilling Program, scientific results, Southeast Greenland margin covering Leg 163, *Proceedings of the Ocean Drilling Program, Scientific Results*, **163**, 53-62.

Thinon, I., Fidalgo-González, L., Avedik, F., Matias, L., Réhault, J.P., Hirn, A. 2003. Deep structure of the Armorican Basin (Bay of Biscay): A review of Norgasis seismic reflection and refraction data. *Journal of the Geological Society, London*, **160**, 99-116.

Thompson, D. 1982. EULDPH: A new technique for making computer-assisted depth estimates from magnetic data. *Geophysics*, 47, 31-37.

Thomson, A. and McWilliam, A. 2001. The structural style and evolution of the Bróna Basin. *In*: Shannon, P.M., Haughton, P.D.W. and Corcoran, D.V. (eds) The Petroleum Exploration of Ireland's Offshore Basins. *Geological Society Special Publication*, **188**, 401-410.

Trueblood, S. and Morton, N. 1991. Comparative sequence stratigraphy and structural style of the Slyne Trough and Hebrides basin. Journal of Geological Society, London, **148**, 197-201.

Underhill, J. and Partington, M. 1993. Jurassic thermal doming and deflation in the North Sea: Implication of the sequence stratigraphic evidence. *In*: Parker, J.R. (ed) *Petroleum Geology of North-west Europe: Proceedings of the 4th Conference*. Geological Society, London, Special Publications, 337-345.

Van Wijk, J.W., Huismans, R.S., Ter Voorde, M. and Cloetingh, S.A.P.L. 2001. Melt generation at volcanic continental margins: No need for a mantle plume? *Geophysical Research Letters*, **28**, 3995-3998.

Verhoef, J., Roest, W.R., Macnab, R., Arkani-Hamed, J. and Members of the Project Team, 1996. *Magnetic anomalies of the Arctic and North Atlantic Oceans and adjacent land areas*. GSC Open File 3125, Geological Survey of Canada, Dartmouth, NS.

Vogt, P. and Avery, O. 1974. Detailed magnetic surveys in the northeast Atlantic and Labrador Sea. *Journal of Geophysical Research*, **79**, 363-389.

Vogt, U., Makris, J., O'Reilly, B.M., Hauser, F., Readman P.W., Jacob, A.W.B. and Shannon P.M. 1998. The Hatton Basin and continental margin: Crustal structure from wide-angle seismic and gravity data. *Journal of Geophysical Research*,

103, 12545-12566.

Walsh, A., Knag, G.O., Morris, M., Quinquis, H., Tricker, P., Bird, C. and Bower, S. 1999. Petroleum geology of the Irish Rockall Trough; a frontier challenge. *In*: Fleet, A.J. and Boldy, S.A.R. (eds) *Petroleum geology of Northwest Europe: Proceedings of the 5th conference*. Geological Society, London, 433-444.

Welsink, H., Dwyer, J. and Knight, R. 1989. Tectono-stratigraphy of the passive margin off Nova Scotia. *In*: Tankard, A.J. and Balkwill, H.R (eds) *Extensionnal Tectonics and Stratigraphy of the North Atlantic Margins*. American Association of Petroleum Geologists (AAPG) Memoirs, **79**, 215-231.

White, R.S. and McKenzie, D.P. 1989. Magmatism at rift zones: the generation of volcanic continental margins and flood basalts. *Journal of Geophysical Research*, **94**, 7685-7729.

White, R.S. 1988. A hot-spot model for early Tertiary volcanism in the N Atlantic. *In*: Morton, A.C. and Parson, L.M. (eds) *Early Tertiary Volcanism and the Opening of the NE Atlantic*. Geological Society Special Publications, **39**, 3-13.

White, R.S., Spence, G.D., Fowler, S.R. and McKenzie, D.P. 1987. Magmatism at rifted continental margins. *Nature*, **330**, 439-444.

Wilson, M. 1993. Geochemical signature of oceanic and continental basalts: a key to mantle dynamics? *Journal of the Geological Society, London*, **150**, 997-1987.

Ziegler, P.-A. 1982. *Geological Atlas of Western and Central Europe*. Elsevier, Amsterdam.

Ziegler, P.-A. 1992. European rift system. *Tectonophysics*, **208**, 91-111.